

**EVALUATION OF SELECTED MUSHROOM EXTRACTS,
DISPIROPIPERAZINE AND DISPIROPYRROLIZIDINE DERIVATIVES
ON ACETYLCHOLINESTERASE ACTIVITY**

by

Khoa Bhanthumnawin

B.Sc., University of Calgary, 2018

THESIS SUBMITTED IN PARTIAL FULFILLMENT OF
THE REQUIREMENTS FOR THE DEGREE OF
MASTER OF SCIENCE
IN
BIOCHEMISTRY

UNIVERSITY OF NORTHERN BRITISH COLUMBIA

December 2023

© Khoa Bhanthumnawin, 2023

Abstract

Acetylcholinesterase is a hydrolase enzyme known for its major role in neurotransmission regulation by breaking down the neurotransmitter acetylcholine at the synapse after every electrochemical signal is successfully relayed between two adjacent neurons. In a healthy human brain, it retains itself on the extracellular surface of neurons, concordantly paints up an artistic beautiful web of an intricate neural network upon staining. However, in an aging human brain experiencing neurodegeneration, the network collapses into plaques that are neurotoxic to the brain. At the center of these individual plaques are heavily aggregated amyloid-beta peptides and fibers enveloping the neurons. This is most often one of the specific traits of Alzheimer's and Parkinson's disease, two most common neurodegenerative diseases. Many studies have provided experimental evidences of stable co-localization and fiber growth promotion existing between the amyloid-beta peptides and acetylcholinesterase. Nevertheless, the specific chemistry and mechanism of how the relationship between the amyloid-beta peptides and acetylcholinesterase is formed and maintained, still remains tentative to date. Most neurodegenerative diseases remain incurable, and most of the available medical treatments focus on alleviating the symptoms and mitigating the disease progression, for instance through the use of acetylcholinesterase inhibitors. But with drawbacks related to treatment effectiveness and undesirable side effects of the current available acetylcholinesterase inhibitors, the continued search for more effective acetylcholinesterase inhibitors has never ceased. The objectives of this *in vitro* study were to examine four small molecules and twenty-one mushroom extracts for their ability to inhibit acetylcholinesterase activity.

To perform the screen, an enzyme assay using Ellman's reagent DTNB was used. The assay utilizes thiocholine produced from the hydrolysis of acetylthiocholine by

acetylcholinesterase to reduce DTNB into TNB²⁻, a colorimetric product that can be used to monitor the changes in the acetylcholinesterase activity level in the presence or absence of inhibitors. Using the established acetylcholinesterase assay, none of the four small molecules showed any inhibitory effect on acetylcholinesterase activity. On the contrary, eight of the mushroom extracts were found to inhibit the acetylcholinesterase activity. These eight extracts were prepared from five mushroom species that have not been extensively researched nor reported for acetylcholinesterase inhibition. Surprisingly, for the remaining thirteen mushroom extracts that did not show inhibition, they were found to enhance the acetylcholinesterase activity. Albeit the unexpected irrelevance to the focus of the study, these thirteen extracts could be useful as biological tools in the general research of regeneration, as acetylcholinesterase has been reported to act as a mediator promoting cell proliferation and regeneration.

Table of Contents

Abstract.....	ii
Table of Contents.....	iv
List of Tables.....	viii
List of Figures.....	ix
List of Supplementary Tables.....	xi
List of Supplementary Figures.....	xii
Acknowledgement and Dedication.....	xiii
Chapter 1 - Introduction	1
1.1 Acetylcholinesterase Enzyme.....	1
1.1.1 Expression and Assembly of Acetylcholinesterase.....	1
1.1.2 The Hydrolysis of Acetylcholine by Acetylcholinesterase.....	4
1.1.3 The Role of Acetylcholinesterase in Cholinergic Neurotransmission.....	8
1.1.4 Upstream Regulation of Acetylcholinesterase Activity.....	12
1.2 Acetylcholinesterase in the Context of Neurodegeneration.....	16
1.2.1 Alzheimer’s Disease.....	18
1.2.2 Parkinson’s Disease.....	20
1.2.3 Huntington’s Disease.....	21
1.2.4 Multiple Sclerosis.....	22
1.3 Acetylcholinesterase Inhibitors in the Treatment of Neurodegenerative Diseases.....	23
1.3.1 Rivastigmine.....	24
1.3.2 Donepezil.....	25
1.3.3 Galanthamine.....	26
1.3.4 Huperzine A.....	27
1.4 The Need to Search for Novel Acetylcholinesterase Inhibitors.....	27
1.4.1 Small Molecules: SPOPP and NP6A.....	28
1.4.2 Small Molecules: 534_1(6) and 534_2(7).....	29
1.4.3 MolTarPred Program.....	31
1.5 Mushrooms as a Potential Source of Acetylcholinesterase Inhibitors.....	32
1.6 Research Objectives.....	36
Chapter 2 - Development of the Acetylcholinesterase Assay and Examination of the Effect of Small Molecules on Acetylcholinesterase Activity.....	37

2.1	Introduction.....	37
2.1.1	Overview of the Acetylcholinesterase Assay Design.....	37
2.1.2	Considerations and Selection for the Main Components of the Acetylcholinesterase Assay	38
	DTNB as an Ideal Reagent for Thiol Quantification.....	38
	Acetylthiocholine Iodide as an Alternative Substrate of Acetylcholinesterase.....	40
	<i>Electrophorus electricus</i> Acetylcholinesterase as an Economical Orthologue Prevalent in Fundamental Research Studies.....	41
	Sodium Phosphate Buffer as a Nurturing Cocktail for an Efficient Functionality of Acetylcholinesterase.....	43
2.2	Materials and Methods.....	44
2.2.1	Preparation of the Main Components of the Acetylcholinesterase Assay – Stock Solutions	44
	20.2 mM of DTNB	44
	346 mM of Acetylthiocholine Iodide	45
	125 units/mL of Acetylcholinesterase	46
	0.1 M of Sodium Phosphate Buffer at pH 8.0	47
2.2.2	Preparation of the Main Components of the Acetylcholinesterase Assay – Standard Solutions	48
	10 mM of DTNB	48
	14 mM of Acetylthiocholine Iodide	48
	9 units/mL of Acetylcholinesterase	49
	4.5 units/mL of Acetylcholinesterase	49
	0.9 units/mL of Acetylcholinesterase	49
	0.09 units/mL of Acetylcholinesterase	50
	0.009 units/mL of Acetylcholinesterase	50
2.3	Results and Discussion	50
2.3.1	Testing the Performance of the Acetylcholinesterase Assay.....	51
2.3.1.1	The First Performance Test: Evaluating the Assay with Different Concentrations of Acetylcholinesterase	51
2.3.1.1.1	Purpose of the First Performance Test	51
2.3.1.1.2	Experimental Procedure of the First Performance Test.....	51
2.3.1.1.3	Raw Data Processing and Graphing Transformation of the First Performance Test	52

2.3.1.1.4	Hypothesis and Predicted Outcomes of the First Performance Test	53
2.3.1.1.5	Observations and Analyses of the First Performance Test.....	53
2.3.1.2	The Second Performance Test: Evaluating the Assay with Different Concentrations of Known Inhibitors of Acetylcholinesterase	76
2.3.1.2.1	Purpose of the Second Performance Test.....	76
2.3.1.2.2	Experimental Procedure of the Second Performance Test	77
2.3.1.2.3	Raw Data Processing and Graphing Transformation of the Second Performance Test.....	79
2.3.1.2.4	Hypothesis and Predicted Outcomes of the Second Performance Test.....	81
2.3.1.2.5	Observations and Analyses of the Second Performance Test	81
2.4	Examination of the Effect of Small Molecules on Acetylcholinesterase Activity	86
2.4.1	Preparation of the Synthetic Small Molecules	86
2.4.1.1	Synthesis of SPOPP and NP6A	86
2.4.1.2	Preparation of Flash Column Chromatography	89
2.4.1.3	Purification of SPOPP and NP6A.....	92
2.4.1.4	Synthesis of 534_1(6) and 534_2(7).....	93
2.4.2	Evaluation of the Effect of Small Molecules on Acetylcholinesterase Activity	93
2.4.2.1	Experimental Procedure.....	93
2.4.2.2	Hypothesis and Predicted Outcomes	95
2.4.2.3	Observations and Analyses	95
Chapter 3 - Investigating the Effect of Mushroom Extracts on Acetylcholinesterase Activity		100
3.1	Introduction.....	100
3.2	Materials and Methods.....	100
3.2.1	Preparation of the Mushroom Extracts.....	100
3.2.1.1	Extraction of the Mushroom Extracts	100
3.3	Results and Discussion	101
3.3.1	Evaluation of the Effect of Crude Mushroom Extracts on Acetylcholinesterase Activity	102
3.3.1.1	Experimental Procedure.....	102
3.3.1.2	Hypothesis and Predicted Outcomes	103
3.3.1.3	Observations and Analyses	104
Chapter 4 - General Discussion		135

4.1	General Remarks.....	135
4.2	Establishment of the Acetylcholinesterase Assay.....	135
4.3	The Effects of the Selective Small Molecules on Acetylcholinesterase Activity.....	137
4.4	The Effects of the Selective Mushroom Extracts on Acetylcholinesterase Activity	138
4.5	Concluding Remarks and Future Directions.....	146
	References.....	148
	Supplementary Data.....	154

List of Tables

Table 1. List of Example Mushroom Species Conducted in the Research of Neurodegeneration.	34
Table 2. List of Example Mushroom Species Reported for <i>In Vitro</i> Inhibition of Acetylcholinesterase Activity.	35
Table 3. Evaluating the Assay with Different Concentrations of Acetylcholinesterase: The First Performance Test, Run 1.....	56
Table 4. Evaluating the Assay with Different Concentrations of Acetylcholinesterase: The First Performance Test, Run 11.....	65
Table 5. Evaluating the Assay with Different Concentrations of Acetylcholinesterase: The First Performance Test, Run 12.....	68
Table 6. Evaluating the Assay with Different Concentrations of Acetylcholinesterase: The First Performance Test, Run 13.....	71
Table 7. Summary of the Preparation of the Mushroom Extracts.	101
Table 8. Summary of Mushroom Extracts that Inhibited Acetylcholinesterase Activity.	116
Table 9. Summary of Mushroom Extracts that Were Negative for Acetylcholinesterase Activity Inhibition.....	124

List of Figures

Figure 1. Schematic Diagram of the Acetylcholinesterase Gene.	2
Figure 2. Schematic Diagram of the Predominant T Form of Acetylcholinesterase in the Central Nervous System of the Human Brain.	3
Figure 3. Schematic Diagram of the Tertiary Protein Structure of Acetylcholinesterase.	6
Figure 4. Schematic Diagram of the Hydrolysis of Acetylcholine at the Catalytic Anionic Site of Acetylcholinesterase.	8
Figure 5. The Chemical Structure of Rivastigmine.	25
Figure 6. The Chemical Structure of Donepezil.	26
Figure 7. The Chemical Structure of Galanthamine.	27
Figure 8. The Chemical Structure of Huperzine A.	27
Figure 9. The Chemical Structures of SPOPP and NP6A.	29
Figure 10. The Chemical Structures of 534_1(6) and 534_2(7).	31
Figure 11. The Reaction Mechanism of the Acetylcholinesterase Assay Using Ellman's Reagent.	38
Figure 12. Evaluating the Assay with Different Concentrations of Acetylcholinesterase: The First Performance Test, Run 3.	58
Figure 13. Evaluating the Assay with Different Concentrations of Acetylcholinesterase: The First Performance Test, Run 11.	66
Figure 14. Evaluating the Assay with Different Concentrations of Acetylcholinesterase: The First Performance Test, Run 12.	69
Figure 15. Evaluating the Assay with Different Concentrations of Acetylcholinesterase: The First Performance Test, Run 13.	72
Figure 16. The Effect of Different Acetylcholinesterase Concentrations on Acetylcholinesterase Activity.	75
Figure 17. The Effect of Different Acetylcholinesterase Concentrations on Acetylcholinesterase Activity.	76
Figure 18. The Effect of Galanthamine Hydrobromide on Acetylcholinesterase Activity.	83
Figure 19. The Effect of Pyridostigmine Bromide on Acetylcholinesterase Activity.	85
Figure 20. The Synthesis of SPOPP and NP6A.	87
Figure 21. The Synthesis of SPOPP and NP6A.	87
Figure 22. Crude Product Solids From the Synthesis of SPOPP and NP6A.	88
Figure 23. Crude Product Solids From the Synthesis of SPOPP and NP6A.	89
Figure 24. The Purification of SPOPP and NP6A.	93
Figure 25. The Effect of SPOPP on Acetylcholinesterase Activity.	96
Figure 26. The Effect of NP6A on Acetylcholinesterase Activity.	97
Figure 27. The Effect of 534_1(6) on Acetylcholinesterase Activity.	98
Figure 28. The Effect of 534_2(7) on Acetylcholinesterase Activity.	99
Figure 29. The Effect of Phellinus igniarius PIE3 on Acetylcholinesterase Activity at Low Extract Concentrations.	106
Figure 30. The Effect of Phellinus igniarius PIE2 on Acetylcholinesterase Activity at Low Extract Concentrations.	108

Figure 31. The Effect of <i>Ganoderma applanatum</i> M5E3 on Acetylcholinesterase Activity at Low Extract Concentrations.....	109
Figure 32. The Effect of <i>Ganoderma applanatum</i> M5E1 on Acetylcholinesterase Activity at Low Extract Concentrations.....	111
Figure 33. The Effect of <i>Ganoderma applanatum</i> M5E1 on Acetylcholinesterase Activity at High Extract Concentrations.....	113
Figure 34. The Effect of <i>Hericium erinaceus</i> 288E3 on Acetylcholinesterase Activity at High Extract Concentrations.....	117
Figure 35. The Effect of <i>Ganoderma applanatum</i> M5E2 on Acetylcholinesterase Activity at High Extract Concentrations.....	118
Figure 36. The Effect of <i>Amanita muscaria</i> 243E1 on Acetylcholinesterase Activity at High Extract Concentrations.....	119
Figure 37. The Effect of <i>Agaricus subrufescens</i> 295E1 on Acetylcholinesterase Activity at High Extract Concentrations.....	120
Figure 38. The Effect of <i>Agaricus subrufescens</i> 295E2 on Acetylcholinesterase Activity at High Extract Concentrations.....	121
Figure 39. The Effect of <i>Hericium erinaceus</i> 288E1 on Acetylcholinesterase Activity at High Extract Concentrations.....	122
Figure 40. The Effect of <i>Inonotus obliquus</i> 285E1 on Acetylcholinesterase Activity at High Extract Concentrations.....	123
Figure 41. The Effect of <i>Amanita muscaria</i> 243E2 on Acetylcholinesterase Activity at High Extract Concentrations.....	125
Figure 42. The Effect of <i>Amanita muscaria</i> 243E3 on Acetylcholinesterase Activity at High Extract Concentrations.....	126
Figure 43. The Effect of <i>Agaricus subrufescens</i> 295E3 on Acetylcholinesterase Activity at High Extract Concentrations.....	127
Figure 44. The Effect of <i>Inonotus obliquus</i> 285E2 on Acetylcholinesterase Activity at High Extract Concentrations.....	128
Figure 45. The Effect of <i>Inonotus obliquus</i> 285E3 on Acetylcholinesterase Activity at High Extract Concentrations.....	129
Figure 46. The Effect of <i>Pleurotus ostreatus</i> 68E2 on Acetylcholinesterase Activity at High Extract Concentrations.....	130
Figure 47. The Effect of <i>Phellinus pini</i> 91E1 on Acetylcholinesterase Activity at High Extract Concentrations.....	131
Figure 48. The Effect of <i>Phellinus igniarius</i> PIE1 on Acetylcholinesterase Activity at High Extract Concentrations.....	132
Figure 49. The Effect of <i>Phellinus pini</i> 91E2 on Acetylcholinesterase Activity at High Extract Concentrations.....	133
Figure 50. The Effect of <i>Phellinus pini</i> 91E3 on Acetylcholinesterase Activity at High Extract Concentrations.....	134

List of Supplementary Tables

Supplementary Table 1. Evaluating the Assay with Different Concentrations of Acetylcholinesterase: The First Performance Test, Run 2.....	155
Supplementary Table 2. Evaluating the Assay with Different Concentrations of Acetylcholinesterase: The First Performance Test, Run 3.....	158
Supplementary Table 3. Evaluating the Assay with Different Concentrations of Acetylcholinesterase: The First Performance Test, Run 4.....	160
Supplementary Table 4. Evaluating the Assay with Different Concentrations of Acetylcholinesterase: The First Performance Test, Run 5.....	163
Supplementary Table 5. Evaluating the Assay with Different Concentrations of Acetylcholinesterase: The First Performance Test, Run 6.....	166
Supplementary Table 6. Evaluating the Assay with Different Concentrations of Acetylcholinesterase: The First Performance Test, Run 7.....	169
Supplementary Table 7. Evaluating the Assay with Different Concentrations of Acetylcholinesterase: The First Performance Test, Run 8.....	172
Supplementary Table 8. Evaluating the Assay with Different Concentrations of Acetylcholinesterase: The First Performance Test, Run 9.....	175
Supplementary Table 9. Evaluating the Assay with Different Concentrations of Acetylcholinesterase: The First Performance Test, Run 10.....	180

List of Supplementary Figures

Supplementary Figure 1. Evaluating the Assay with Different Concentrations of Acetylcholinesterase: The First Performance Test, Run 2.....	156
Supplementary Figure 2. Evaluating the Assay with Different Concentrations of Acetylcholinesterase: The First Performance Test Run 4.....	161
Supplementary Figure 3. Evaluating the Assay with Different Concentrations of Acetylcholinesterase: The First Performance Test, Run 5.....	164
Supplementary Figure 4. Evaluating the Assay with Different Concentrations of Acetylcholinesterase: The First Performance Test, Run 6.....	167
Supplementary Figure 5. Evaluating the Assay with Different Concentrations of Acetylcholinesterase: The First Performance Test, Run 7.....	170
Supplementary Figure 6. Evaluating the Assay with Different Concentrations of Acetylcholinesterase: The First Performance Test, Run 8.....	173
Supplementary Figure 7. Evaluating the Assay with Different Concentrations of Acetylcholinesterase: The First Performance Test, Run 9.....	176

Acknowledgement and Dedication

Set sailing towards the end of 2023, as I looked back on my journey throughout the years upon completing this piece of writing, I would like to acknowledge and express my sincere gratitude towards these individuals:

Dr. Chow Lee, for giving me an opportunity to get back into science when I had nowhere else to go, and for his mentorship and constructive criticisms to help me grow as a scientist.

Dr. Kendra Furber and Dr. Kerry Reimer, for their mentorship and support with productive feedback on my coursework and thesis.

Maggie Li, for helping me overcome many unforeseen circumstances that unexpectedly unfolded during ongoing experiments with her creativity and advice.

Hooi Xian Lee and Victor Liu, for providing the test samples, teaching and sharing tips on how to perform well on some of the tricky parts of certain lab techniques.

I would not have been able to come this far, had it not been for their guidance. Therefore, I am greatly in debt to each and every one of these individuals.

Thank you for your kind guidance throughout these passing years again. It was an honor.

Sincerely,

Khoa Doan Bhanthumnawin

Chapter 1

Introduction

1.1 Acetylcholinesterase Enzyme

Acetylcholinesterase is a hydrolase enzyme known for its major role in regulating cholinergic neurotransmission by catabolizing the neurotransmitter acetylcholine at the synapse after every nerve impulse transmission between two adjacent neurons. The enzyme is known to exist in four different isoforms, distinguished by the subunit types altered through various post-translational modifications: R, S, H, and T. Each of these subunit types may also have more than one molecular form, characterized mainly by a combination of the following three phenotypes: homomeric or heteromeric, amphiphilic or non-amphiphilic, and soluble or membrane-bound.

In contrast to the highly conserved catalytic domain of the enzyme, the diverse subunit types and their unique molecular forms mostly result from specific types of post-translational modifications targeted at the flexible C-terminal domain. This domain is not necessary for the catalytic function of the enzyme. In the central nervous system of the human brain, the predominant form of acetylcholinesterase is a membrane-bound amphiphilic heteromer of four T subunits attached to the proline-rich membrane anchor. The proline-rich membrane anchor is abbreviated as PRiMA.¹

1.1.1 Expression and Assembly of Acetylcholinesterase

The predominant T form is expressed from the acetylcholinesterase gene, which comprises six exons. However, only exons 2, 3, and 4 code for the catalytic domain, while exon 6 is alternatively spliced into one of the splice variants that codes for the unique C-terminal domains of T subunits and contains a message directing the attachment of those subunits to the PRiMA anchor subsequently (Figure 1).²

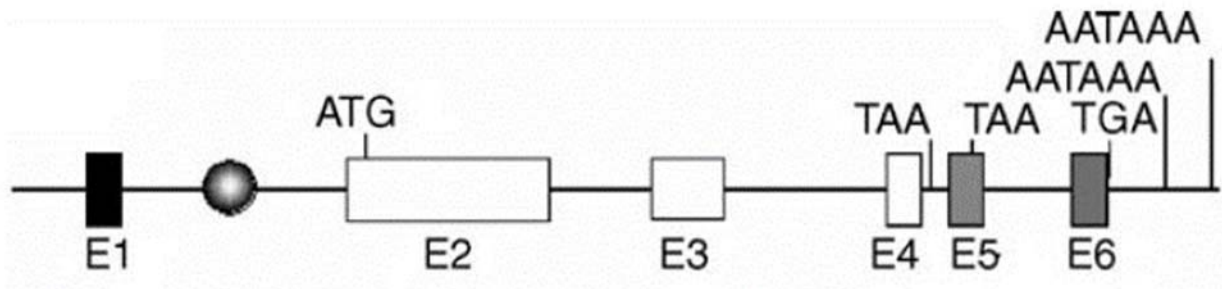


Figure 1. Schematic Diagram of the Acetylcholinesterase Gene.

The rectangles represent exons. The circle represents a regulatory intron. ATG represents the start codon AUG. TAA and TGA represent the stop codons UAA and UGA. AATAAA represents the polyadenylation signal.^{2,61}

Like many other enzymes, all acetylcholinesterase mRNA transcripts are highly localized within the nucleus and delivered to the rough endoplasmic reticulum, where translation of the enzyme occurs. During translation, the enzyme's protein structure undergoes several modifications, such as glycosylation with asparagine-linked oligosaccharides and the assembly of T subunits to the PRiMA anchor. After translation, it is a common statistic across all cell types expressing acetylcholinesterase that 20% or fewer of the enzymes are able to exit the rough endoplasmic reticulum as correctly folded protein structures maintaining an active catalytic activity. For the majority that are unable to exit, they are eventually degraded within the rough endoplasmic reticulum.

Furthermore, the asparagine-linked oligosaccharides glycosylated to the enzyme are fine-tuned to oligomers that are resistant to endoglycosidase H in the Golgi apparatus.³ Endoglycosidase H is a hydrolase enzyme that catabolizes oligosaccharides with a high content of mannose monosaccharides. Because the presence of mannose monosaccharides is strongly tied to a properly functional catalytic activity of acetylcholinesterase, it is imperative that the asparagine-linked oligosaccharides are resistant to endoglycosidase H.⁴

Upon exiting the Golgi apparatus, the fully mature acetylcholinesterase is parceled into vesicles via a clathrin-mediated mechanism, to which these vesicles are delivered to the extracellular surface.³ For successful presentation on the extracellular surface, the PRiMA anchor is a crucial structural component that the enzyme cannot be without. The peptide sequence of the anchor contains a seventeen-amino acid long proline-rich attachment domain abbreviated as PRAD located within the N-terminal domain. It is used to bind to the tryptophan amphiphilic tetramerization domain abbreviated as WAT located within the C-terminal domain of the peptide sequence of acetylcholinesterase. This binding is responsible for the assembly of T subunits to the PRiMA anchor and the presentation of the enzyme on the extracellular surface (Figure 2).⁵

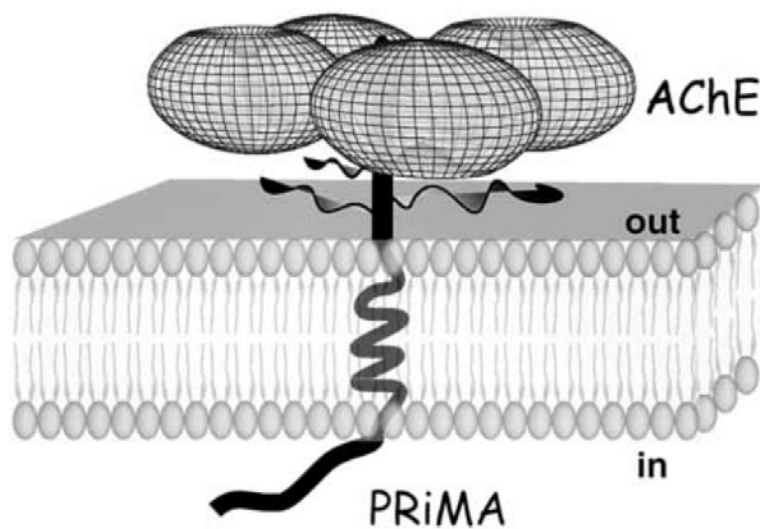


Figure 2. Schematic Diagram of the Predominant T Form of Acetylcholinesterase in the Central Nervous System of the Human Brain.

The predominant T form of acetylcholinesterase in the central nervous system of the human brain is a membrane-bound amphiphilic heteromeric tetramer of T subunits attached to the proline-rich membrane anchor PRiMA. The peptide sequence of the PRiMA anchor contains a seventeen-amino acid long proline-rich attachment domain called PRAD located within the N-terminal domain. It binds to the tryptophan amphiphilic tetramerization domain called WAT located within the C-terminal domain of the acetylcholinesterase peptide sequence. This binding signals the assembly of T subunits to the PRiMA anchor and the presentation of acetylcholinesterase on the extracellular surface of the pre-synaptic neuron at the synapse.^{5 62}

Moreover, it has also been suggested to play an important role in maintaining the structural stability and promoting the maturation of the enzyme. Incubation and reabsorption of the peptide sequence of PRAD alone was shown to significantly increase the catalytic activity of acetylcholinesterase on the extracellular surface by 400%.⁶ This indicates that PRAD may maintain the structural stability and promote the maturation of acetylcholinesterase by increasing the probability of the enzyme bypassing translational and post-translational checkpoints as a correctly folded protein structure maintaining an active catalytic activity.

On the extracellular surface, recent studies experimenting with highly polarized cells in culture have supported and suggested a common finding that all forms of acetylcholinesterase, including the predominant T form in the central nervous system, are targeted to the apical membrane, which translates to the growing axon tip of a neuron. In other words, the predominant T form of acetylcholinesterase in the central nervous system has been suggested to localize on the extracellular surface of the pre-synaptic neuron at the synapse.³

1.1.2 The Hydrolysis of Acetylcholine by Acetylcholinesterase

At the synapse, acetylcholinesterase hydrolyzes its substrate acetylcholine into acetic acid and choline. Within its quaternary structure, there exists a deep gorge, akin to a partially cracked soft-boiled egg. Near the outer opening of this gorge is the peripheral anionic site, abbreviated as the P-site. The P-site is rich in aromatic residues, with tryptophan being the most prevalent. Tryptophan's side chain has a highly electron-rich doublet aromatic ring. In the presence of the highly unstable cationic nitrogen of acetylcholine, they eventually form an intermolecular π -cation bond, providing stability to the cationic nitrogen of acetylcholine. Additionally, the para-hydroxyl group on the singlet aromatic ring of tyrosine's side chain can form a weak intermolecular

hydrogen bond with the carbonyl group on the acetyl end of acetylcholine, offering further stability to the entire substrate.

Much like the carnivorous pitcher plant, the process of luring acetylcholine into the deep gorge begins at the P-site, starting with the doublet aromatic ring of the tryptophan-286 residue. Once drawn into the gorge like a trapped insect, the acetylcholine molecule is guided into the lower choline-binding pocket deep within the gorge. At this site, the molecule once again forms π -cation bonding with the surrounding aromatic residues, including tryptophan-86 and tyrosine-337. These residues realign and correctly position the molecule towards the catalytic triad, found at the catalytic anionic site, abbreviated as the A-site. This is a crucial step that allows the acyl-binding pocket, located slightly to the upper left of the choline-binding pocket, to firmly secure the acetyl end of the molecule, preparing it for direct cleavage by the catalytic triad (Figure 3).⁷

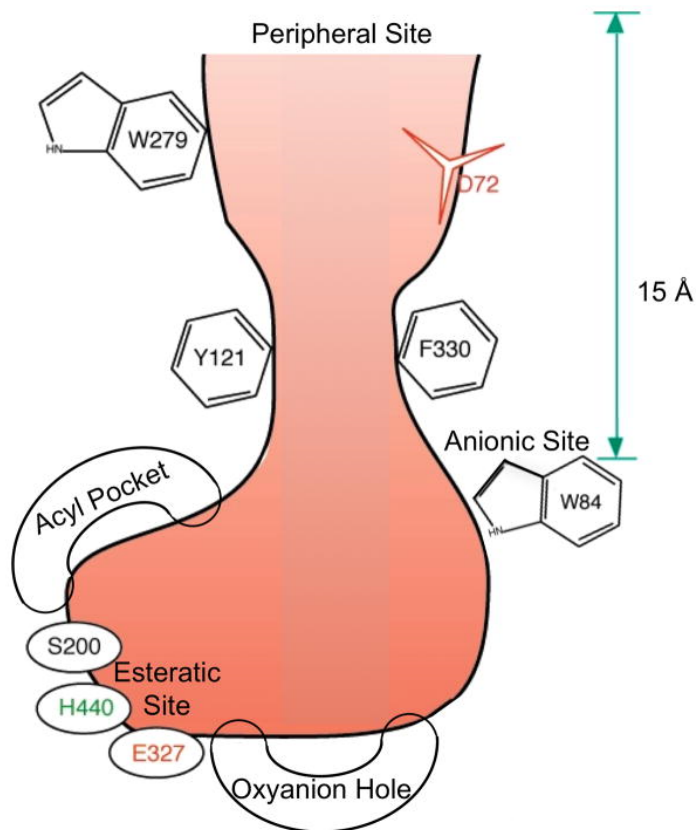


Figure 3. Schematic Diagram of the Tertiary Protein Structure of Acetylcholinesterase.

The peripheral anionic site, abbreviated as the P-site, is responsible for drawing acetylcholine into the lower catalytic anionic site, abbreviated as the A-site, through π -cation bonding. At the A-site, acetylcholine is held centered, to which it will be cleaved by the catalytic triad consisting of glutamate, histidine, and serine.⁷

The catalytic triad consists of three key residues: glutamate-334, histidine-447, and serine-203. They are arranged in a specific sequence where electron donation flows from glutamate to histidine and then to serine. The hydrolysis process begins with deprotonated glutamate-334 donating a pair of electrons and abstracting a proton from histidine-447. A deprotonated histidine-447 then donates a pair of electrons and abstracts a proton from serine-203, forming an anionic oxygen on serine-203. This anionic oxygen subsequently attacks the carbonyl group, breaking the acetyl end apart from the acetylcholine molecule.

As acetylcholine breaks apart, its anionic oxygen on the choline end donates a pair of electrons and abstracts a proton from histidine-447, returning the residue to its deprotonated state before the choline end is released from the enzyme. After separating the acetyl end, the serine-acetyl complex bends backward and is stabilized by an amide backbone in the vicinity. Following this, a water molecule infiltrates the catalytic site, and one of its protons is abstracted in exchange for a pair of electrons from the deprotonated histidine-447. These electrons are then utilized to attack the carbonyl group, releasing the acetyl end from the serine-acetyl complex as acetic acid. During the release of acetic acid, the anionic oxygen on serine-203 also donates a pair of electrons and abstracts a proton from the protonated histidine-447, restoring the residue to its deprotonated state once again. Finally, the deprotonated histidine-447 donates a pair of electrons and abstracts a proton from the protonated glutamate-334, completing the hydrolysis of acetylcholine by acetylcholinesterase (Figure 4).⁸

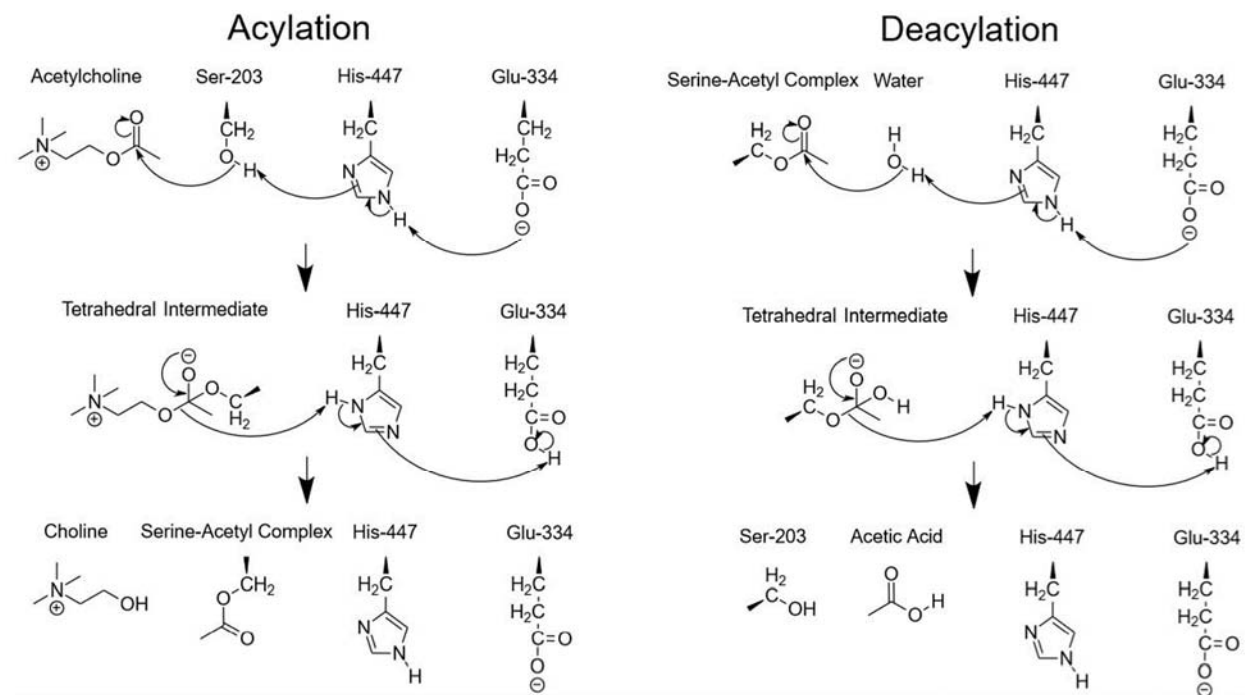


Figure 4. Schematic Diagram of the Hydrolysis of Acetylcholine at the Catalytic Anionic Site of Acetylcholinesterase.

The catalytic triad of the catalytic anionic site of acetylcholinesterase consists of three key residues: glutamate-334, histidine-447, and serine-203. They are arranged in a specific sequence where electron donation flows from glutamate to histidine and then to serine. The hydrolysis process begins with deprotonated glutamate-334 donating a pair of electrons and abstracting a proton from histidine-447. The small double-headed black arrow signifies the continuation of the electron flow, as explained above.

1.1.3 The Role of Acetylcholinesterase in Cholinergic Neurotransmission

As a regulator of cholinergic neurotransmission, the primary role of acetylcholinesterase is to prevent the continued excitation of the post-synaptic neuron by catabolizing acetylcholine. To induce an excitation or inhibition like any other neurotransmitter, acetylcholine is required to bind to a threshold number of acetylcholine receptors located on the membrane of the dendrite or cell body of the opposing post-synaptic neuron after it diffuses across the synapse.

Acetylcholine typically excites neurons. If it is not neutralized, it may continue binding to these acetylcholine receptors, leading to continued excitation of the post-synaptic neuron, potentially resulting in severe consequences. According to the Camp et al. (2005) study, a

homozygous knockout of exon 6 of the acetylcholinesterase gene in murine brains resulted in homozygotes experiencing more frequent seizures than both the heterozygotes and the wild types. These seizures exacerbated mental deficits related to memory, learning, and behavioral processes. Since exon 6 is alternatively spliced into one of the splice variants coding for the unique C-terminal domains of T subunits that direct the attachment of those subunits to the PRiMA anchor, the complete loss of exon 6 would be expected to result in a complete loss of anchorage of the T subunits to the PRiMA anchor. This would impair the presentation of acetylcholinesterase to the extracellular surface of the pre-synaptic neuron. Consistently, measurements of acetylcholinesterase activity in brain tissues showed a complete loss of activity in the homozygotes compared to the wild types, confirming the expected impaired presentation of acetylcholinesterase to the extracellular surface of the pre-synaptic neuron. Without acetylcholinesterase, the loss of control over appropriate neuron excitation may explain for the hyperexcitability, as seen with the increased frequency of seizures observed in the homozygotes.²

In addition to its primary role, recent research studies have further linked cellular communications between acetylcholinesterase and the muscarinic acetylcholine receptors mAChR1 and mAChR2 as a part of biological processes involved in cholinergic neurotransmission regulation. Both muscarinic acetylcholine receptors are abbreviated as M1 and M2 receptors. The M1 receptor is the predominant form of the five muscarinic acetylcholine receptors in the central nervous system and is primarily clustered on the extracellular surface of the post-synaptic neuron at the synapse. It plays a major role in stimulating neurons to excite upon binding with acetylcholine. The M2 receptor is moderately expressed in the central nervous system and is found on the extracellular surface of both pre- and post-synaptic neurons at the synapse. It contributes to the inhibition of the post-synaptic neuron and,⁹ notably, is involved in the autoregulation of

acetylcholine release into the synapse when bound by acetylcholine. Similar to the M2 receptor, the M4 receptor is also moderately expressed in the central nervous system and plays a role in this autoregulation. However, after an extended period of debate, it has been concluded that the M2 receptor has a more dominant role in this autoregulation.¹⁰

In murine brains, a homozygous knockout of the acetylcholinesterase gene was shown to lead to a reduction in the localization of the M1 receptor and a complete abolition of the localization of the M2 receptor on the extracellular surface of post- and pre-synaptic neurons, respectively. However, the mRNA expression levels of both receptors remained largely unchanged. This suggests that the absence of acetylcholinesterase may signal the internalization and degradation or redistribution of both receptors within the cell.^{11 12} Furthermore, the absence of acetylcholinesterase at the synapse appeared to affect the cellular responsiveness of both receptors differently. In the case of the M1 receptor, in the same studies, treatment with one of its agonists called oxotremorine did not substantially increase the activation signal of the MAPK/ERK pathway in the homozygotes compared to the wild types. The MAPK/ERK pathway is one of many that plays a crucial role in promoting brain plasticity and cognitive processes such as memory and learning. This suggests a desensitization of the M1 receptor in the absence of acetylcholinesterase at the synapse, and this desensitization may also extend to cholinergic signaling as a whole.¹¹

Regarding the M2 receptor, in a separate study where the release of acetylcholine into the synapse was monitored in slices of murine brain tissues following *in vitro* electrical stimulation, treatment with one of its antagonists called atropine, while an active acetylcholinesterase was left undisturbed, resulted in an increased efflux of acetylcholine by 66%, or 166% in net total, over the span of 12 mins compared to the basal efflux of the control. Conversely, treatment with one of the irreversible inhibitors of acetylcholinesterase called diisopropyl fluorophosphate, while an

active M2 receptor was left undisturbed, resulted in a decreased efflux of acetylcholine by 60%, or 40% in net total, over the same time span compared to the basal efflux of the control. This pattern, similar to the absence of acetylcholinesterase with the irreversible inhibition of its catalytic activity, suggests an enhancement in the sensitivity of the M2 receptor in response to acetylcholine binding, serving as a second line of defense to regulate the amount of acetylcholine released into the synapse, should the primary function of acetylcholinesterase in preventing continued neuron excitation be compromised.¹³

Taken together, the studies support the idea that acetylcholinesterase indirectly regulates the M1 and M2 receptors at a certain level. The presence of an irreversibly inactive acetylcholinesterase, or absence of an active acetylcholinesterase, was shown to not only significantly quell the number of M1 and M2 receptors presented on the extracellular surface at the synapse, but also impact their cellular responsiveness towards acetylcholine in opposite ways. These changes in receptor behavior may represent cellular responses aimed at mitigating continued neuron excitation, in order to cope with an acetylcholinesterase whose primary function is compromised.

Hypothetically, the M1 receptor becomes less sensitive and is internalized more to prevent acetylcholine from reaching the activation threshold required to induce excitation in the post-synaptic neuron, especially when unhydrolyzed acetylcholine is present in the synapse. On the other hand, the M2 receptor becomes more sensitive to enhance the autoinhibition of the acetylcholine release, preventing the excessive buildup of unhydrolyzed acetylcholine in the synapse. As a result of preventing this buildup, more M2 receptors are internalized as a response to balance the overall energy allocation within the cell, especially in the presence of lower levels of unhydrolyzed acetylcholine in the synapse.

However, it is important to note that these cellular responses may not completely prevent continued neuron excitation by unhydrolyzed acetylcholine. This is because acetylcholine can also bind to other acetylcholine receptors to induce excitation, such as the nicotinic acetylcholine receptor. Moreover, a desensitized M1 receptor does not necessarily mean it is completely insensitive, thus unhydrolyzed acetylcholine may still stimulate neurons to excite through the receptor. These proposed suggestions are consistent with the evidence from homozygous knockout mice with a complete loss of exon 6 of the acetylcholinesterase gene, as they experienced more frequent seizures compared to both the heterozygotes and the wild types.²

As for the specific mechanisms of this indirect regulation imposed on the M1 and M2 receptors in the absence of acetylcholinesterase, it is possible that extracellular signals play a role in the internalization and desensitization of the M1 receptor, and in the internalization of the M2 receptor. This is supported by the observation that treatment with their antagonist atropine could rescue the presentation of both receptors on the extracellular surface at the synapse. There may also be intracellular signals involved in the hypersensitization of the M2 receptor.^{11 12 13} Likewise, there may also be a different set of specific mechanisms of this indirect regulation in the presence of an active acetylcholinesterase.

In summary, acetylcholinesterase's role as a regulator of cholinergic neurotransmission goes beyond preventing continued neuron excitation by catabolizing acetylcholine. It also involves an indirect control of acetylcholine flow into the synapse and the sensitivity of cholinergic signaling by regulating the localization and cellular responsiveness of M1 and M2 receptors towards acetylcholine.

1.1.4 Upstream Regulation of Acetylcholinesterase Activity

Regulating neurotransmission is not a simple task, as it requires a delicate and steady neutral balance avoiding the extremes. For such a crucial function, it is unlikely that acetylcholinesterase is the sole regulator of cholinergic neurotransmission. Therefore, there may be other upstream regulatory checkpoints that control acetylcholinesterase activity at the synapse in a sequential order. At the post-transcriptional level, there have been reports of a microRNA called miRNA-132 that inhibits acetylcholinesterase expression as one of its target genes. This microRNA was found to be highly enriched in neurons.¹⁴ Either a disruption of the regulation or a decrease in the level of miRNA-132 has been shown to upregulate acetylcholinesterase expression, leading to mental deficits related to memory, learning, and behavioral processes.¹⁵ Similar to the homozygous knockout of the acetylcholinesterase gene or its exon 6 alone, this suggests that hypercatabolic activity on acetylcholine due to the overexpression of acetylcholinesterase at the synapse may not be beneficial for brain function, further emphasizing the importance of maintaining a neutral balance in cholinergic signaling during neurotransmission regulation. Reports on the regulation of acetylcholinesterase activity by miRNA-132 support observations recorded for the homozygous knockout treatment of the M1 receptor gene in the murine brain. In both cases, excessive catabolism of acetylcholine due to the overexpression of acetylcholinesterase and the reduction in cholinergic signaling due to the complete loss of the M1 receptor resulted in mental deficits related to short-term memory.¹⁰

At the post-translational level, there have been reports of a protein called presenilin 1, which appears to be an indispensable factor governing the glycosylation pattern on the protein structure of acetylcholinesterase. This glycosylation pattern is strongly linked to the proper catalytic activity of the enzyme on the extracellular surface of the pre-synaptic neuron at the synapse. According to a lectin binding analysis conducted by the Cortes-Gomez et al. (2023) study,

the majority of acetylcholinesterase activity in brain extracts obtained from control subjects was found to bind to *Concanavalina ensiformis* A and *Lens culinaris* lectins. These two lectins are known to recognize and bind to α -mannose monosaccharides. While the majority of the enzyme activity bound to the lectins, the majority of the enzyme was found to remain in fractions that did not bind to the lectins, comprising 89% to 92% of the total. This suggests that the observed majority of active acetylcholinesterase bound to the lectins only corresponded to a very small portion of the total enzyme amount, in line with the common finding that only about 20% or fewer active acetylcholinesterase can normally reach the extracellular surface. In brain extracts obtained from Alzheimer's disease subjects, the percentage of active acetylcholinesterase bound to the lectins was further reduced. These findings suggest that the glycosylation pattern, enriched in mannose monosaccharides within the protein structure of acetylcholinesterase, may play a direct role in shaping the proper catalytic function of the catalytic anionic site of the enzyme. Changes in this pattern may negatively impact acetylcholinesterase activity at the synapse, especially in the context of neurodegeneration.⁴

The involvement of presenilin 1 in the regulation of acetylcholinesterase glycosylation was further supported when its overexpression was shown to significantly increase the percentage of active acetylcholinesterase bound to the lectins, with an average increase of 25% to 30% compared to the control. This was accompanied by a larger intracellular migration across the Golgi apparatus to the extracellular surface. Even its suppression by small interfering RNA greatly shifted the majority of active acetylcholinesterase from being recognized by any of the lectins used, even though there was minimal change to the total expression level of the enzyme. These findings suggest that presenilin 1 may not only govern the glycosylation of acetylcholinesterase with highly enriched mannose monosaccharides, but it may also play a role in directing the presentation of

active acetylcholinesterase to the extracellular surface, akin to the peptide sequence of PRAD. Furthermore, disturbances affecting its functions may lead to disruptions in this specific glycosylation pattern, resulting in a shift and reduction in the portion of active acetylcholinesterase presented on the extracellular surface of the pre-synaptic neuron at the synapse.⁴

At the ligand level, apart from the acetylcholinesterase inhibitors used to alleviate the symptoms of neurodegenerative diseases, very little is known about potential endogenous ligands in the brain that directly bind and regulate acetylcholinesterase activity. However, to date, one potential candidate appears to be cholesterol. According to the Paul et al. (2017) study, feeding a hypercholesterolemic diet to mice led to an overall decrease in acetylcholinesterase activity in the brain compared to mice fed with a healthy diet. This decrease was observed across different brain regions, with enzyme activity reduced by at least 29%, and in some cases, as high as 57%. It was also associated with an increase in cholesterol content in the brain and disruption of the blood-brain barrier. At the phenotypic level, hypercholesterolemic mice also displayed mental deficits related to short-term memory, which is consistent with the seizures experienced by murine homozygotes when exon 6 of the acetylcholinesterase gene was deleted.^{2 16}

Based on the general knowledge of the role of cholesterol in the brain, it is a major component that makes up the myelin sheaths, enhancing the nerve impulse by providing an evolutionary upgrade in the form of electrical currents racing across the nodes of Ranvier at a propagation speed that is 500 times faster upon depolarization.¹⁷ Due to its crucial importance, cholesterol is not permeable through the blood-brain barrier, and its level is tightly regulated in the brain through repeated cycles of synthesis and recycling, with minimal uptake from circulation. When there is an excess amount, it is secreted from the brain after being converted into either one of its two main oxysterol derivatives, 24-hydroxycholesterol and 27-hydroxycholesterol. In

addition to aiding the excretion of excess cholesterol from the brain, these two oxysterols can also act as potent inhibitors against the production of amyloid-beta peptides, as their levels have been reported to be downregulated in Alzheimer's disease.¹⁸

Returning to the aforementioned study on the effects of hypercholesterolemia in the murine brain, although it remains unclear how high cholesterol content can disrupt the blood-brain barrier, and how cholesterol interacts to decrease acetylcholinesterase activity in the brain, all the evidences presented so far are in line with one another, strongly linking the pathological role of cholesterol and the regulatory role of its oxysterol derivatives to neurodegeneration.

1.2 Acetylcholinesterase in the Context of Neurodegeneration

In a healthy human brain, acetylcholinesterase remains on the extracellular surface of pre-synaptic neurons at the synapse, creating a beautiful and intricate neural network when stained. However, in an aging human brain experiencing neurodegeneration, this network tends to deteriorate into plaques, resembling chunks of cookies and their leftover crumbs of various sizes that are neurotoxic to the brain. At the center of these individual plaques are heavily aggregated amyloid-beta peptides and fibers that envelop the neurons. This is often one of the major characteristic features of common neurodegenerative diseases like Alzheimer's and Parkinson's diseases. In the early stages, these plaques exist as pre-plaques, which can be either small and slightly diffused with a diameter of roughly 40 μm , or large and widely diffused with a diameter of up to 300 μm . As the disease progresses, they eventually concentrate and become fully developed plaques with a densely packed core.¹⁹

Various previous *in vitro* studies have corroborated and strongly suggested a stable co-localization of amyloid-beta peptides and acetylcholinesterase. In an experiment by Alvarez et al. (1998), amyloid-beta peptides and acetylcholinesterase derived from cell extracts of bovine brain

tissues were subjected to a sedimentation velocity analysis to examine their binding affinity towards each other and their potential for co-localization. The analysis relied on centrifuging a test sample through a gradient of sucrose concentrations contained within a single test tube. Theoretically, the denser a molecule is, the deeper it will be able to advance to heavier concentrations at the bottom of the test tube. Thus, the shifts in position based on the mass of molecules in a mixture can be used to detect co-localization when compared to controls containing only individual molecules. By dividing the mixture into fractions and using the isotope iodine-125 to label the amyloid-beta peptides and Ellman's reagent 5,5'-dithiobis-2-nitrobenzoic acid abbreviated as DTNB to label the acetylcholinesterase, their relative positions along the sucrose gradient after centrifugation were determined. The results showed that the amyloid-beta peptides by themselves were denser and mostly concentrated in fractions derived from the bottom of the test tube. In contrast, acetylcholinesterase by itself was mainly concentrated in fractions derived from positions midway through the test tube. Interestingly, when amyloid-beta peptides were mixed with acetylcholinesterase, roughly two-thirds of the labeled acetylcholinesterase shifted together with the labeled amyloid-beta peptides to fractions derived from the bottom of the test tube, strongly suggesting their co-localization.²⁰

In another experiment, the amyloid-beta peptide-acetylcholinesterase complex derived from cell extracts of bovine brain tissues was subjected to various stringent experimental conditions of extremely high ionic strength and strong denaturation, followed by centrifugation, to examine the overall stability of the complex. Theoretically, the heavier complex is expected to concentrate into a pellet at the bottom of a test tube through sufficiently rough centrifugation. The presence of acetylcholinesterase activity in the remaining supernatant at the top would determine the relative proportion of acetylcholinesterase that manages to break free from the complex, which

can then be translated to the overall stability of the complex. By using DTNB to label the acetylcholinesterase activity in the supernatant, the results showed that, except for 1% SDS and 6 M of guanidine isothiocyanate, the relative proportion of enzyme activity decreased to roughly half or nearly completely diminished when the complex was subjected separately to stringent experimental conditions. Overall, both experiments suggest the existence of a profoundly strong stability inherent in the amyloid-beta peptide-acetylcholinesterase complex, bound together by hydrophobic interactions.²¹

In addition to stable co-localization, other *in vitro* experiments have also shown that acetylcholinesterase contributes to the growth of amyloid-beta peptides.²² Furthermore, the interaction of acetylcholinesterase with the complex corresponds to greater neurotoxicity, as observed by lower cell viability in the MTT assay, followed by a reduction in cell density and truncated axon growth of neurons in cell cultures.²⁰

1.2.1 Alzheimer's Disease

Based on the substantial accumulation of observations and experimental data obtained from numerous scientific studies to date, Alzheimer's disease, the most common neurodegenerative disease, serves as the foundation for developing several hypotheses aimed at explaining its pathogenesis. Although these hypotheses remain incomplete, they provide valuable insights into creating an overall depiction of Alzheimer's disease pathogenesis, particularly from the perspective of cholinergic neurotransmission. With hope, these insights may extend to the pathogenesis of other neurodegenerative diseases as well.

Among these hypotheses, the amyloid-beta peptides are considered a major focal point. According to the amyloid hypothesis, amyloid-beta peptides are generated from the amyloid precursor protein through hydrolysis by the γ -secretase complex, of which presenilin 1 is a

component. This hydrolysis process depends on acetylcholinesterase. In addition to facilitating the production of amyloid-beta peptides, acetylcholinesterase also directly binds to amyloid-beta peptides, forming highly stable complexes that enhance their fibrilization into long fiber stretches. Notably, acetylcholinesterase's involvement in these three processes is independent of its catalytic anionic site.

Overall, amyloid-beta peptides begin as short peptide sequences of approximately forty amino acids in length. They then transform into complexes when coupled with acetylcholinesterase, subsequently forming fibers and eventually aggregating densely enough to be termed plaques. Consequently, the presence of amyloid-beta-acetylcholinesterase complexes is generally more neurotoxic than amyloid-beta peptides alone. Interestingly, there is also a positive correlation between the increase of the soluble monomeric form of acetylcholinesterase, shifting away from its membrane-bound tetrameric form, and the increase in amyloid-beta plaque density as the disease progresses.²³

In a second hypothesis called the tau hypothesis, the focus is on the tau protein. Under physiological conditions, it binds and stabilizes microtubules, facilitating the delivery of nutrients and essential molecules from the cell body to the dendrite and axon within a neuron. In Alzheimer's disease, it detaches from microtubules and attaches to other tau proteins in a disorderly manner, forming neurofibrillary tangles. These tangles obstruct the flow and transportation of biomolecules, ultimately negatively impacting communication between neurons. The abnormal behavior of the tau protein is associated with its hyperphosphorylation, and it is also linked to an increased expression of acetylcholinesterase, neither of which occurs under physiological conditions. Consequently, the increased expression of acetylcholinesterase results in

the co-localization of the enzyme with the tau protein in the cytoplasm. Uncertainly, this somehow leads to increased acetylcholinesterase activity that depletes acetylcholine at the synapse later on.

In a third hypothesis called the cholinergic hypothesis, acetylcholinesterase becomes the central focus. Throughout Alzheimer's disease, acetylcholinesterase activity mildly decreases in the early stages, but becomes overly active as the disease progresses to the late stages. Accompanying this overactivity of acetylcholinesterase are the decreased level of miRNA-132 and the increased apoptosis of neurons that gradually develop over time.²³

1.2.2 Parkinson's Disease

Parkinson's disease is the second most common neurodegenerative disease. Its pathology is mainly characterized by clumps of misfolded proteins within the neuron, of which one type is called Lewy bodies. Similar to amyloid-beta peptides, these Lewy bodies comprise of repeating units of the alpha-synuclein protein that can extend into long stretches of fibers. In the context of Parkinson's disease, the bodies are not properly degraded and overwhelm the neuron, resulting in neurotoxicity as amyloid-beta peptides would.⁵⁷ Similar to Alzheimer's disease, the formation of amyloid-beta plaques is also present in Parkinson's disease, and acetylcholinesterase may also be involved in stabilizing and enhancing their formation. Unlike Alzheimer's disease, the neurotoxic effects of amyloid-beta plaques may not only exacerbate dementia, but also influence mood and physical mobility. Often, mood changes tend to be pessimistic, associated with mental states of depression, anxiety, and apathy. Impaired physical mobility leads to disruptions in a subject's sense of balance, resulting in postural instability and gait difficulty. Hyperphosphorylation of the tau protein and its association with acetylcholinesterase may contribute to visual and olfactory dysfunctions in Parkinson's disease as well.

In general, there is a slight difference from Alzheimer's disease in that acetylcholinesterase activity is more significantly dampened throughout Parkinson's disease, but followed again by a sudden increase in activity upon the apoptosis of neurons. Additionally, the significantly lower acetylcholinesterase activity in Parkinson's disease not only leads to more pronounced deficits affecting cognitive processes in the central nervous system, but also affects major sensory communications between the sense organs and the peripheral nervous system. Overall, there is a similar mode of action for acetylcholinesterase, but a slight difference in the duration of enzyme activity at different levels between Alzheimer's and Parkinson's disease. Concerning the magnitude of the adverse effects contributed by acetylcholinesterase, it appears that Parkinson's disease displays more severe deficits, which tend to extend further beyond the central nervous system compared to Alzheimer's disease.²³

1.2.3 Huntington's Disease

Unlike Alzheimer's and Parkinson's diseases, Huntington's disease does not result in the eventual death of neurons through apoptosis. Its pathology is mainly characterized by a distinctive mutation in the *HTT* gene. The *HTT* gene is an abbreviation for the word "Huntington". Although the normal function of this gene is not fully understood, it is known to be an extremely important factor in the development of the central nervous system. In Huntington's disease, the mutation carried by this gene contains many repeats of the base sequence CAG, which translates to a mutated protein consisting of an abnormally long chain of glutamine repeats. The mutated protein is then cleaved by different proteases into many different types of fragments that cause neurotoxicity. Of those fragments, the most studied one is called HTT exon 1. This fragment is highly malleable, capable of transforming into different conformations that combine with other proteins, including amyloid-beta peptides, to form neurotoxic tangles. As a result, this leads to a

persistent impairment of neurons.⁵⁸ In addition to this type of impairment, a reduction in the expression of acetylcholinesterase on the extracellular surface at the synapse is associated to it. Simultaneously, a decrease in the expression of both choline acetyltransferase, an enzyme responsible for synthesizing acetylcholine, and the vesicular acetylcholine transporter, a protein responsible for loading acetylcholine into secretory vesicles before its release as a neurotransmitter into the synapse, is also observed. Consequently, it has been suggested that the reduced expression of acetylcholinesterase may represent a cellular response to balance overall energy allocation within the cell, as the amount of acetylcholine to be synthesized, released, and subsequently catabolized is expected to be lower under the conditions of this disease.²³

1.2.4 Multiple Sclerosis

Differing from Alzheimer's and Parkinson's diseases, the pathology of multiple sclerosis is mainly characterized by demyelinating lesions along the neuron. With regards to the acetylcholinesterase enzyme, it experiences a significant and cyclic bipolar swing in activity in multiple sclerosis, seemingly trapped in an endless cycle between the relapsing phase and the remitting phase. In the relapsing phase, the expression of acetylcholinesterase increases by more than 60% on average compared to normal level, followed by a rapid increase in enzyme activity that depletes acetylcholine level. Alongside this increased enzyme activity, high levels of pro-inflammatory cytokines are observed. These cytokines can develop and cause permanent damage to the myelin sheaths surrounding the axon over time.

In the remitting phase, the expression of acetylcholinesterase and its enzyme activity decrease significantly. In some cases, a decreased activity level of both choline acetyltransferase and the vesicular acetylcholine transporter, which coincides with the rapid increase in acetylcholinesterase activity during the relapsing phase, and vice versa during the remitting phase,

is also observed. Interestingly, a decreased level of miRNA-132 is linked to the drastic increase in acetylcholinesterase activity during the relapsing phase as well.

Taken together, in addition to its overall role in modulating cholinergic neurotransmission in multiple sclerosis, these findings suggest a role in anti-inflammation that is inherent in cholinergic signaling. This implies that acetylcholinesterase may have the ability to diminish the anti-inflammatory response directed by cholinergic neurotransmission. However, the specific mechanisms by which acetylcholinesterase contributes to the worsening severity of multiple sclerosis during each cycle of relapsing and remitting, and how it gradually overwhelms and desensitizes the anti-inflammatory response of cholinergic signaling over the course of the disease, remain unclear.²³

1.3 Acetylcholinesterase Inhibitors in the Treatment of Neurodegenerative Diseases

Neurodegenerative diseases remain incurable, and most available medical treatments primarily focus on alleviating symptoms and slowing their progression for a limited time, typically through the use of acetylcholinesterase inhibitors. Currently, the acetylcholinesterase inhibitors used for therapeutic purposes are all reversible inhibitors. They are primarily employed to address symptoms related to cognitive processes such as memory, learning, and judgement. Most of these inhibitors are synthetic compounds.²⁴ Their drug potency in treating the symptoms of neurodegenerative diseases has an average IC₅₀ range, which can vary from as low as 0.02 μM to as high as 25 μM.²⁵

Regarding treatment effectiveness, most of these inhibitors can only manage mild to moderate stages of cognitive deterioration, and their modest effects typically last for a short period of time, usually confined to around two years. In addition, they often come with a range of undesirable common side effects that tend to affect the central nervous system and the digestive

system. These side effects can include headache, dizziness, low fever, seizures, as well as appetite loss, abdominal pain, vomiting, and diarrhea.²⁴ Rivastigmine, donepezil, galanthamine, and huperzine A are among the most commonly known acetylcholinesterase inhibitors.

1.3.1 Rivastigmine

Rivastigmine is a synthetic compound that inhibits acetylcholinesterase and butyrylcholinesterase (Figure 5). It is approved for alleviating symptoms in mild to moderate stages of Alzheimer's and Parkinson's diseases, and can be administered orally or transdermally. In some cases, transdermal administration of the drug has proven effective even against severe stages of these diseases, making it the more popular mode of drug administration for two primary reasons. The first reason is that it eliminates the need for patients to ingest the drug, which can be challenging even as a simple task, particularly for those who may have difficulty remembering to do so. The second reason is that it bypasses the gastrointestinal tract, leading to fewer side effects.

The drug primarily targets acetylcholinesterase to increase cholinergic signaling by reducing the level of amyloid-beta peptides, thereby improving cognitive abilities necessary for daily activities. Rivastigmine can also enhance a patient's mood by reducing sleep disturbances, anxiety, hallucinations, and the frequency of falls due to impaired mobility in Parkinson's disease. However, rivastigmine is associated with a wide range of adverse side effects, primarily related to gastrointestinal disturbances, and also includes weight loss, skin allergies, irregular heartbeat, vascular disorders, and psychiatric disorders, among others. Additionally, its effects typically last only a few years, and in some cases, as short as six months to a year, in both diseases. Furthermore, the results of rivastigmine treatment for Huntington's disease show significant discrepancies, and it offers insignificant improvements in the treatment of multiple sclerosis.²³

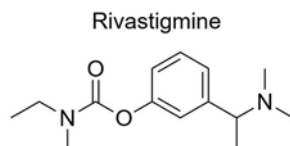


Figure 5. The Chemical Structure of Rivastigmine.

1.3.2 Donepezil

Donepezil is a synthetic inhibitor that selectively targets acetylcholinesterase (Figure 6). It shares many similarities with rivastigmine, but there are still some subtle differences between the two. Originally, donepezil is approved for alleviating symptoms of mild to severe stages of Alzheimer's disease, although in some cases, it is used to alleviate symptoms of mild to moderate stages of Parkinson's disease as well. It is administered orally, with the notable advantage being its minimal interaction and interference with the effects of other drugs when patients are undergoing multiple drug treatments simultaneously.

In addition to reducing the level of amyloid-beta peptides by targeting acetylcholinesterase, the drug may also inhibit the formation of neurofibrillary tangles resulting from the aggregation of hyperphosphorylated tau protein. This capability can lead to an improvement in cognitive abilities for both diseases. In Parkinson's disease, it may also enhance a patient's mood by mitigating depression and reducing the frequency of hallucinations. However, similar to rivastigmine, donepezil carries a significant number of side effects, including those related to gastrointestinal disturbances, which can extend to muscle cramps and insomnia. Furthermore, its effects are modest and not long-lasting. Additionally, the results of donepezil treatment show significant discrepancies when it comes to both Huntington's disease and multiple sclerosis.²³

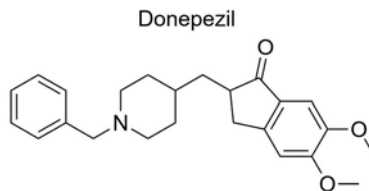


Figure 6. The Chemical Structure of Donepezil.

1.3.3 Galanthamine

Galanthamine is a natural alkaloid belonging to the *Amaryllidaceae* family that selectively inhibits acetylcholinesterase (Figure 7). Notably, its inhibition of acetylcholinesterase is 53 times stronger than that of butyrylcholinesterase. It is approved for alleviating symptoms in mild to moderate stages of Alzheimer's disease. Similar to rivastigmine, the drug enhances cognitive abilities primarily by targeting acetylcholinesterase to increase cholinergic signaling through a reduction in amyloid-beta peptides. One advantage over other acetylcholinesterase inhibitors is its extensive volume of distribution, which means it circulates throughout the entire body, increasing the likelihood of reaching the brain to exert its effects rather than being primarily confined to the bloodstream.

In addition to Alzheimer's disease, galanthamine may hold potential for the treatment of Huntington's disease. However, like most other inhibitors, it carries a significant number of side effects, including those mentioned earlier. Furthermore, its effects are modest, not long-lasting, and tend to diminish after one to one and a half years. Moreover, the results of galanthamine treatment exhibit significant discrepancies in the context of Parkinson's disease, and there is no available recorded data on its treatment effects against multiple sclerosis.²³

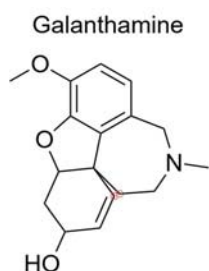


Figure 7. The Chemical Structure of Galanthamine.

1.3.4 Huperzine A

Huperzine A is a natural alkaloid derived from the *Huperzia serrata* species, which selectively inhibits acetylcholinesterase (Figure 8). It has not been registered as a drug for any neurodegenerative disease, except in China, where it has been approved for the treatment of symptoms in mild to moderate stages of Alzheimer's disease. Similar to rivastigmine, this substance appears to enhance cholinergic signaling by inhibiting acetylcholinesterase and reducing the level of amyloid-beta peptides. However, there is insufficient data to determine its side effects, and there is no available recorded data on its treatment effects against other neurodegenerative diseases.²³

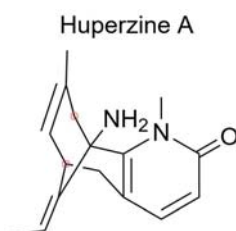


Figure 8. The Chemical Structure of Huperzine A.

1.4 The Need to Search for Novel Acetylcholinesterase Inhibitors

From the available information, it appears that despite these well-known acetylcholinesterase inhibitors targeting acetylcholinesterase, whether to hinder its interaction with

aberrant biochemical structures detrimental to cholinergic neurotransmission under disease conditions, or to suppress its overpowering catabolism of acetylcholine upon upregulation, their overall treatment effects are generally modest and not long-lasting.

One possible explanation for this is that their continuous inhibition of acetylcholinesterase activity at varying strengths over an extended period of time may lead to a gradual restriction of the activity of M1 and M2 receptors at the synapse. As a potential compensatory cellular response to prolonged acetylcholinesterase activity suppression, three subsequent events may occur as consequences: the desensitization of the M1 receptor's neuronal excitatory response to acetylcholine binding; the hypersensitization of the M2 receptor's autoinhibitory response to acetylcholine secretion into the synapse; and the excessive internalization of both receptors for intracellular degradation.

Besides the modest and short-term treatment effects, these inhibitors fail to consistently yield positive treatment results in most neurodegenerative diseases other than Alzheimer's disease. Additionally, their adverse side effects significantly impact on the central nervous system and the digestive system. Consequently, these drawbacks highlight the need to search for more effective acetylcholinesterase inhibitors capable of prolonging disease treatment while maintaining a balanced inhibition of cholinergic neurotransmission. Such inhibitors should ideally require less frequent administration. With this in mind, this study was undertaken to examine several small molecules and mushroom extracts in an effort to identify potential novel acetylcholinesterase inhibitors.

1.4.1 Small Molecules: SPOPP and NP6A

SPOPP and NP6A are dispiropiperazine derivatives synthesized from an azomethine ylide cycloaddition reaction using acenaphthenequinone and L-proline as substrates (Figure 9). The

reaction mixture is simmered under reflux in methanol for 3 h at 35°C. These chemical derivatives have been reported as excellent cell cycle checkpoint inhibitors of the G2/M phase when combined with DNA-damaging agents or radiation treatment to combat cancer. The insufficient exploration of this topic led to its selection as the focal point of research conducted by former team member Victor Liu from the Lee lab.

Previously, treatment with SPOPP was demonstrated to induce cell cycle arrest at the G2/M phase and significantly reduce cell viability through apoptosis or necrosis in various cancer cell lines, including leukemia, glioblastoma, colon cancer, cervical cancer, ovarian cancer, and breast cancer. The G2/M phase arrest was confirmed by examining the expression levels of cyclin B1, a crucial regulator of the transition from the G2 phase to the M phase, and phosphohistone H3, a biomarker signaling a disruption in this transition. Cyclin B1 level was shown to decrease, while phosphohistone H3 level increased rapidly. Furthermore, a closer examination revealed a disarray of mitotic spindle fiber formation misaligned at the cell's equator and detectable DNA damage as early as 1 h after treatment. In contrast to SPOPP, treatment with NP6A did not yield significant results.²⁶

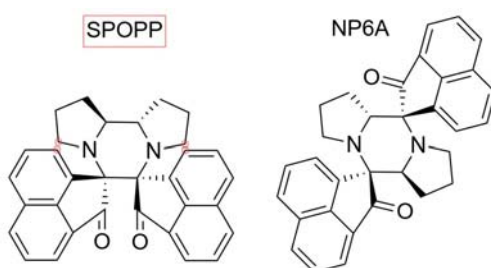


Figure 9. The Chemical Structures of SPOPP and NP6A.

1.4.2 Small Molecules: 534_1(6) and 534_2(7)

534_1(6) and 534_2(7) are dispiropyrrolizidine derivatives synthesized through a similar reaction to SPOPP and NP6A, albeit under slightly different reaction conditions (Figure 10). Simmering under reflux in either methanol or acetonitrile for as long as 1 to 48 h at a fairly hot temperature of 65°C, in addition to the initial reaction between acenaphthenequinone and L-proline, the by-products from the first reaction are further reacted with (2*E*)-2-(2-bromobenzylidene)-1-indanone to produce 534_1(6) and 534_2(7). These chemical derivatives have been reported to be bioactive molecules with a wide range of therapeutic properties, including anticancer, antioxidant, antimicrobial, antifungal, and inhibition of acetylcholinesterase activity.

Previously, former team member Lee Hooi Xian from the Lee lab conducted research focusing on screening 534_1(6) and 534_2(7) for their potential as novel inhibitors of KRAS, a crucial drug target in colorectal cancer treatment. The motivation for her research stemmed from the limited availability of effective inhibitors, with few positive treatment responses from patients using existing drugs. Experimental results showed that treatment with either 20 µM of 534_1(6) or 534_2(7) significantly downregulated the expression of KRAS by more than 50% after 48 h. However, the specific mechanisms of their suppression on KRAS expression remained tentative and required further studies.²⁷ While dispiropyrrolizidine derivatives may exhibit an inhibitory effect against acetylcholinesterase activity, 534_1(6) and 534_2(7) have not been reported to show any inhibition of acetylcholinesterase activity.

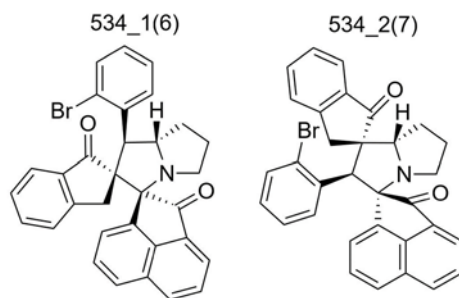


Figure 10. The Chemical Structures of 534_1(6) and 534_2(7).

1.4.3 MolTarPred Program

Using a web-based ligand-centric computational program for small molecule target prediction called MolTarPred, SPOPP and NP6A were predicted to bind to acetylcholinesterase. In simple terms, the MolTarPred program comprises a large database containing numerous small molecules, each known to bind to at least one protein target. When a new small molecule is entered into the program, the program compares structural similarities between the new input and the small molecules in the database to search for potential matches. When a match is found, the program predicts the binding affinities of the new input for protein targets already known to be bound by the matched small molecule in the database. Subsequently, based on the structural similarities between the new input and the matched small molecule, and the known binding affinities between the protein targets and the matched small molecule, the binding affinities between the newly input small molecule and the protein targets are ranked by numbers, with 1 being the least reliable and 10 being the most reliable. These rankings are then considered predictions, or in mathematical terms, probabilities.

According to the program, acetylcholinesterase was identified as the number one protein target predicted to be bound by both SPOPP and NP6A, from a list of several potential protein targets. The ranking for SPOPP and acetylcholinesterase was 7, while that for NP6A was 4. Later on, former team member from the Lee lab of the University of Northern British Columbia Lee

Hooi Xian discovered 534_1(6) and 534_2(7) possessing molecular structures similar to SPOPP and NP6A. In this Master's thesis, an evaluation of these four small molecules for their potential ability to inhibit acetylcholinesterase activity was described.

1.5 Mushrooms as a Potential Source of Acetylcholinesterase Inhibitors

In addition to small molecules, there are also several acetylcholinesterase inhibitors derived from natural sources. Mushrooms, in particular, stand out as a unique natural resource with numerous latent therapeutic applications yet to be fully explored. Globally, there are an estimated three to six million mushroom species, but only 3% to 8% of them are accurately classified. Among these, just over twenty-five are considered edible, and only a few are cultivated, mass-produced, and consumed worldwide. Needless to say, those with significant therapeutic applications are scarce, even more so in the context of neurodegenerative diseases.²⁸

For those with specific therapeutic applications in neurodegenerative diseases, there are only a handful of them. The two most commonly mentioned are *Hericiium erinaceus* and *Volvariella volvacea*. *Hericiium erinaceus* possesses anti-aging and anti-dementia properties, and its neuroprotective effects can support the biosynthesis of nerve growth factors. It is often used to prevent common neurodegenerative diseases like Alzheimer's and Parkinson's diseases. *Volvariella volvacea* has a high antioxidant effect and can help regulate excessive neuron excitation throughout the nervous system. It is often used to prevent cardiovascular and neurodegenerative diseases.

In addition to these two, there are less common mushroom species like *Flammulina velutipes* and *Phellinus gilvus*. *Flammulina velutipes* is often used to reduce cholesterol level in the human body, lower pro-inflammation in the event of a food allergy, and act as a preservative to protect meat and seafood from oxidation. It primarily exhibits anticancer effects, although its

inhibitory effect on acetylcholinesterase activity is also noted. *Phellinus gilvus* is commonly used to treat inflammation, stomachache, and tumors. It primarily offers anticancer and anti-inflammation effects, with some mention of neuroprotective effects for this species.²⁹

While not many mushroom species are directly applied for therapeutic use, numerous experiments are being conducted on different cell lines to explore their medicinal properties for potential therapeutic applications in neurodegenerative diseases (Table 1). However, the scope of these experiments is largely limited to the examination of the pathogenesis of Alzheimer's and Parkinson's diseases.³⁰ Regarding the inhibition of acetylcholinesterase activity, there are also many mushroom species being studied, but a comprehensive understanding of the extent to which they inhibit acetylcholinesterase activity remains mostly incomplete (Table 2).^{31 32 33 34 35 36 37 38 39}

40 41

Medicinal Property	Mushroom Species	Type of Neurodegenerative Disease
Anti-amyloidogenesis	<i>Pleurotus ostreatus</i>	Alzheimer's Disease
Anti-apoptosis	<i>Amauroderma rugosum</i>	Neurotoxicity
	<i>Armillaria mellea</i>	Alzheimer's Disease
	<i>Morchella importuna</i>	Neurodegenerative Diseases
	<i>Pleurotus eryngii</i>	Aging
	<i>Tremella fuciformis</i>	Neurodegenerative Diseases
Anti-cholinergic signaling	<i>Amanita caesarea</i>	Alzheimer's Disease
	<i>Armillaria mellea</i>	Alzheimer's Disease
	<i>Flammulina velutipes</i>	Cognitive Impairment
	<i>Hericium erinaceus</i>	Alzheimer's Disease
Anti-neuroinflammation	<i>Amanita caesarea</i>	Alzheimer's Disease
	<i>Antrodia camphorata</i>	Parkinson's Disease
	<i>Ganoderma lucidum</i>	Alzheimer's Disease
Anti-neurotoxicity	<i>Hericium erinaceus</i>	Alzheimer's Disease
Antioxidant	<i>Amanita caesarea</i>	Alzheimer's Disease
	<i>Auricularia auricula-judae</i>	Aging
	<i>Cantharellus cibarius</i>	Neurodegenerative Diseases
	<i>Dictyophora indusiata</i>	Neurodegenerative Diseases
	<i>Flammulina velutipes</i>	Alzheimer's Disease
	<i>Ganoderma atrum</i>	Aging
	<i>Ganoderma lucidum</i>	Alzheimer's Disease
	<i>Inonotus obliquus</i>	Alzheimer's Disease
	<i>Pleurotus ostreatus</i>	Alzheimer's Disease
	<i>Tricholoma lobayense</i>	Aging

Table 1. List of Example Mushroom Species Conducted in the Research of Neurodegeneration.

These mushroom species are known examples that are being experimented on different cell lines in the research of neurodegeneration. Some have multiple medicinal properties, but most are limited against Alzheimer's and Parkinson's diseases.³⁰

Mushroom Species	Extract	IC₅₀ (mg/mL)	Concentration Range (mg/mL)
<i>Agaricus bisporus</i>	Ethyl Acetate	2.27700	N/A
<i>Agaricus bitorquis</i>	Ethyl Acetate	0.74500	N/A
<i>Agaricus essettei</i>	Ethyl Acetate	0.91800	N/A
<i>Amanita strobiliformis</i>	Hot Water	0.00727	N/A
<i>Ganoderma adpersum</i>	Hot Water	10.56% inhibition at 0.20000 mg/mL	N/A
<i>Ganoderma applanatum</i>	Hot Water	11.87% inhibition at 0.20000 mg/mL	N/A
<i>Ganoderma lucidium</i>	Hot Water	1.01000	0.060 - 2.000
<i>Ganoderma mediosinense</i>	70% Methanol	43.86000	N/A
<i>Ganoderma mediosinense</i>	Ethyl Acetate	0.81000	N/A
<i>Ganoderma ramosissimum</i>	70% Methanol	58.24000	N/A
<i>Hericium novae-zealandiae</i>	Water	8.00000 - 8.70000	3.000 - 32.000
<i>Inonotus obliquus</i>	80% Methanol	N/A	N/A
<i>Phellinus igniarius</i>	Hot Water	21.14% inhibition at 0.20000 mg/mL	N/A
<i>Phellinus pini</i>	Hot Water	29.32% inhibition at 0.20000 mg/mL	N/A
<i>Pleurotus florida</i>	Hydromethanol	59.13000	N/A
<i>Pleurotus ostreatus</i>	Methanol	13.00% inhibition at 0.20000 mg/mL	0.025 - 0.200
<i>Pleurotus ostreatus</i>	Hot Water	8.62% inhibition at 0.20000 mg/mL	N/A
<i>Pleurotus pulmonarius</i>	80% Methanol	68.60% inhibition at 0.50000 mg/mL	0.063 - 1.000

Table 2. List of Example Mushroom Species Reported for *In Vitro* Inhibition of Acetylcholinesterase Activity.

These mushroom species are known examples that can inhibit the *in vitro* acetylcholinesterase activity. However, the extent to which they inhibit acetylcholinesterase activity remains mostly incomplete. The highlighted species were a part of those examined for their inhibitory effect on acetylcholinesterase activity in this study.^{31 32 33 34 35 36 37 38 39 40 41}

Therefore, there is a need to further establish, explore, and identify mushroom species that can be beneficial for the treatment of not only common neurodegenerative diseases, but also less common ones. As a result, the second research objective turned to the examination of extracts from eight mushroom species for their potential inhibitory effect on acetylcholinesterase activity. Since

there is a lack of comprehensive data on the full concentration range of inhibition on acetylcholinesterase activity and the IC₅₀ value across various studies for a few of the mushroom species listed in Table 2, the following species were chosen for re-examination to determine whether their potential inhibitory effect on acetylcholinesterase activity could be replicated: *Ganoderma applanatum*, *Inonotus obliquus*, *Phellinus igniarius*, *Phellinus pini*, and *Pleurotus ostreatus*. Additionally, three more species were included in the study, each of which has never been reported to exhibit any inhibitory effect on acetylcholinesterase activity. These species were *Agaricus subrufescens*, *Amanita muscaria*, and *Hericium erinaceus*.

With the exception of *Agaricus subrufescens*, each of these eight mushroom species has either been reported for inhibition against acetylcholinesterase activity; has not been reported for such inhibition but has been reported for inhibition against other targets of neurodegeneration; or has other species from the same genus reported for inhibition against acetylcholinesterase activity and/or inhibition against other targets of neurodegeneration. Therefore, given the significant overlap of medicinal properties within species and across species of the same genus, it was hypothesized that there is a high chance that each of the eight species may potentially contain at least one extract that can exert significant inhibition on acetylcholinesterase activity.

1.6 Research Objectives

The goals of this study were to test the following hypotheses:

- I. The four small molecules SPOPP, NP6A, 534_1(6), and 534_2(7) have an inhibitory effect against acetylcholinesterase activity.
- II. The extracts from the selected eight mushroom species collected from the forests in Northern British Columbia have an inhibitory effect against acetylcholinesterase activity.

Chapter 2

Development of the Acetylcholinesterase Assay and Examination of the Effect of Small Molecules on Acetylcholinesterase Activity

2.1 Introduction

2.1.1 Overview of the Acetylcholinesterase Assay Design

To assess the inhibitory effect of small molecules or mushroom extracts on acetylcholinesterase, an enzyme assay using Ellman's reagent 5,5'-dithiobis-2-nitrobenzoic acid (DTNB) was employed. This assay involved five key components: sodium phosphate buffer, *Electrophorus electricus* (South American electric eel) acetylcholinesterase, acetylthiocholine iodide, the test sample (either a small molecule or mushroom extract), and DTNB.

In theory to how this assay works, acetylcholinesterase initially hydrolyzes acetylthiocholine into acetic acid and thiocholine. Thiocholine, acting as a reducing agent, then reduces DTNB into 2-nitro-5-thiobenzoic acid, abbreviated as TNB^{2-} , by breaking the disulfide linkage of DTNB (Figure 11).⁴² The presence of TNB^{2-} results in a yellow coloration, which its absorbance can be measured at the wavelength of 412 nm. The intensity of the yellow color, and therefore the absorbance, is directly proportional to the amount of TNB^{2-} .

preferred subject of research due to its significant role in medical science as an antioxidant and anticancer agent. While there are alternative reagents and methods for thiol quantification, such as para-chloromercuribenzoic acid, ethylmaleimide, nitrobenzo-2-oxa-1,3-diazole, pyridine disulfide, and the use of papain reactivation, DTNB remained the most suitable choice for this study's enzyme assay design.⁴³ The specific reasons for the disadvantages of substituting DTNB with these reagents for thiol quantification were explained in the following paragraphs.

Para-chloromercuribenzoic acid, abbreviated as pCMB, is used to react with thiols, producing a product with its absorbance measured at the wavelength of 255 nm. However, the product is not colorimetric, and its absorbance falls within the UV range of 100 to 400 nm, which can also be absorbed by non-thiols. Additionally, pCMB can have non-specific reactions with some non-thiols. Furthermore, UV detection requires experimental tools made of quartz, which are more expensive than common materials like glass and plastic.⁴³

As for pyridine disulfide, it reacts with thiols to generate an acidic form that quickly rearranges into a ketone form called thiopyridone, with the absorbance of thiopyridone measured in the range from 324 nm to 343 nm. Similar to the product of pCMB, the issues associated with relying on UV detection are as explained. Additionally, aside from the irreversible nature of the reaction, pyridine disulfide is poorly soluble in neutral and basic solutions,⁴³ which are crucial conditions for the optimal performance of the acetylcholinesterase assay. Moreover, it is capable of permeating through biological membranes.⁴⁴

Unlike pCMB and pyridine disulfide, the disadvantages of using ethylmaleimide, nitrobenzo-2-oxa-1,3-diazole, or papain reactivation are more related to their performance efficiency than design compatibility. Ethylmaleimide is used to react with thiols, initiating a reaction in which its absorbance is measured as it decreases, at the wavelength of 300 nm.⁴³ Apart

from the issues associated with relying on UV detection, the approach, while appropriate, may seem counterintuitive, as it involves visualizing increasing enzyme activity corresponding to diminishing color.

Nitrobenzo-2-oxa-1,3-diazole, abbreviated as NBD, is used to react with thiols to generate a covalent product, with the absorbance of the product measured at the wavelength of 425 nm. However, achieving sufficient colorimetric detection of the covalent product requires a thiol to NBD ratio of 1:10, in contrast to a thiol to DTNB ratio of 1:1 needed to achieve the same visual effect.⁴³ This significant difference in the ratio leads to considerably higher costs.

Papain reactivation relies on the inactivation of a cysteine hydrolase by methyl methanethiosulfonate, followed by its reactivation upon exposure to thiols. When subjected to its substrate n-benzoyl-L-arginine-p-nitroanilide, the reaction generates a product with its absorbance measured at the wavelength of 410 nm. Although the product is 100 times more sensitive than DTNB for the same initial amount of thiols, the maximum amount of thiols that can be quantified through papain reactivation is 100 times less than with DTNB.⁴³ In the specific assay design of this study, DTNB has none of the disadvantages mentioned above in a relative comparison among all the thiol quantifiers discussed so far. Therefore, as the most suitable option by far, it was the only appropriate thiol quantifier for this study.

Acetylthiocholine Iodide as an Alternative Substrate of Acetylcholinesterase

To facilitate the efficient reduction of DTNB, acetylthiocholine iodide was chosen as the substrate of acetylcholinesterase, replacing the enzyme's natural substrate acetylcholine. The primary objective was to produce a product that contains a free thiol group for the ready reduction of DTNB. During the hydrolysis by acetylcholinesterase, acetylthiocholine is enzymatically

cleaved into acetic acid and thiocholine, whereas acetylcholine is cleaved into acetic acid and choline. Thiocholine contains a free thiol group, while choline does not (Figure 11).

***Electrophorus electricus* Acetylcholinesterase as an Economical Orthologue**

Prevalent in Fundamental Research Studies

The selected orthologue of acetylcholinesterase was *Electrophorus electricus* (South American electric eel), instead of *Homo sapiens* (human). In a cross-species genetic comparative study involving *Homo sapiens* (human), *Mus musculus* (house mouse), *Rattus norvegicus* (brown rat), *Felis silvestris catus* (cat), *Oryctolagus cuniculus* (European rabbit), *Bos taurus* (cow), *Torpedo californica* (Pacific electric ray), and *Drosophila melanogaster* (common fruit fly), the amino acid sequence of the primary structure of acetylcholinesterase showed a percentage identity of 80.13% among mammals, which decreased to 56.14% when *Torpedo californica* was included and further decreased to 27.68% when *Drosophila melanogaster* was included. However, the amino acid sequence of the active site of the enzyme exhibited a 100.00% identity among mammals, which decreased to 92.00% when *Torpedo californica* was included and further decreased to 76.00% when *Drosophila melanogaster* was included. Despite the significant differences in the overall amino acid sequence of the enzyme, the active site's amino acid sequence remained highly conserved across species. It was suggested that this conservation may result in a highly similar tertiary structural fold of the enzyme among species. This, along with the conservation of the active site, imply that the enzyme's functionality is likely highly conserved across species.⁴⁵

Although *Electrophorus electricus* was not part of the comparative analysis, it was also expected to be functionally conserved when compared to other species. According to other scientific studies, the amino acid sequence of acetylcholinesterase showed a percentage identity of

50% between the *Electrophorus electricus* and the mammalian orthologues. As for the percentage identity of the amino acid sequence of the enzyme's active site, it was reported to be 83% between these orthologues.^{59 60} Taken together, these two percentage identity values were reported similarly to the ones mentioned above for the *Torpedo californica* orthologue, matching the given expectation since both are electric fish species. Nevertheless, in theory, if acetylcholinesterase activity is 100% functionally conserved across species, its binding affinity for a ligand should also be very similar among different orthologues. This means that a small molecule inhibitor, acting as a ligand, is expected to exhibit a very similar degree of inhibition on acetylcholinesterase from different species.

In support of the aforementioned cross-species comparative study of the amino acid sequence of acetylcholinesterase, another study cross-examined the effect of eight different known inhibitors on *Electrophorus electricus* and *Homo sapiens* acetylcholinesterase. Considering the negligible difference in the baseline activity of *Homo sapiens* acetylcholinesterase attributed to biological sex and age factors from human blood donors, the study found that the variation in acetylcholinesterase activity between species in the presence of each known inhibitor was modest and primarily a result of the distinct chemical properties of the inhibitors. The research revealed that *Electrophorus electricus* acetylcholinesterase was more sensitive to inhibitors of oxon metabolites, whereas *Homo sapiens* acetylcholinesterase was more sensitive to carbamate inhibitors.⁴⁶ For instance, when tested on *Electrophorus electricus* acetylcholinesterase, the IC₅₀ values for oxon metabolites chlorpyrifos-oxon (CPO), phosmet-oxon (PMO), and diazinon-oxon (DZO) were 0.027 μM, 0.070 μM, and 1.030 μM, respectively. In contrast, the IC₅₀ values for carbamates pirimicarb (PI) and rivastigmine (RI) were 61 μM and 53 μM, respectively.⁴⁶ When tested on *Homo sapiens* acetylcholinesterase, the average IC₅₀ values for oxon metabolites CPO,

PMO, and DZO were $0.300 \pm 0.100 \mu\text{M}$, $1.900 \pm 1.100 \mu\text{M}$, and $2.500 \pm 0.800 \mu\text{M}$, respectively, while the average IC_{50} values for carbamates PI and RI were $20.000 \pm 4.300 \mu\text{M}$ and $9.900 \pm 3.100 \mu\text{M}$, respectively. These results highlighted that the interspecies conservation of acetylcholinesterase activity in response to binding a ligand is rigorous, though not entirely perfect.

The findings are consistent with those of the aforementioned cross-species comparative study of the amino acid sequence of acetylcholinesterase. They collectively reflect the overarching reality that finding or synthesizing a species-specific acetylcholinesterase inhibitor, whether naturally or artificially, appears to be exceedingly challenging. One plausible explanation for the minor difference in acetylcholinesterase activity across species in the presence of each known inhibitor could be due to minor variations in the spatial arrangement of the active site in the acetylcholinesterase orthologues.⁴⁶

In conclusion, although the choice of an acetylcholinesterase orthologue for use in the enzyme assay design of this study may not seem essential, significant cost difference exists among the orthologues available on the market. For example, an amount of *Electrophorus electricus* acetylcholinesterase that is 100 times greater than the amount of *Homo sapiens* acetylcholinesterase can be purchased for a similar price according to Sigma Aldrich. Therefore, opting for *Electrophorus electricus* acetylcholinesterase appears to be the more financially reasonable choice.

Sodium Phosphate Buffer as a Nurturing Cocktail for an Efficient Functionality of Acetylcholinesterase

Finally, the choice of buffer in this study was 0.1 M of sodium phosphate buffer at pH 8.0. Several critical reasons underpinned the selection of pH 8.0. First, it minimizes the protonation of TNB^{2-} , as the bright shade of yellow is a reflection of TNB^{2-} in its ionized state. The pK_a of TNB^{2-}

is 4.53, and at pH 5.53, 6.53, and 7.53, the percentage of ionized TNB²⁻ was reported to increase from 50% to 91% and then greater than 99%, respectively.⁴³ Secondly, the pH 8.0 was chosen to keep the thiocholine, produced from the hydrolysis of acetylthiocholine by acetylcholinesterase, in its deprotonated form. This maintains the single negative charge of its free thiol group, allowing it to readily attack and break up the disulfide linkage of DTNB. Thirdly, the pH 8.0 falls within the optimal range of *Electrophorus electricus* acetylcholinesterase activity, which ranges from pH 8.0 to 9.5.⁴⁷

Regarding the concentration, 0.1 M was selected to provide the buffer with moderate ionic strength. Excessive ionic strength on either end of the spectrum could lead to adverse consequences for assay performance. Very high ionic strength may impede the π -cation interaction between the positively charged nitrogen atom of acetylthiocholine and the electron-rich aromatic rings of the side chain of multiple tryptophan residues situated within the peripheral anionic site of acetylcholinesterase. This obstruction would hinder the efficient catabolism of the substrate by the enzyme. Conversely, excessively low ionic strength may result in the aggregation of the side chains of charged residues within the enzyme, potentially leading to denaturation of the enzyme.

2.2 Materials and Methods

2.2.1 Preparation of the Main Components of the Acetylcholinesterase Assay – Stock

Solutions

20.2 mM of DTNB

DTNB in powder form was accurately weighed at 0.0500 g on a small piece of weighing paper that had been folded into a triangular shape and placed on an analytical balance. Once weighed, the powder was carefully transferred to a 13-mL round-bottom polypropylene test tube. This was accomplished by positioning the pointed end of the weighing paper against the tube, and

gently pouring the powder into it. To ensure that every speck of powder was collected, the weighing paper was rinsed with a small amount of 100% ethanol, with all the washings directed into the same tube.

Following this, the tube was gradually filled with 100% ethanol until it reached a total volume of 6.25 mL. This was done using a 10-mL pipette attached to a pipette gun. Once filled, the DTNB solution in the tube was gently mixed by pipetting the contents back and forth, using the same 10-mL pipette attached to the pipette gun. Subsequently, the solution was divided into seven equal portions, each comprising approximately 850 μ L. All seven portions were then separately transferred into seven 1.5-mL microcentrifuge tubes using 1000- μ L pipette tips attached to a 1000- μ L pipettor.

Finally, each of the seven 1.5-mL microcentrifuge tubes was wrapped in aluminum foil to protect the DTNB solution from exposure to light and stored in a -20°C freezer. The procedure was conducted in a dark room with limited external light penetration due to DTNB's sensitivity to light, starting from the moment when the DTNB powder was transferred to the 13-mL round-bottom polypropylene test tube.

346 mM of Acetylthiocholine Iodide

Acetylthiocholine iodide in powder form was accurately weighed at 0.1000 g on a small piece of weighing paper that had been folded into a triangular shape and placed on an analytical balance. Once weighed, the powder was carefully transferred to a 13-mL round-bottom polypropylene test tube. This was accomplished by positioning the pointed end of the weighing paper against the tube, and gently pouring the powder into it. To ensure that every speck of powder was collected, the weighing paper was rinsed with a small amount of 0.1 M of sodium phosphate buffer at pH 8.0, with all the washings directed into the same tube.

Following this, the tube was gradually filled with 0.1 M of sodium phosphate buffer at pH 8.0 until it reached a total volume of 1000 μ L. This was done using a 1000- μ L pipette tip attached to a 1000- μ L pipettor. Once filled, the acetylthiocholine iodide solution in the tube was gently mixed by pipetting the contents back and forth, using the same 1000- μ L pipette tip attached to the 1000- μ L pipettor. Subsequently, the solution was divided into five equal portions, each comprising approximately 200 μ L. All five portions were then separately transferred into five 1.5-mL microcentrifuge tubes using 200- μ L pipette tips attached to a 200- μ L pipettor. Finally, all five 1.5-mL microcentrifuge tubes were stored in the -20°C freezer.

125 units/mL of Acetylcholinesterase

Tris-HCl buffer at pH 7.4 with a volume of 200 μ L at 1.0 M concentration was carefully transferred to a 13-mL round-bottom polypropylene test tube. This was done using a 200- μ L pipette tip attached to the 200- μ L pipettor. Following this, the tube was gradually filled with autoclaved water until it reached a total volume of 10.00 mL. This was done using a 10-mL pipette attached to the pipette gun. This diluted the concentration of the buffer to 20 mM.

Once filled, 2.30 mL of the buffer at 20 mM was carefully transferred to a small glass bottle containing *Electrophorus electricus* acetylcholinesterase in powder form. This was done using a 5-mL pipette attached to the pipette gun. The enzyme solution in the glass bottle was gently mixed by pipetting the contents back and forth, using a 1000- μ L pipette tip attached to the 1000- μ L pipettor. Once mixed, the enzyme solution was carefully transferred back to a new 13-mL round-bottom polypropylene test tube. This was done using 1000- μ L pipette tips attached to the 1000- μ L pipettor. Subsequently, the solution was divided into twenty-three equal portions, each comprising approximately 100 μ L. All twenty-three portions were then separately transferred into twenty-

three 1.5-mL microcentrifuge tubes using 200- μ L pipette tips attached to the 200- μ L pipettor. Finally, all twenty-three 1.5-mL microcentrifuge tubes were stored in the -20°C freezer.

0.1 M of Sodium Phosphate Buffer at pH 8.0

Sodium dihydrogen phosphate in powder form was accurately weighed at 13.80 g on a large weighing boat that had been placed on a top loading balance. Once weighed, the powder was carefully transferred to a 250-mL Erlenmeyer flask. This was accomplished by positioning the pointed end of the weighing boat against the flask, and gently pouring the powder into it. To ensure that every speck of powder was collected, the weighing boat was rinsed with a small amount of autoclaved water, with all the washings directed into the same flask. The same process was done for 14.20 g of sodium hydrogen phosphate in powder form in another separate 250-mL Erlenmeyer flask.

Following this, each flask was gradually filled with autoclaved water until it reached a total volume of 80.0 mL. This was done using a 100-mL graduated cylinder to measure and transfer the water. Once filled, both flasks were gently swirled by hand, with swift yet rhythmic movements, to ensure thorough mixing of the contents. Subsequently, both phosphate solutions were individually transferred back to two clean 100-mL graduated cylinders from their respective flasks. In the graduated cylinders, both solutions were gradually filled with autoclaved water again, until they reached a total volume of 100.0 mL. This was done using a long glass Pasteur pipette.

After that, 6.80 mL of the sodium dihydrogen phosphate solution and 93.20 mL of the sodium hydrogen phosphate solution were transferred together to a 1000-mL glass bottle. This was done using a 10-mL pipette and a 25-mL pipette attached to the pipette gun, respectively. This created the sodium phosphate buffer with a concentration of 1.0 M at pH 8.0. Then, the bottle was gradually filled with autoclaved water again, until it reached a total volume of 1000 mL. This was

done using a 1000-mL graduated cylinder to measure and transfer the water. This diluted the concentration of the buffer to 0.1 M. Finally, the 1000-mL glass bottle was stored on the lab bench at room temperature.

2.2.2 Preparation of the Main Components of the Acetylcholinesterase Assay – Standard Solutions

10 mM of DTNB

DTNB with a volume of 500 μL at 20.2 mM concentration was carefully transferred to a 1.5-mL microcentrifuge tube. This was done using a 1000- μL pipette tip attached to the 1000- μL pipettor. Following this, the tube was gradually filled with 100% ethanol until it reached a total volume of 1000 μL . This was done using another 1000- μL pipette tip attached to the 1000- μL pipettor. Once filled, the DTNB solution in the tube was gently mixed by pipetting the contents back and forth, using the same 1000- μL pipette tip attached to the 1000- μL pipettor. This diluted the concentration of DTNB to 10 mM. Finally, the 1.5-mL microcentrifuge tube was wrapped in aluminum foil and stored in the -20°C freezer.

14 mM of Acetylthiocholine Iodide

Acetylthiocholine iodide with a volume of 40 μL at 346 mM concentration was carefully transferred to a 1.5-mL microcentrifuge tube. This was done using a 200- μL pipette tip attached to the 200- μL pipettor. Following this, the tube was gradually filled with 0.1 M of sodium phosphate buffer at pH 8.0 until it reached a total volume of 1000 μL . This was done using a 1000- μL pipette tip attached to the 1000- μL pipettor. Once filled, the acetylthiocholine iodide solution in the tube was gently mixed by pipetting the contents back and forth, using the same 1000- μL pipette tip attached to the 1000- μL pipettor. This diluted the concentration of acetylthiocholine iodide to 14 mM. Finally, the 1.5-mL microcentrifuge tube was stored in the -20°C freezer.

9 units/mL of Acetylcholinesterase

Acetylcholinesterase with a volume of 72 μL at 125 units/mL concentration was carefully transferred to a 1.5-mL microcentrifuge tube. This was done using a 200- μL pipette tip attached to the 200- μL pipettor. Following this, the tube was gradually filled with 20 mM of Tris-HCl buffer at pH 7.4 until it reached a total volume of 1000 μL . This was done using a 1000- μL pipette tip attached to the 1000- μL pipettor. Once filled, the enzyme solution in the tube was gently mixed by pipetting the contents back and forth, using the same 1000- μL pipette tip attached to the 1000- μL pipettor. This diluted the concentration of acetylcholinesterase to 9 units/mL. Finally, the 1.5-mL microcentrifuge tube was stored in the -20°C freezer.

4.5 units/mL of Acetylcholinesterase

Acetylcholinesterase with a volume of 50 μL at 9 units/mL concentration was carefully transferred to a 1.5-mL microcentrifuge tube. This was done using a 200- μL pipette tip attached to the 200- μL pipettor. Following this, the tube was gradually filled with 20 mM of Tris-HCl buffer at pH 7.4 until it reached a total volume of 100 μL . This was done using another 200- μL pipette tip attached to the 200- μL pipettor. Once filled, the enzyme solution in the tube was gently mixed by pipetting the contents back and forth, using the same 200- μL pipette tip attached to the 200- μL pipettor. This diluted the concentration of acetylcholinesterase to 4.5 units/mL. Finally, the 1.5-mL microcentrifuge tube was stored in the -20°C freezer.

0.9 units/mL of Acetylcholinesterase

Acetylcholinesterase with a volume of 20 μL at 9 units/mL concentration was carefully transferred to a 1.5-mL microcentrifuge tube. This was done using a 200- μL pipette tip attached to the 200- μL pipettor. Following this, the tube was gradually filled with 20 mM of Tris-HCl buffer at pH 7.4 until it reached a total volume of 200 μL . This was done using another 200- μL pipette

tip attached to the 200- μ L pipettor. Once filled, the enzyme solution in the tube was gently mixed by pipetting the contents back and forth, using the same 200- μ L pipette tip attached to the 200- μ L pipettor. This diluted the concentration of acetylcholinesterase to 0.9 units/mL. Finally, the 1.5-mL microcentrifuge tube was stored in the -20°C freezer.

0.09 units/mL of Acetylcholinesterase

Acetylcholinesterase with a volume of 10 μ L at 0.9 units/mL concentration was carefully transferred to a 1.5-mL microcentrifuge tube. This was done using a 200- μ L pipette tip attached to the 200- μ L pipettor. Following this, the tube was gradually filled with 20 mM of Tris-HCl buffer at pH 7.4 until it reached a total volume of 100 μ L. This was done using another 200- μ L pipette tip attached to the 200- μ L pipettor. Once filled, the enzyme solution in the tube was gently mixed by pipetting the contents back and forth, using the same 200- μ L pipette tip attached to the 200- μ L pipettor. This diluted the concentration of acetylcholinesterase to 0.09 units/mL. Finally, the 1.5-mL microcentrifuge tube was stored in the -20°C freezer.

0.009 units/mL of Acetylcholinesterase

Acetylcholinesterase with a volume of 10 μ L at 0.09 units/mL concentration was carefully transferred to a 1.5-mL microcentrifuge tube. This was done using a 200- μ L pipette tip attached to the 200- μ L pipettor. Following this, the tube was gradually filled with 20 mM of Tris-HCl buffer at pH 7.4 until it reached a total volume of 100 μ L. This was done using another 200- μ L pipette tip attached to the 200- μ L pipettor. Once filled, the enzyme solution in the tube was gently mixed by pipetting the contents back and forth, using the same 200- μ L pipette tip attached to the 200- μ L pipettor. This diluted the concentration of acetylcholinesterase to 0.009 units/mL. Finally, the 1.5-mL microcentrifuge tube was stored in the -20°C freezer.

2.3 Results and Discussion

2.3.1 Testing the Performance of the Acetylcholinesterase Assay

2.3.1.1 The First Performance Test: Evaluating the Assay with Different Concentrations of Acetylcholinesterase

2.3.1.1.1 Purpose of the First Performance Test

Before the acetylcholinesterase assay could be used to experiment with the test samples, it underwent two different performance tests to assess its ability to detect potential acetylcholinesterase inhibitors. The first performance test focused on the assay's capability to generate appropriate absorbance readings with increasing concentrations of acetylcholinesterase. This test served two purposes. First, it aimed to confirm that the assay would function correctly without the addition of any test sample. Hypothetically, assuming all other factors, including time, remain constant, the change in TNB^{2-} absorbance should increase as the concentration of acetylcholinesterase increases. This is because a greater amount of enzyme leads to the production of more thiocholine, resulting in more DTNB reduction and TNB^{2-} generation, ultimately causing a larger change in absorbance over the same time span.

The second purpose was to identify one specific concentration of acetylcholinesterase that would produce a suitably steep slope representing a constant linear change in TNB^{2-} absorbance over time. This choice would simplify the detection of potential acetylcholinesterase inhibitors. By assessing the steepness of the linear slope, it becomes easier to distinguish the absorbance signal in the presence of a potential enzyme inhibitor. With a lower amount of thiocholine generated due to inhibited enzyme activity, the change in absorbance is smaller, resulting in a slower rate of increase. As a result, the slope of the constant linear change in TNB^{2-} absorbance is shallower when compared to the absence of the inhibitor.

2.3.1.1.2 Experimental Procedure of the First Performance Test

Experiments were carried out using 96-well microtiter plates. In this test, only four out of five components of the assay were included: sodium phosphate buffer, *Electrophorus electricus* acetylcholinesterase, acetylthiocholine iodide, and DTNB. On the plate, each row was divided into one control well and five different treatment wells.

In the control well, the following components were added: 180 μL of 0.1 M of sodium phosphate buffer at pH 8.0, 0 μL of acetylcholinesterase, 10 μL of 14 mM of acetylthiocholine iodide, and 10 μL of 10 mM of DTNB.

In each treatment well, the following components were added: 160 μL of 0.1 M of sodium phosphate buffer at pH 8.0, 20 μL of a specific concentration of acetylcholinesterase, 10 μL of 14 mM of acetylthiocholine iodide, and 10 μL of 10 mM of DTNB. The concentration of acetylcholinesterase was divided into five increasing concentrations ordered from least to most concentrated: 0.009, 0.09, 0.9, 4.5, and 9 units/mL of acetylcholinesterase.

There were three rows in total, each representing one technical replicate. The three technical replicates were combined to form one experimental replicate corresponding to a single run. For each experimental replicate, the change in the absorbance of TNB^{2-} was detected at the wavelength of 412 nm and recorded every 2 mins for a total of 30 mins using the Synergy 2 plate reader machine. A total of three experimental replicates were performed.

2.3.1.1.3 Raw Data Processing and Graphing Transformation of the First Performance Test

For each of the five different concentrations of acetylcholinesterase used in the treatment, the raw absorbance values were recorded every 2 mins for a total of 30 mins and then directly plotted onto a graph of absorbance against time. In cases where values were marked with an

“overflow” signal, they were automatically assigned a value of 4.000 to indicate that they had exceeded the upper limit of the plate reader machine’s detection range.

The objective was to demonstrate that the rate of TNB²⁻ absorbance increase corresponding to the level of acetylcholinesterase activity exhibited significant changes over the 30-min time span when treated with various concentrations of acetylcholinesterase. Each raw absorbance value at every time point was derived from the average of nine different raw absorbance values recorded across nine different technical replicates, corresponding to three different experimental replicates. Each absorbance value plotted on the graph was accompanied by a standard deviation value calculated from the provided raw data.

2.3.1.1.4 Hypothesis and Predicted Outcomes of the First Performance Test

According to the hypothesis, as the concentration of acetylcholinesterase increases, the rate of TNB²⁻ absorbance increase should accelerate, leading to a more significant change in absorbance. It may even reach the stationary phase of enzyme activity at a specific enzyme concentration, gradually transitioning from an initially linear trend to a logarithmic trend as saturation is achieved.

2.3.1.1.5 Observations and Analyses of the First Performance Test

In run 1, as the concentration of acetylcholinesterase increased, the rate of TNB²⁻ absorbance showed an initial slow linear increase, which gradually transitioned into a logarithmic trend, starting from 0.9 units/mL of acetylcholinesterase or higher. This pattern was consistently observed across three technical replicates.

However, the graphical representation of the rate of TNB²⁻ absorbance increase in all three technical replicates were suboptimal. The lines were neither smooth nor steady as expected, given that they should have followed proper linear or logarithmic trends. Instead, they appeared jagged,

indicating fluctuations in the absorbance readings. These fluctuations sometimes were minor, while at other times, they were significant. Notably, in a few instances, lower enzyme concentrations yielded higher absorbance readings than higher concentrations at the same time point.

After the run, it was suspected that the issue may have been related to inadequate mixing of the wells. The only mixing action during the run involved swirling the microtiter plate for a few secs after all components had been added to the wells. Additionally, many absorbance readings from time points in the second half of the 30-min time span for wells treated with 0.9 units/mL of acetylcholinesterase or higher exceeded the upper limit of the plate reader machine's detection range. Due to this, and given the similarity of their graphical data, the treatments with acetylcholinesterase concentrations of 4.5 units/mL and 9.0 units/mL were discontinued in subsequent runs. The data of the treatment with the 0.9 units/mL concentration was used to make relative comparisons instead (Table 3).

Replicate 1

	[unit/mL]	0.0	0.009	0.09	0.9	4.5	9.0
Minutes							
0		0.116	0.127	0.189	0.620	1.077	0.785
2		0.131	0.159	0.275	1.094	1.944	2.365
4		0.137	0.190	0.273	1.490	2.345	2.605
6		0.143	0.222	0.444	1.474	2.696	2.868
8		0.149	0.255	0.484	1.563	2.757	2.937
10		0.155	0.261	0.514	1.852	3.052	2.956
12		0.159	0.302	0.549	2.246	3.026	3.021
14		0.162	0.331	0.590	2.646	2.939	3.106
16		0.166	0.365	0.629	3.287	3.186	3.167
18		0.171	0.451	0.666	OVRFLW	OVRFLW	3.213
20		0.175	0.488	0.705	OVRFLW	OVRFLW	3.242
22		0.179	0.532	0.742	OVRFLW	OVRFLW	3.271
24		0.182	0.563	0.802	OVRFLW	OVRFLW	3.301
26		0.187	0.583	0.875	OVRFLW	OVRFLW	3.342
28		0.191	0.602	1.141	OVRFLW	OVRFLW	3.342
30		0.196	0.620	1.185	OVRFLW	OVRFLW	3.386



Replicate 2

	[unit/mL]	0.0	0.009	0.09	0.9	4.5	9.0
Minutes							
0		0.116	0.254	0.182	0.261	1.360	0.608
2		0.128	0.319	0.257	0.823	2.131	0.781
4		0.133	0.374	0.368	1.196	2.459	0.756
6		0.141	0.393	0.392	1.569	2.517	0.731
8		0.215	0.408	0.433	1.884	2.488	0.751
10		0.354	0.424	0.485	2.242	2.797	0.816
12		0.431	0.445	0.544	2.559	2.792	1.040
14		0.455	0.457	0.577	2.785	2.830	1.309
16		0.465	0.468	0.640	2.958	2.908	1.748
18		0.483	0.474	0.695	3.098	3.017	2.093
20		0.545	0.482	0.816	3.200	3.326	2.337
22		0.551	0.489	0.888	3.340	OVRFLW	2.221
24		0.551	0.497	0.968	3.404	OVRFLW	2.500
26		0.560	0.500	1.045	3.477	OVRFLW	3.681
28		0.566	0.513	1.113	3.554	OVRFLW	OVRFLW
30		0.573	0.518	1.182	3.648	OVRFLW	OVRFLW



Replicate 3

	[unit/mL]	0.0	0.009	0.09	0.9	4.5	9.0
Minutes							
0		0.107	0.207	0.159	0.199	0.436	0.762
2		0.118	0.314	0.196	0.923	0.881	3.461
4		0.124	0.239	0.293	1.154	1.343	3.732
6		0.129	0.213	0.357	1.681	1.896	3.486
8		0.134	0.299	0.400	2.188	2.238	OVRFLW
10		0.139	0.379	0.436	2.550	2.329	3.945
12		0.143	0.399	0.469	2.951	2.411	3.840
14		0.148	0.422	0.498	3.342	2.455	3.448
16		0.153	0.442	0.527	3.541	2.512	OVRFLW
18		0.159	0.492	0.561	OVRFLW	2.558	OVRFLW
20		0.165	0.491	0.597	OVRFLW	2.588	OVRFLW
22		0.170	0.493	0.634	OVRFLW	2.633	OVRFLW
24		0.177	0.500	0.664	OVRFLW	2.669	OVRFLW
26		0.182	0.506	0.692	OVRFLW	2.709	OVRFLW
28		0.186	0.511	0.742	OVRFLW	2.757	OVRFLW
30		0.191	0.516	0.808	OVRFLW	2.802	OVRFLW



Table 3. Evaluating the Assay with Different Concentrations of Acetylcholinesterase: The First Performance Test, Run 1.

The test aimed to assess the assay's ability to generate appropriate absorbance readings in response to increasing concentrations of acetylcholinesterase. It analyzed the rate of TNB²⁻ absorbance increase over a 30-min time span as acetylcholinesterase concentration increased. The term "OVRFLW", or "Overflow", denoted absorbance readings that exceeded the upper limit of the Synergy 2 plate reader machine's detection range and could not be measured. Black highlighted sections in the tables represented unusual data where absorbance readings resulting from treatments with lower enzyme concentrations were higher than those from treatments with higher enzyme concentrations. The lower panels of graphs depicted the changes in TNB²⁻ absorbance in response to increasing concentrations of acetylcholinesterase over the course of 30 mins. The experiment was repeated three times (n = 3).

In run 2, experimental conditions from run 1 were replicated, with one notable change: the order of the components added to the treatment wells was adjusted. In run 1, the order was as follows: 160 μ L of 0.1 M of sodium phosphate buffer at pH 8.0, 20 μ L of a specific concentration of acetylcholinesterase, 10 μ L of 10 mM of DTNB, and 10 μ L of 14 mM of acetylthiocholine

iodide. In run 2, the order was adjusted to: 20 μL of a specific concentration of acetylcholinesterase, 10 μL of 10 mM of DTNB, 160 μL of 0.1 M of sodium phosphate buffer at pH 8.0, and 10 μL of 14 mM of acetylthiocholine iodide. Unfortunately, this adjustment significantly impaired the assay's performance.

The graphical representation of the rate of TNB^{2-} absorbance increase almost entirely flattened out across most wells in the three technical replicates throughout the 30-min time span. Additionally, none of the wells displayed the characteristic bright shade of yellow associated with TNB^{2-} production. It was suspected that adding components with smaller volumes first may have caused them to dry up, especially the critical acetylcholinesterase, leading to aggregation and loss of functionality. This damage could not be reversed by adding the sodium phosphate buffer later in an attempt to rehydrate the enzyme. Reordering the components to the original sequence from run 1 in subsequent runs was necessary, at least until any further adjustments were made (Supplementary Table 1 and Supplementary Figure 1).

In run 3, experimental conditions from run 1 were replicated, but with an increased mixing time. After adding all components to the wells, the swirling time of the microtiter plate was increased to 30 secs before the plate was loaded into the plate reader machine. The results closely resembled those of run 1 for all three technical replicates, albeit with some improvement in assay performance quality.

The graphical representation of the rate of TNB^{2-} absorbance increase was smoother but still not completely consistent and steady. As such, minor fluctuations in the absorbance readings persisted. Surprisingly, the formation of crystals in some wells was noticed for the first time (Figure 12). The formation of these crystals corresponded to wells where absorbance readings exhibited minor fluctuations.

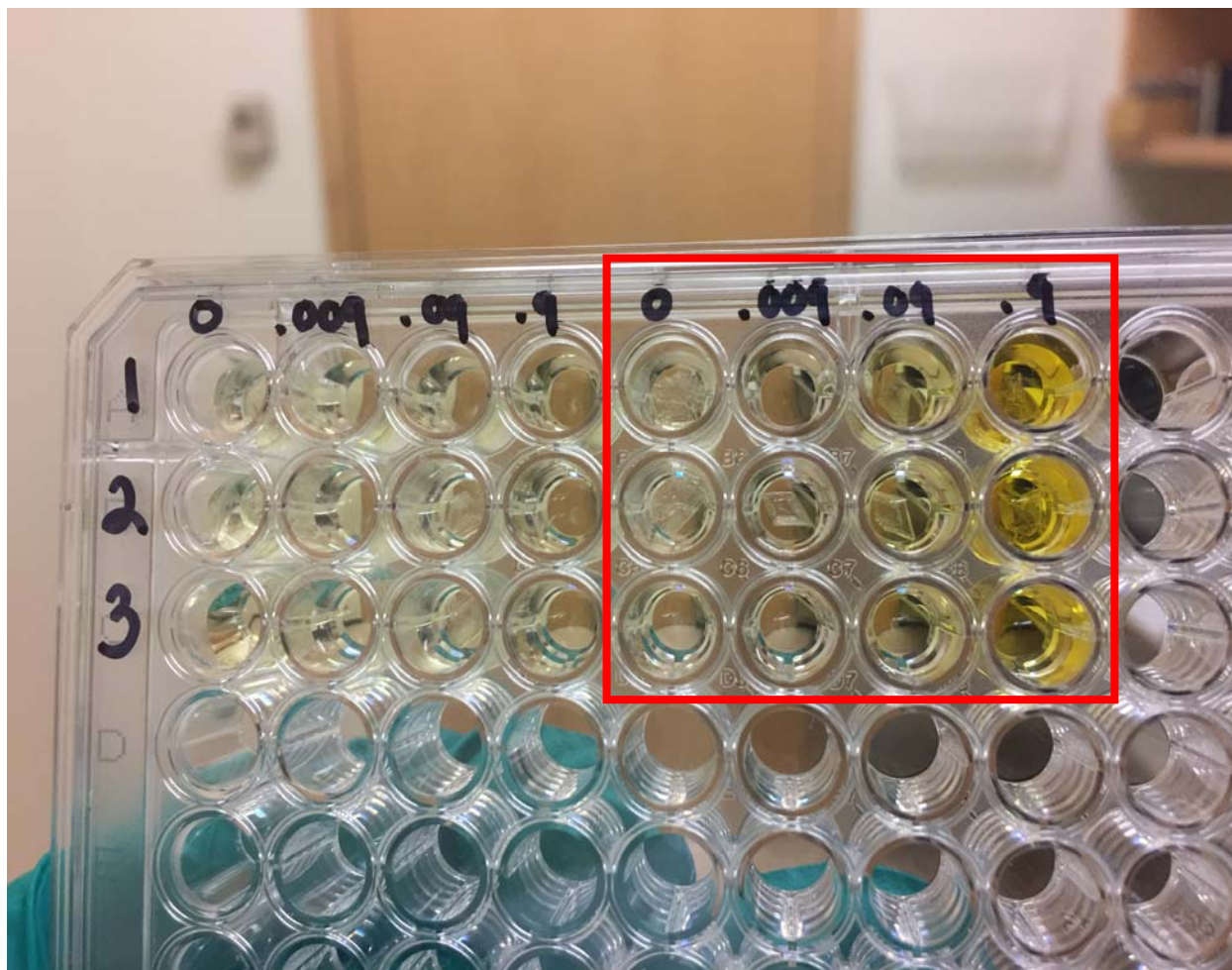


Figure 12. Evaluating the Assay with Different Concentrations of Acetylcholinesterase: The First Performance Test, Run 3.

The test aimed to assess the assay's ability to generate appropriate absorbance readings in response to increasing concentrations of acetylcholinesterase. It analyzed the rate of TNB^{2-} absorbance increase over a 30-min time span as acetylcholinesterase concentration increased. A photo of the microtiter plate (the second 4x3 set on the right within the red box) used for the run was also attached to illustrate the unexpected results. The experiment was repeated three times ($n = 3$).

After the run, it was strongly suspected that these unusual crystals were the root cause of the inconsistency in absorbance readings and the fluctuations in the graphical representation of the rate of TNB^{2-} absorbance increase. However, at the time, the exact cause of the crystal formation was uncertain. To address this, additional literature research was conducted, leading to the identification of five main possible factors contributing to the formation of these crystals: low pH,

temperature, contamination, mixing, and concentration. In the subsequent runs, these factors were either eliminated or carefully controlled to investigate whether the problem with crystallization could be resolved (Supplementary Table 2).

In run 4, experimental conditions from run 1 were replicated, with a few notable exceptions. To ensure the pH of the sodium phosphate buffer was correct, a piece of pH test strip was soaked with a few drops of the buffer. The pH was recorded to be approximately 8.0. To maintain the correct temperature of all components, they were placed in a cool area on the lab bench to slowly thaw to room temperature, avoiding reliance on the warmth of human hands. To prevent contamination, the control wells with 0 units/mL of acetylcholinesterase and the treatment wells with three different acetylcholinesterase concentrations of 0.009, 0.09, and 0.9 units/mL from all three technical replicates were arranged and separated horizontally by one column of wells based on the order of enzyme concentration.

Regarding mixing, instead of swirling the microtiter plate for 30 secs after adding all components to the wells, before the plate was loaded into the plate reader machine, the solution in each individual well was gently pipetted up and down with a small volume of approximately 10 to 20 μ L each time a component was added, until all components were included. The results closely resembled what was observed in run 3 for all three technical replicates. The most noteworthy observation was the absence of crystal formation in any wells before the plate was loaded into the plate reader machine. However, after completing the run, crystals had formed in two of twelve wells. Additionally, the wells with crystals displayed significantly higher absorbance readings and fluctuations compared to those without crystals, even among wells treated with the same enzyme concentration.

This further confirmed with high certainty that these peculiar crystals were the root cause of the inconsistency in absorbance readings and the fluctuations in the graphical representation of the rate of TNB²⁻ absorbance increase. Simultaneously, this shed light on the nature of the crystal formation. One significant finding was that the time taken for the crystals to form appeared to vary considerably. They could form immediately after all components were added to the wells before mixing, during the mixing process, or even while the microtiter plate was being processed in the plate reader machine.

Overall, while the crystallization problem persisted, the three main factors suspected to contribute to the crystal formation were eliminated in this run. Since the issue remained unresolved despite careful control and monitoring of these factors, the two remaining factors, mixing and concentration, were examined in the subsequent runs to determine if any progress towards resolution of the problem could be made (Supplementary Table 3 and Supplementary Figure 2).

In run 5, experimental conditions from run 4 were replicated, with one exception. Concerning the mixing action, instead of gently pipetting the solution up and down with a small volume of approximately 10 to 20 μL each time a component was added to each individual well, until all components were included, the solution in each individual well was gently pipetted up and down with a larger volume of 100 μL , but only after all components were added to the wells. Following this, the microtiter plate was swirled again for 30 secs before being loaded into the plate reader machine.

The results closely mirrored those observed in run 1 for all three technical replicates. However, a notable difference was the graphical representation of the rate of TNB²⁻ absorbance increase, which was smooth and consistent, following either a linear or logarithmic trend. There were no fluctuations in the graphical lines over the entire 30-min time span, and the absorbance

readings exhibited high consistency across the technical replicates. Notably, there was no crystallization at all during this run.

Initially, the mixing factor was suspected as the cause of the crystal formation (Supplementary Table 4 and Supplementary Figure 3). However, run 6 did not reproduce the results observed in run 5. Despite repeating everything exactly as in run 5, the crystallization problem resurfaced, and the results resembled those observed in runs 3 and 4. This ruled out the mixing factor as the possible cause of the crystal formation. Consequently, concentration became the sole remaining factor under scrutiny. Building on the observations from run 4 of the first performance test, another significant detail emerged in run 6 was the appearance of crystallization immediately after the addition of acetylthiocholine iodide to the wells. As such, the concentration of acetylthiocholine iodide became the primary suspect. It was examined in the subsequent runs to determine whether any resolution to the problem could be achieved. If the concentration of acetylthiocholine iodide was indeed the cause of crystallization, then the crystallization process should cease when the concentration of acetylthiocholine iodide was diluted (Supplementary Table 5 and Supplementary Figure 4).

In run 7, experimental conditions from run 5 were replicated, except for the adjustment in the added amount and concentration of acetylthiocholine iodide, which was changed from 10 μ L of 14 mM of acetylthiocholine iodide to 10 μ L of 1.4 mM of acetylthiocholine iodide. This adjustment resulted in a 10-fold dilution of the acetylthiocholine iodide concentration. The results were fairly reproducible to what was observed in run 5, with the only significant difference being that the displayed absorbance readings were much lower due to the substrate concentration being diluted (Supplementary Table 6 and Supplementary Figure 5).

Similarly, in run 8, experimental conditions from run 5 were replicated, except the adjustment in the added amount and concentration of acetylthiocholine iodide, which was changed from 10 μ L of 14 mM of acetylthiocholine iodide to 10 μ L of 7 mM of acetylthiocholine iodide. This adjustment resulted in a 2-fold dilution of the acetylthiocholine iodide concentration. Once again, the results were sufficiently reproducible to what was observed in run 5, with the only significant difference being that the displayed absorbance readings were slightly lower due to the substrate concentration being diluted. However, the absorbance readings were much higher than those in run 7.

Overall, at this point, the results from both runs 7 and 8 seemed to suggest that the concentration of acetylthiocholine iodide was the primary source of the problem leading to the crystal formation. However, it was later discovered that the concentration of the sodium phosphate buffer used had been incorrect throughout the first eight runs of the first performance test. Instead of 0.1 M, it had mistakenly been prepared as 1.0 M. Recalling back to the time during the preparation of both the stock and standard solutions of acetylthiocholine iodide, heavy precipitation quickly formed over time shortly after mixing the sodium phosphate buffer with the acetylthiocholine iodide powder. Although the precipitates had slightly different shapes, their appearance closely resembled the crystals formed during the runs.

As a result, the suspicion shifted to the sodium phosphate buffer in the following runs, and it became the focus of the examination. Assuming that the real source of the problem lied with the buffer's concentration, it was expected that the crystallization process would not recur even if 14 mM of acetylthiocholine iodide were to be reused, as long as the buffer's concentration used to dissolve it was indeed 0.1 M (Supplementary Table 7 and Supplementary Figure 6).

In run 9, experimental conditions from run 5 were replicated, with the only change being the adjustment of the sodium phosphate buffer concentration used to prepare 14 mM of acetylthiocholine iodide, which was corrected to 0.1 M. The results were almost entirely reproducible to what was observed in run 5. The only minor difference of note was that the treatment with 0.009 units/mL of acetylcholinesterase resulted in slightly lower absorbance readings across the 30-min time span compared to the treatment with 0 units/mL of acetylcholinesterase, even though the total change in absorbance over 30 mins was much greater for the treatment with 0.009 units/mL of acetylcholinesterase than for the treatment with 0 units/mL of acetylcholinesterase.

To confirm the previously incorrect concentration of sodium phosphate buffer as the real source of the crystallization problem, four more runs were performed to assess the reproducibility of run 9. The results were completely reproducible to what was observed in run 5, and even better than what was observed in run 9 for runs 11 through 13 (Tables 4-6 and Figures 13-15, respectively).

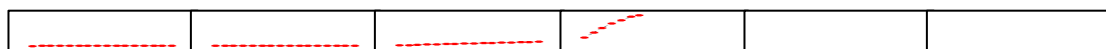
Replicate 1

	[unit/mL]	0.0	0.009	0.09	0.9	4.5	9.0
Minutes							
0		0.138	0.148	0.222	1.169	OVRFLW	OVRFLW
2		0.139	0.149	0.254	1.773	OVRFLW	OVRFLW
4		0.139	0.152	0.284	2.357	OVRFLW	OVRFLW
6		0.139	0.153	0.316	2.872	OVRFLW	OVRFLW
8		0.140	0.156	0.347	3.338	OVRFLW	OVRFLW
10		0.140	0.158	0.379	3.704	OVRFLW	OVRFLW
12		0.140	0.160	0.408	3.992	OVRFLW	OVRFLW
14		0.140	0.162	0.438	OVRFLW	OVRFLW	OVRFLW
16		0.140	0.164	0.468	OVRFLW	OVRFLW	OVRFLW
18		0.141	0.166	0.496	OVRFLW	OVRFLW	OVRFLW
20		0.141	0.167	0.524	OVRFLW	OVRFLW	OVRFLW
22		0.141	0.169	0.555	OVRFLW	OVRFLW	OVRFLW
24		0.141	0.171	0.585	OVRFLW	OVRFLW	OVRFLW
26		0.141	0.173	0.612	OVRFLW	OVRFLW	OVRFLW
28		0.143	0.175	0.641	OVRFLW	OVRFLW	OVRFLW
30		0.143	0.177	0.667	OVRFLW	OVRFLW	OVRFLW



Replicate 2

	[unit/mL]	0.0	0.009	0.09	0.9	4.5	9.0
Minutes							
0		0.128	0.139	0.208	1.192	OVRFLW	OVRFLW
2		0.133	0.141	0.241	1.817	OVRFLW	OVRFLW
4		0.134	0.143	0.274	2.423	OVRFLW	OVRFLW
6		0.134	0.145	0.308	2.981	OVRFLW	OVRFLW
8		0.135	0.147	0.340	3.403	OVRFLW	OVRFLW
10		0.136	0.150	0.371	3.848	OVRFLW	OVRFLW
12		0.136	0.152	0.403	4.012	OVRFLW	OVRFLW
14		0.136	0.155	0.434	OVRFLW	OVRFLW	OVRFLW
16		0.137	0.157	0.465	OVRFLW	OVRFLW	OVRFLW
18		0.137	0.159	0.495	OVRFLW	OVRFLW	OVRFLW
20		0.137	0.162	0.526	OVRFLW	OVRFLW	OVRFLW
22		0.138	0.164	0.556	OVRFLW	OVRFLW	OVRFLW
24		0.138	0.166	0.586	OVRFLW	OVRFLW	OVRFLW
26		0.138	0.168	0.615	OVRFLW	OVRFLW	OVRFLW
28		0.138	0.170	0.645	OVRFLW	OVRFLW	OVRFLW
30		0.139	0.172	0.677	OVRFLW	OVRFLW	OVRFLW



Replicate 3

	[unit/mL]	0.0	0.009	0.09	0.9	4.5	9.0
Minutes							
0		0.138	0.141	0.221	1.132	OVRFLW	OVRFLW
2		0.138	0.142	0.253	1.778	OVRFLW	OVRFLW
4		0.138	0.145	0.288	2.396	OVRFLW	OVRFLW
6		0.139	0.146	0.322	2.942	OVRFLW	OVRFLW
8		0.138	0.149	0.357	3.425	OVRFLW	OVRFLW
10		0.139	0.152	0.391	3.779	OVRFLW	OVRFLW
12		0.140	0.154	0.425	OVRFLW	OVRFLW	OVRFLW
14		0.141	0.156	0.458	OVRFLW	OVRFLW	OVRFLW
16		0.140	0.158	0.491	OVRFLW	OVRFLW	OVRFLW
18		0.141	0.160	0.524	OVRFLW	OVRFLW	OVRFLW
20		0.141	0.162	0.555	OVRFLW	OVRFLW	OVRFLW
22		0.143	0.164	0.585	OVRFLW	OVRFLW	OVRFLW
24		0.142	0.166	0.617	OVRFLW	OVRFLW	OVRFLW
26		0.141	0.169	0.648	OVRFLW	OVRFLW	OVRFLW
28		0.142	0.171	0.679	OVRFLW	OVRFLW	OVRFLW
30		0.143	0.172	0.708	OVRFLW	OVRFLW	OVRFLW



Table 4. Evaluating the Assay with Different Concentrations of Acetylcholinesterase: The First Performance Test, Run 11.

The test aimed to assess the assay’s ability to generate appropriate absorbance readings in response to increasing concentrations of acetylcholinesterase. It analyzed the rate of TNB²⁻ absorbance increase over a 30-min time span as acetylcholinesterase concentration increased. The term “OVRFLW”, or “Overflow”, denoted absorbance readings that exceeded the upper limit of the Synergy 2 plate reader machine’s detection range and could not be measured. The lower panels of graphs depicted the changes in TNB²⁻ absorbance in response to increasing concentrations of acetylcholinesterase over the course of 30 mins. The experiment was repeated three times (n = 3).

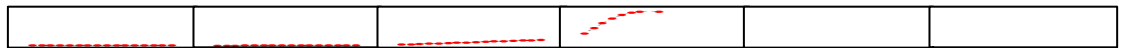


Figure 13. Evaluating the Assay with Different Concentrations of Acetylcholinesterase: The First Performance Test, Run 11.

A photo of the microtiter plate (inside the red box) used for the run was also attached to illustrate the complete reproducibility of the results obtained from run 5 when treated with the correct amount and concentration of acetylthiocholine iodide, along with the correct concentration of sodium phosphate buffer in which the acetylthiocholine iodide was dissolved. This was evident from the absence of the crystal formation in all wells, and from the consistent absorbance readings across the 30-min time span for all three technical replicates.

Replicate 1

	[unit/mL]	0.0	0.009	0.09	0.9	4.5	9.0
Minutes							
0		0.156	0.152	0.261	1.520	OVRFLW	OVRFLW
2		0.157	0.154	0.298	2.146	OVRFLW	OVRFLW
4		0.157	0.153	0.333	2.723	OVRFLW	OVRFLW
6		0.157	0.156	0.367	3.235	OVRFLW	OVRFLW
8		0.157	0.157	0.405	3.651	OVRFLW	OVRFLW
10		0.157	0.160	0.438	3.885	OVRFLW	OVRFLW
12		0.157	0.163	0.468	4.019	OVRFLW	OVRFLW
14		0.158	0.163	0.506	OVRFLW	OVRFLW	OVRFLW
16		0.157	0.164	0.548	4.029	OVRFLW	OVRFLW
18		0.157	0.167	0.587	OVRFLW	OVRFLW	OVRFLW
20		0.158	0.168	0.625	OVRFLW	OVRFLW	OVRFLW
22		0.158	0.171	0.661	OVRFLW	OVRFLW	OVRFLW
24		0.158	0.172	0.697	OVRFLW	OVRFLW	OVRFLW
26		0.158	0.174	0.730	OVRFLW	OVRFLW	OVRFLW
28		0.158	0.176	0.766	OVRFLW	OVRFLW	OVRFLW
30		0.159	0.178	0.799	OVRFLW	OVRFLW	OVRFLW



Replicate 2

	[unit/mL]	0.0	0.009	0.09	0.9	4.5	9.0
Minutes							
0		0.149	0.161	0.270	1.310	OVRFLW	OVRFLW
2		0.150	0.164	0.307	1.889	OVRFLW	OVRFLW
4		0.150	0.165	0.344	2.412	OVRFLW	OVRFLW
6		0.151	0.166	0.380	2.877	OVRFLW	OVRFLW
8		0.151	0.168	0.414	3.289	OVRFLW	OVRFLW
10		0.151	0.168	0.448	3.555	OVRFLW	OVRFLW
12		0.151	0.170	0.483	3.815	OVRFLW	OVRFLW
14		0.152	0.172	0.520	3.918	OVRFLW	OVRFLW
16		0.152	0.173	0.556	OVRFLW	OVRFLW	OVRFLW
18		0.152	0.175	0.590	OVRFLW	OVRFLW	OVRFLW
20		0.152	0.177	0.629	OVRFLW	OVRFLW	OVRFLW
22		0.152	0.178	0.650	OVRFLW	OVRFLW	OVRFLW
24		0.153	0.180	0.694	OVRFLW	OVRFLW	OVRFLW
26		0.152	0.180	0.729	OVRFLW	OVRFLW	OVRFLW
28		0.153	0.181	0.764	OVRFLW	OVRFLW	OVRFLW
30		0.153	0.184	0.805	OVRFLW	OVRFLW	OVRFLW



Replicate 3

	[unit/mL]	0.0	0.009	0.09	0.9	4.5	9.0
Minutes							
0		0.157	0.159	0.237	1.129	OVRFLW	OVRFLW
2		0.157	0.161	0.266	1.688	OVRFLW	OVRFLW
4		0.158	0.164	0.294	2.201	OVRFLW	OVRFLW
6		0.159	0.165	0.322	2.663	OVRFLW	OVRFLW
8		0.159	0.168	0.349	3.066	OVRFLW	OVRFLW
10		0.158	0.170	0.377	3.462	OVRFLW	OVRFLW
12		0.159	0.173	0.406	3.748	OVRFLW	OVRFLW
14		0.158	0.175	0.428	4.038	OVRFLW	OVRFLW
16		0.158	0.178	0.457	OVRFLW	OVRFLW	OVRFLW
18		0.159	0.180	0.475	OVRFLW	OVRFLW	OVRFLW
20		0.158	0.181	0.504	OVRFLW	OVRFLW	OVRFLW
22		0.158	0.184	0.536	OVRFLW	OVRFLW	OVRFLW
24		0.159	0.188	0.569	OVRFLW	OVRFLW	OVRFLW
26		0.154	0.186	0.608	OVRFLW	OVRFLW	OVRFLW
28		0.157	0.187	0.635	OVRFLW	OVRFLW	OVRFLW
30		0.153	0.193	0.665	OVRFLW	OVRFLW	OVRFLW



Table 5. Evaluating the Assay with Different Concentrations of Acetylcholinesterase: The First Performance Test, Run 12.

The test aimed to assess the assay’s ability to generate appropriate absorbance readings in response to increasing concentrations of acetylcholinesterase. It analyzed the rate of TNB²⁻ absorbance increase over a 30-min time span as acetylcholinesterase concentration increased. The term “OVRFLW”, or “Overflow”, denoted absorbance readings that exceeded the upper limit of the Synergy 2 plate reader machine’s detection range and could not be measured. Black highlighted sections in the tables represented unusual data where absorbance readings resulting from treatments with lower enzyme concentrations were higher than those from treatments with higher enzyme concentrations. The lower panels of graphs depicted the changes in TNB²⁻ absorbance in response to increasing concentrations of acetylcholinesterase over the course of 30 mins. The experiment was repeated three times (n = 3).



Figure 14. Evaluating the Assay with Different Concentrations of Acetylcholinesterase: The First Performance Test, Run 12.

A photo of the microtiter plate (inside the red box) used for the run was also attached to illustrate the complete reproducibility of the results obtained from run 5 when treated with the correct amount and concentration of acetylthiocholine iodide, along with the correct concentration of sodium phosphate buffer in which the acetylthiocholine iodide was dissolved. This was evident from the absence of the crystal formation in all wells, and from the consistent absorbance readings across the 30-min time span for all three technical replicates.

Replicate 1

	[unit/mL]	0.0	0.009	0.09	0.9	4.5	9.0
Minutes							
0		0.157	0.160	0.222	1.293	OVRFLW	OVRFLW
2		0.157	0.163	0.247	1.893	OVRFLW	OVRFLW
4		0.157	0.165	0.268	2.477	OVRFLW	OVRFLW
6		0.157	0.167	0.292	3.025	OVRFLW	OVRFLW
8		0.157	0.169	0.313	3.529	OVRFLW	OVRFLW
10		0.156	0.169	0.341	3.957	OVRFLW	OVRFLW
12		0.154	0.169	0.366	OVRFLW	OVRFLW	OVRFLW
14		0.157	0.173	0.392	OVRFLW	OVRFLW	OVRFLW
16		0.152	0.183	0.415	OVRFLW	OVRFLW	OVRFLW
18		0.150	0.188	0.440	OVRFLW	OVRFLW	OVRFLW
20		0.156	0.194	0.462	OVRFLW	OVRFLW	OVRFLW
22		0.159	0.198	0.486	OVRFLW	OVRFLW	OVRFLW
24		0.159	0.201	0.507	OVRFLW	OVRFLW	OVRFLW
26		0.160	0.205	0.529	OVRFLW	OVRFLW	OVRFLW
28		0.161	0.208	0.552	OVRFLW	OVRFLW	OVRFLW
30		0.162	0.212	0.575	OVRFLW	OVRFLW	OVRFLW



Replicate 2

	[unit/mL]	0.0	0.009	0.09	0.9	4.5	9.0
Minutes							
0		0.147	0.152	0.207	0.981	OVRFLW	OVRFLW
2		0.147	0.154	0.229	1.466	OVRFLW	OVRFLW
4		0.148	0.156	0.252	1.889	OVRFLW	OVRFLW
6		0.148	0.158	0.273	2.316	OVRFLW	OVRFLW
8		0.149	0.159	0.296	2.745	OVRFLW	OVRFLW
10		0.149	0.162	0.319	3.056	OVRFLW	OVRFLW
12		0.149	0.164	0.341	3.360	OVRFLW	OVRFLW
14		0.149	0.165	0.363	3.590	OVRFLW	OVRFLW
16		0.149	0.166	0.385	3.846	OVRFLW	OVRFLW
18		0.149	0.168	0.407	3.890	OVRFLW	OVRFLW
20		0.149	0.170	0.428	4.042	OVRFLW	OVRFLW
22		0.150	0.169	0.450	OVRFLW	OVRFLW	OVRFLW
24		0.149	0.171	0.469	OVRFLW	OVRFLW	OVRFLW
26		0.150	0.175	0.489	OVRFLW	OVRFLW	OVRFLW
28		0.150	0.179	0.512	OVRFLW	OVRFLW	OVRFLW
30		0.150	0.184	0.534	OVRFLW	OVRFLW	OVRFLW



Replicate 3

	[unit/mL]	0.0	0.009	0.09	0.9	4.5	9.0
Minutes							
0		0.156	0.159	0.253	1.040	OVRFLW	OVRFLW
2		0.156	0.163	0.290	1.600	OVRFLW	OVRFLW
4		0.157	0.166	0.326	2.131	OVRFLW	OVRFLW
6		0.158	0.170	0.362	2.613	OVRFLW	OVRFLW
8		0.158	0.173	0.398	3.089	OVRFLW	OVRFLW
10		0.159	0.177	0.435	3.451	OVRFLW	OVRFLW
12		0.159	0.180	0.472	3.796	OVRFLW	OVRFLW
14		0.160	0.184	0.504	OVRFLW	OVRFLW	OVRFLW
16		0.161	0.187	0.540	OVRFLW	OVRFLW	OVRFLW
18		0.162	0.191	0.580	OVRFLW	OVRFLW	OVRFLW
20		0.163	0.194	0.614	OVRFLW	OVRFLW	OVRFLW
22		0.163	0.197	0.647	OVRFLW	OVRFLW	OVRFLW
24		0.164	0.201	0.682	OVRFLW	OVRFLW	OVRFLW
26		0.164	0.203	0.717	OVRFLW	OVRFLW	OVRFLW
28		0.165	0.207	0.749	OVRFLW	OVRFLW	OVRFLW
30		0.166	0.210	0.782	OVRFLW	OVRFLW	OVRFLW



Table 6. Evaluating the Assay with Different Concentrations of Acetylcholinesterase: The First Performance Test, Run 13.

The test aimed to assess the assay’s ability to generate appropriate absorbance readings in response to increasing concentrations of acetylcholinesterase. It analyzed the rate of TNB²⁻ absorbance increase over a 30-min time span as acetylcholinesterase concentration increased. The term “OVRFLW”, or “Overflow”, denoted absorbance readings that exceeded the upper limit of the Synergy 2 plate reader machine’s detection range and could not be measured. The lower panels of graphs depicted the changes in TNB²⁻ absorbance in response to increasing concentrations of acetylcholinesterase over the course of 30 mins. The experiment was repeated three times (n = 3).

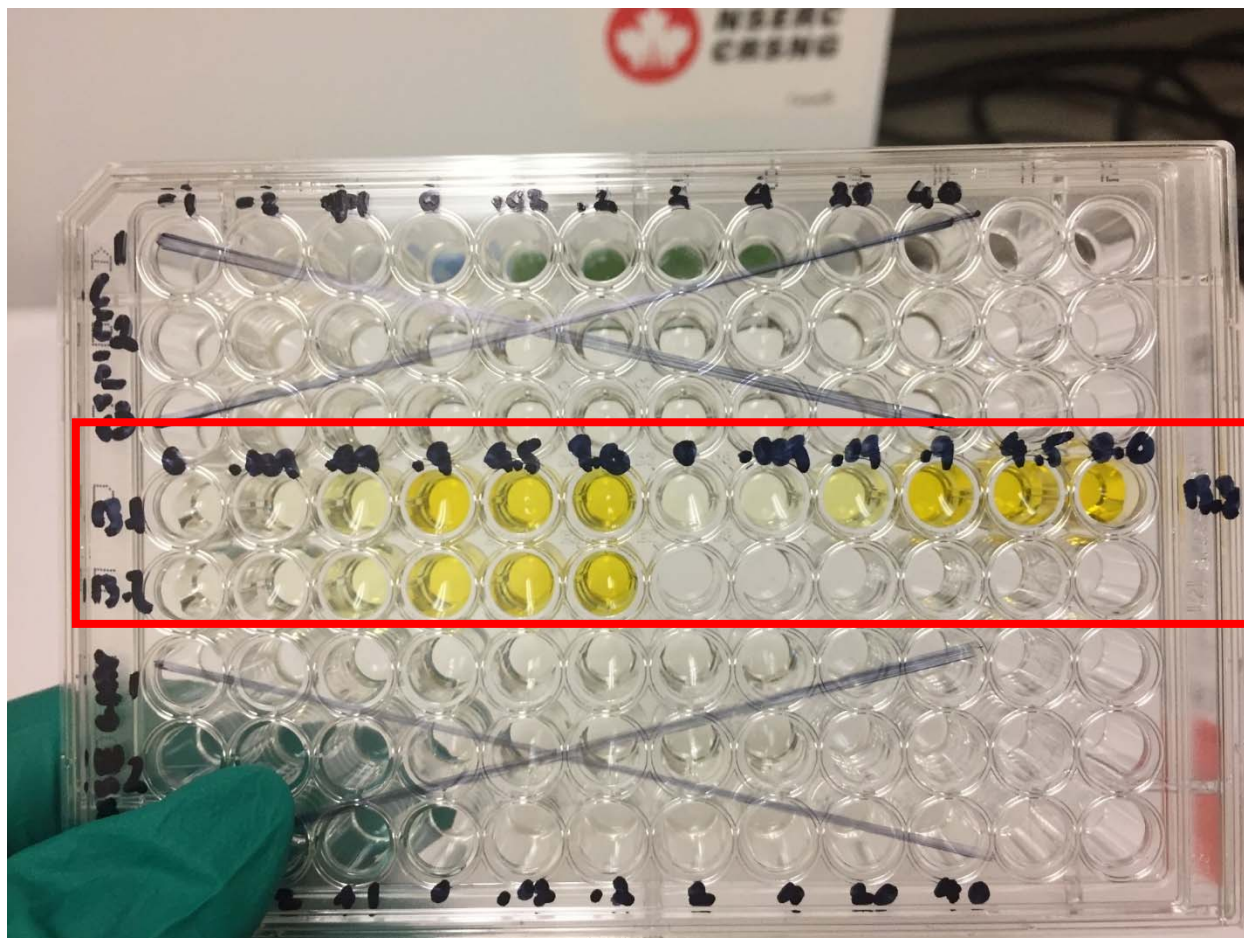


Figure 15. Evaluating the Assay with Different Concentrations of Acetylcholinesterase: The First Performance Test, Run 13.

A photo of the microtiter plate (inside the red box) used for the run was also attached to illustrate the complete reproducibility of the results obtained from run 5 when treated with the correct amount and concentration of acetylthiocholine iodide, along with the correct concentration of sodium phosphate buffer in which the acetylthiocholine iodide was dissolved. This was evident from the absence of the crystal formation in all wells, and from the consistent absorbance readings across the 30-min time span for all three technical replicates.

In conclusion, this confirmed with absolute certainty that the previously incorrect concentration of sodium phosphate buffer at 1.0 M was the sole error causing the formation of crystals within some of the microtiter plate wells. These crystals could form at various stages, either immediately after all components were added to the wells before mixing, during mixing, or while the microtiter plate was being processed in the plate reader machine. The major negative

impact of these crystals on the assay's performance was their disruption of the direct pathway of light passing through the wells, leading to the inconsistency in absorbance readings, and substantial, unsteady fluctuations in the graphical representation of the rate of TNB²⁻ absorbance increase (Supplementary Table 8 and Supplementary Figure 7).

As the issue of crystallization was being resolved, some additional adjustments were made to the assay's procedure during the last four runs of the first performance test. In run 10, six technical replicates were performed over five consecutive periods spanning roughly 8 h. The first period consisted two technical replicates, followed by the remaining four technical replicates, each within one of the remaining four periods. It was observed that the rate of TNB²⁻ absorbance increase for treatments with lower acetylcholinesterase concentrations slowed down over time, to the point where it became so sluggish that it almost resembled a flat line on the graph. This pattern was consistent for the same treatment with one enzyme concentration over the span of 8 h, regardless of the acetylcholinesterase concentration used.

It was suspected that the enzyme lost its stability over time, including its functionality, even when stored on ice throughout the experiment. To prevent this from recurring, a new batch of fresh standard solutions of acetylcholinesterase was prepared every time a run was performed, to maintain the structural and functional stability of the enzyme. Additionally, the step of swirling the microtiter plate for 30 secs before loading it into the plate reader machine was removed. It was considered unnecessary as it did not significantly contribute to the efficiency of well mixing. It was evident that within the confined space of each well, swirling the microtiter plate by hand could not generate enough force to create a swirling motion adequate for efficient mixing. Therefore, gently pipetting the solution up and down in every well with a large volume of 100 μ L after adding

all components to the wells was the sole practical option to achieve efficient mixing. These two new adjustments were subsequently applied in runs 11 through 13 (Supplementary Table 9).

Of all thirteen runs conducted in the first performance test, runs 11 through 13 stood out as the only ones where the assay's performance reached the highest level of optimization. Consequently, their data were selected for processing to serve as the final results of the first performance test. Notably, the two acetylcholinesterase concentrations of 4.5 units/mL and 9.0 units/mL, which had been excluded after the first run due to a significant number of absorbance readings going beyond the upper limit of the plate reader machine's detection range, were reintroduced in runs 10 through 13 for the purpose of data completion.

Based on the mean data from the last three runs of the first performance test, corresponding to three experimental replicates, a graph of absorbance plotted against time for five different concentrations of acetylcholinesterase was created. As the concentration of acetylcholinesterase increased, the rate of TNB²⁻ absorbance increase became faster, resulting in a more substantial change in absorbance over the same 30-min time frame. Additionally, the rate of TNB²⁻ absorbance increase became increasingly rapid, to the point where saturation could instantly be reached at the zeroth min with extremely high concentrations of acetylcholinesterase. This shift in the graphical trend indicated that the rate of TNB²⁻ absorbance increase transitioned from initially being linear at low enzyme concentrations to logarithmic at higher concentrations (Figure 16).

***In Vitro* Acetylcholinesterase Activity with Increasing Enzyme Concentration [unit/mL]**

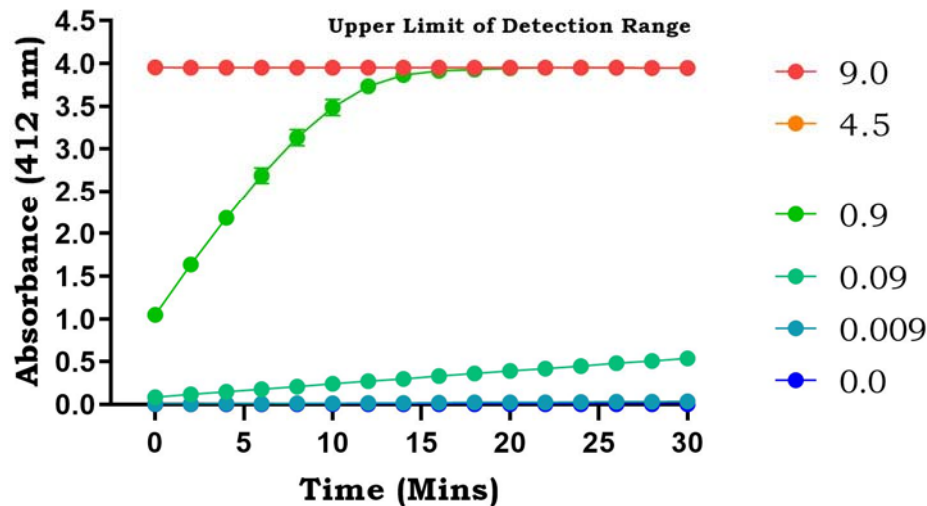


Figure 16. The Effect of Different Acetylcholinesterase Concentrations on Acetylcholinesterase Activity.

The variation in the *in vitro* acetylcholinesterase activity was determined by the change in absorbance over a 30-min time span, with the acetylcholinesterase concentration primarily increasing by factors of ten. Each data point on the graph represented the mean absorbance reading recorded for the treatment with one specific acetylcholinesterase concentration at one specific timepoint, with a 2-min interval between measurements. Each mean absorbance reading was averaged from runs 11 through 13 of the first performance test, representing an average obtained from three experimental replicates, corresponding to nine technical replicates ($n = 9$). The absorbance value of 4.0 represented the upper limit of the absorbance detection range of the Synergy 2 plate reader machine, beyond which no numerical value could be recorded. Owing to extremely small standard deviations, the error bars for most data points were not visible.

The results not only supported the hypothesis, but also demonstrated that the assay functioned correctly on its own without the addition of any test sample. Focusing on the results, the acetylcholinesterase concentration of 0.09 units/mL was the only one to produce a suitably steep slope representing a consistent linear change in TNB^{2-} absorbance over time. This meant that should there be a potential inhibitor of the enzyme, the decline in the steepness of the linear slope would be easily noticeable. A decrease in thiocholine content would result in a lower TNB^{2-} amount and a slower rate of TNB^{2-} absorbance increase over time, causing the previously straight incline to become flatter and more horizontally leveled. With its favorable range of absorbance

and moderate incline, the concentration of 0.09 units/mL was chosen for use in runs where test samples were added (Figure 17).

***In Vitro* Acetylcholinesterase Activity with Increasing Enzyme Concentration [unit/mL]**

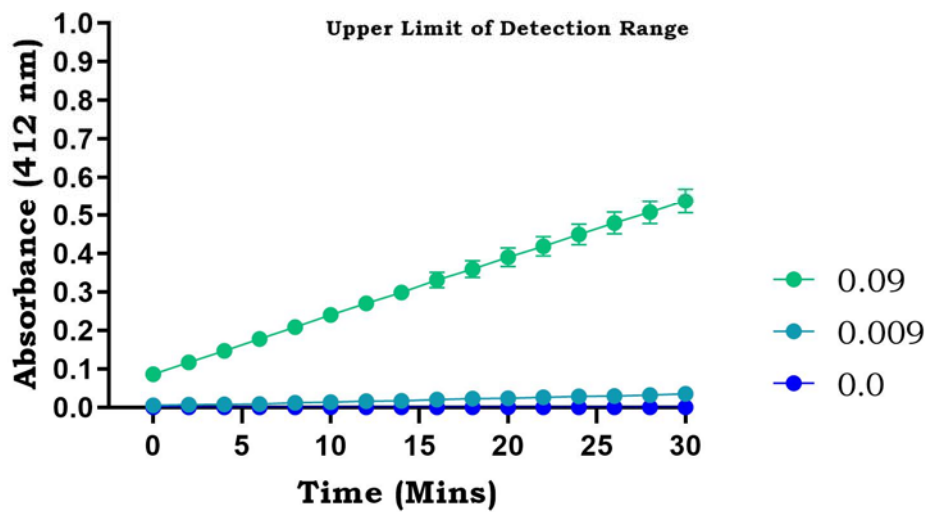


Figure 17. The Effect of Different Acetylcholinesterase Concentrations on Acetylcholinesterase Activity.

The data from Figure 6 were re-plotted to more effectively illustrate the effect of lower acetylcholinesterase concentrations on acetylcholinesterase activity.

2.3.1.2 The Second Performance Test: Evaluating the Assay with Different

Concentrations of Known Inhibitors of Acetylcholinesterase

2.3.1.2.1 Purpose of the Second Performance Test

The second performance test aimed to assess the assay's ability to generate decreasing absorbance readings in response to increasing concentrations of a known acetylcholinesterase inhibitor. This test served two purposes. First, it sought to ensure that the assay operated effectively when a test sample was introduced. Hypothetically, assuming all other factors, including time, remain constant, the change in TNB²⁻ absorbance should decrease as the concentration of a

potential acetylcholinesterase inhibitor increases. This is because a higher concentration of the enzyme inhibitor would result in a reduced production of thiocholine, leading to a lower amount of DTNB reduction and TNB²⁻ generation, ultimately yielding a smaller change in absorbance over the same time span.

The second purpose was to utilize the inhibition strength on acetylcholinesterase activity of the known inhibitor as a reference point for comparison. This reference would help assess the inhibition strength on the enzyme's activity by any potential inhibitors discovered in this study.

2.3.1.2.2 Experimental Procedure of the Second Performance Test

Experiments were carried out using 96-well microtiter plates. In this test, all five components of the assay were included: sodium phosphate buffer, *Electrophorus electricus* acetylcholinesterase, acetylthiocholine iodide, DTNB, and a small molecule as the test sample. On the plate, each row was divided into four different control wells and six different treatment wells.

For the control wells, there were four different types: first negative control, second negative control, first positive control, and second positive control.

In the first negative control well, the following components were added: 180 μ L of 0.1 M of sodium phosphate buffer at pH 8.0, 10 μ L of 10 mM of DTNB, and 10 μ L of 14 mM of acetylthiocholine iodide.

In the second negative control well, the following components were added: 170 μ L of 0.1 M of sodium phosphate buffer at pH 8.0, 20 μ L of 0.09 units/mL of acetylcholinesterase, and 10 μ L of 10 mM of DTNB. The purpose of the two negative controls was to ensure that the assay would not exhibit any activity in case one of the two crucial components, the enzyme or its substrate, was missing.

In the first positive control well, the following components were added: 160 μL of 0.1 M of sodium phosphate buffer at pH 8.0, 20 μL of 0.09 units/mL of acetylcholinesterase, 10 μL of 10 mM of DTNB, and 10 μL of 14 mM of acetylthiocholine iodide. Repeating what was done in the first performance test, including the first positive control was essential to ensure that the assay would function correctly without the addition of any test sample.

In the second positive control well, the following components were added: 140 μL of 0.1 M of sodium phosphate buffer at pH 8.0, 20 μL of 0.09 units/mL of acetylcholinesterase, 10 μL of 10 mM of DTNB, 20 μL of a specific concentration of a solvent used to dissolve the known inhibitor of acetylcholinesterase, and 10 μL of 14 mM of acetylthiocholine iodide. In contrast to the first positive control, this was intended to ensure that any inhibitory effect on acetylcholinesterase activity would not likely be attributed to the solvent used to dissolve the known enzyme inhibitor.

In each treatment well, the following components were added: 140 μL of 0.1 M of sodium phosphate buffer at pH 8.0, 20 μL of 0.09 units/mL of acetylcholinesterase, 10 μL of 10 mM of DTNB, 20 μL of a specific concentration of a known inhibitor of acetylcholinesterase, and 10 μL of 14 mM of acetylthiocholine iodide. The concentration of the known enzyme inhibitor was divided into six increasing concentrations ordered from least to most concentrated: 0.02, 0.2, 2, 4, 20, and 40 μM . Once all concentrations of the known enzyme inhibitor were added to the treatment wells, the wells underwent a 15-min incubation period before acetylthiocholine iodide was introduced to initiate the assay.

There were three rows in total, each representing one technical replicate. The three technical replicates were combined to form one experimental replicate corresponding to a single run. For each experimental replicate, the change in the absorbance of TNB^{2-} was detected at the

wavelength of 412 nm and recorded every 2 mins for a total of 30 mins using the Synergy 2 plate reader machine. A total of three experimental replicates were performed.

In addition to the treatment with the known acetylcholinesterase inhibitor, the experimental procedure of the second performance test also included a treatment with a known non-inhibitor of the enzyme. Testing a pair of test samples with opposite effects on acetylcholinesterase would ensure that only compounds structurally compatible with the enzyme's active site and chemically compatible with the surrounding atoms within the active site could exhibit an inhibitory effect on the enzyme's activity. Aside from the known non-inhibitor of acetylcholinesterase, a second known inhibitor of the enzyme was also included.

Aspirin, which has no reported history of inhibiting acetylcholinesterase, was selected as the known non-inhibitor. The known inhibitors of acetylcholinesterase chosen were galanthamine hydrobromide and pyridostigmine bromide. Both are well-known and well-studied reversible inhibitors that selectively target different sites within the enzyme to inhibit its activity. Galanthamine hydrobromide selectively binds to aromatic residues within the peripheral anionic site of the enzyme, while pyridostigmine bromide selectively binds to the hydroxyl side chain of the serine residue in the catalytic triad located within the catalytic anionic site of the enzyme.²⁴ The effect of aspirin on acetylcholinesterase activity was tested individually with either galanthamine hydrobromide or pyridostigmine bromide, forming two separate experimental sets.

2.3.1.2.3 Raw Data Processing and Graphing Transformation of the Second Performance Test

In each technical replicate, for each of the negative control, positive control, and treatment with one concentration of a small molecule, the total change in TNB^{2-} absorbance over the 30-min time span was calculated by subtracting the raw absorbance value recorded at the zeroth min from

the value recorded at the thirtieth min. As there were two negative controls, the final total change in TNB²⁻ absorbance was determined by averaging the total changes from the two controls. The same process was repeated for the two positive controls.

Next, the true average total change in TNB²⁻ absorbance observed for the positive control was calculated by subtracting the average total change for the negative control from the average total change for the positive control. This step removed background absorbance contributed by any solution in the positive control well apart from DTNB. This revealed the actual change in absorbance due to DTNB reduction to TNB²⁻.

The true average total change in TNB²⁻ absorbance observed for the positive control, along with the total changes for the treatments with the six different concentrations of the small molecule, were normalized to a range from 0% to 100% enzyme activity. The 100% mark was represented by the true average total change in TNB²⁻ absorbance observed for the positive control. This normalization allowed a relative comparison of how acetylcholinesterase activity would decrease as the concentration of the small molecule increased by factors of ten, if the small molecule acted as an actual inhibitor of acetylcholinesterase.

In cases where an inhibitory effect occurred and sufficient data were available, a sigmoidal dosage-response graph was created. This graph plotted percentage values of enzyme activity against the increasing concentrations of the small molecule. Each percentage value at a specific concentration was an average of nine different percentage values calculated from raw absorbance data recorded in nine technical replicates, corresponding to three different experimental replicates. A standard deviation value for each percentage value was also provided based on the raw data.

Following this, the IC₅₀ value was calculated based on the shape of the sigmoidal curve, considering the length and depth of both the upper and lower portions surrounding the inflection

point. The normalization and the IC₅₀ value calculation were computed using the PRISM graphing software. The x-axis of the graph was presented in a logarithmic scale to match the S-shaped sigmoidal trend of a dosage-response graph.

Once the graph for the small molecule was completed, it was merged into a final overall graph with the graph of another small molecule that did not inhibit acetylcholinesterase activity. This comparison allowed for a clear distinction in the impact on the acetylcholinesterase activity when exposed to an inhibitor versus a non-inhibitor.

2.3.1.2.4 Hypothesis and Predicted Outcomes of the Second Performance Test

According to the hypothesis, as the concentration of a known acetylcholinesterase inhibitor increases, the linear rate of TNB²⁻ absorbance increase should slow down, leading to a smaller change in absorbance. This gradual decrease would cause the initially steep incline, which starts at a certain degree, to flatten into a straight horizontal line.

On a dose-response graph where the percentage of enzyme activity is plotted against the concentration of small molecule, an increase in the concentration of a known acetylcholinesterase inhibitor by factors of ten should result in a decrease in the percentage of enzyme activity. This decrease should follow a sigmoidal trend, producing a reverse S-shaped curve.

2.3.1.2.5 Observations and Analyses of the Second Performance Test

In the second performance test, a graph of the percentage of enzyme activity plotted against concentration was created based on the mean data from three experimental replicates. In the first experimental set, the effects of aspirin and galanthamine hydrobromide on acetylcholinesterase activity were compared.

As the concentration of aspirin increased, mainly by a factor of ten within the range of 0.02 to 40 μ M, the percentage of enzyme activity remained relatively stable and close to the levels

observed in the positive controls. This suggested that aspirin had no significant effect on acetylcholinesterase activity. In contrast, as the concentration of galanthamine hydrobromide increased in a similar manner, the percentage of enzyme activity significantly decreased, following a sigmoidal trend and ultimately reaching complete inhibition at 100%. The standard deviations of the mean data for the aspirin treatment were substantial, indicating random fluctuations in the percentage of enzyme activity, while the standard deviations of the mean data for the galanthamine hydrobromide treatment were small, suggesting minimal variability.

In summary, the data showed that aspirin had no impact on acetylcholinesterase activity, while galanthamine hydrobromide clearly inhibited the enzyme's activity. The concentration of galanthamine hydrobromide required to inhibit acetylcholinesterase activity by 50%, or the IC₅₀ value, was calculated to be 0.313 μM . Excluding eight outliers from a total of eighty-one search results, which represent scientific studies conducted from the year 2000 to 2021 and were sourced from the ChEMBL database of the European Molecular Biology Laboratory at that time, the reported IC₅₀ values for the inhibition of galanthamine hydrobromide on the activity of *Electrophorus electricus* acetylcholinesterase in the nanomolar unit showed a range from 0.200 μM to 1.500 μM . Among these results, thirty-three reported IC₅₀ values were below 0.700 μM . The most frequently occurring value among those thirty-three search results was in the six hundred nanomolar range.⁴⁸ The IC₅₀ value obtained in this study for galanthamine hydrobromide, required to inhibit acetylcholinesterase activity, fell within this reported range. It was notably close to the most common value found in the research studies. As a result, this value was considered consistent and reliable (Figure 18).

***In Vitro* Acetylcholinesterase Activity in the Presence of Its Known Inhibitor Galanthamine Hydrobromide**

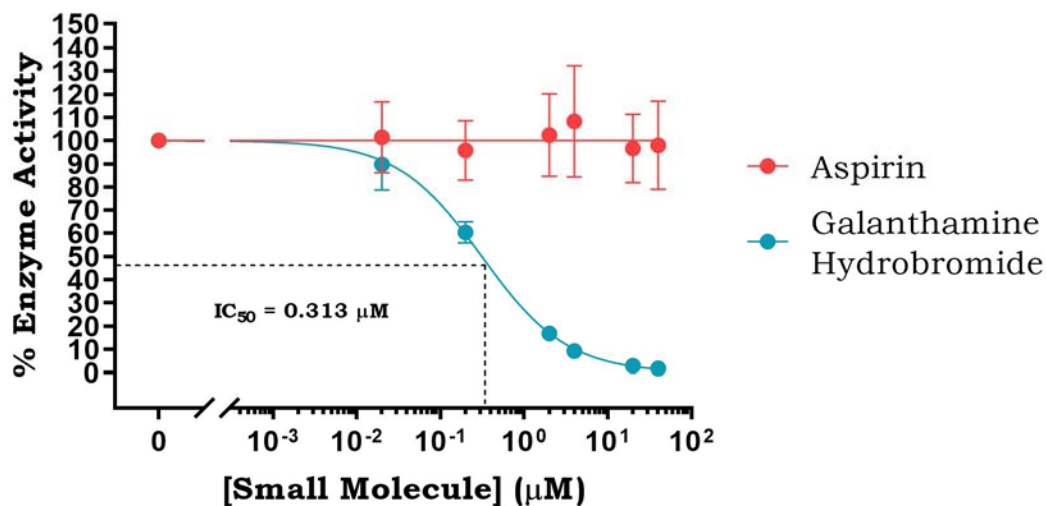


Figure 18. The Effect of Galanthamine Hydrobromide on Acetylcholinesterase Activity.

The shift in percentage of *in vitro* acetylcholinesterase activity when the enzyme was separately exposed to different small molecules at increasing concentrations primarily by factors of ten, over a 30-min time span. Aspirin is a known non-inhibitor of acetylcholinesterase. Galanthamine hydrobromide is a known inhibitor of acetylcholinesterase. Each data point on the graph represented the mean percentage value of acetylcholinesterase activity recorded for the treatment with one specific small molecule, and at one specific small molecule concentration. Each mean percentage value of acetylcholinesterase activity was averaged from three experimental replicates, corresponding to nine technical replicates ($n = 9$). Each set of upper and lower bars surrounding each data point on the graph represented the standard deviation of a mean percentage value of acetylcholinesterase activity. The IC_{50} value represented the concentration of galanthamine hydrobromide required to inhibit acetylcholinesterase activity by 50%.

In the second experimental set, the effect of aspirin was compared to the effect of pyridostigmine bromide on acetylcholinesterase activity. As the concentration of aspirin increased, mainly by a factor of ten within the range of 0.02 to 40 µM, the percentage of enzyme activity remained relatively stable and close to the levels observed in the positive controls again. While the trendline appeared to show a slight decrease after the third data point, it did not seem to be a substantial decrease, as the last three data points remained fairly consistent, with a slight increase observed from the fourth data point to the sixth data point. Similar to the testing of aspirin in the first experimental set, the presence of aspirin did not significantly alter acetylcholinesterase

activity in comparison to the levels observed in the positive controls in the second experimental set. The results, characterized by large standard deviations, confirmed that aspirin had no substantial effect on the activity of acetylcholinesterase.

In contrast to aspirin, as the concentration of pyridostigmine bromide increased in a similar manner, the percentage of enzyme activity significantly decreased, following a sigmoidal trend. However, the trend did not reach a complete inhibition of enzyme activity at 100%, as seen with the testing of galanthamine hydrobromide in the first experimental set. Examining data variability between experimental replicates, it was evident that the standard deviations of the mean data for the pyridostigmine bromide treatment were small, indicating that pyridostigmine bromide also had an inhibitory effect on acetylcholinesterase activity. However, its inhibitory effect on the enzyme activity was approximately eighteen times weaker than the effect of galanthamine hydrobromide, as reflected in the IC_{50} value of 5.530 μM . The IC_{50} value of pyridostigmine bromide demonstrated that a significantly higher concentration was required to achieve the same degree of inhibition on acetylcholinesterase activity compared to what was observed with galanthamine hydrobromide. Contrary to galanthamine hydrobromide, there were no reliable, up-to-date extensive research studies nor reports on the inhibitory effect of pyridostigmine bromide specifically on *Electrophorus electricus* acetylcholinesterase activity, as no relevant information was found in the ChEMBL database of the European Molecular Biology Laboratory, nor on the National Center for Biotechnology Information website at the time. Despite the absence of literature values for comparison, the experimental IC_{50} value of 5.530 μM was considered reliable due to the precise data with low variability between experimental replicates. In addition to a weaker inhibitory effect, the effective concentration range was also smaller for pyridostigmine bromide, as indicated by the

narrower and steeper slope around the inflection point of the sigmoidal trend compared to the slope observed for galanthamine hydrobromide (Figure 19).

***In Vitro* Acetylcholinesterase Activity in the Presence of Its Known Inhibitor Pyridostigmine Bromide**

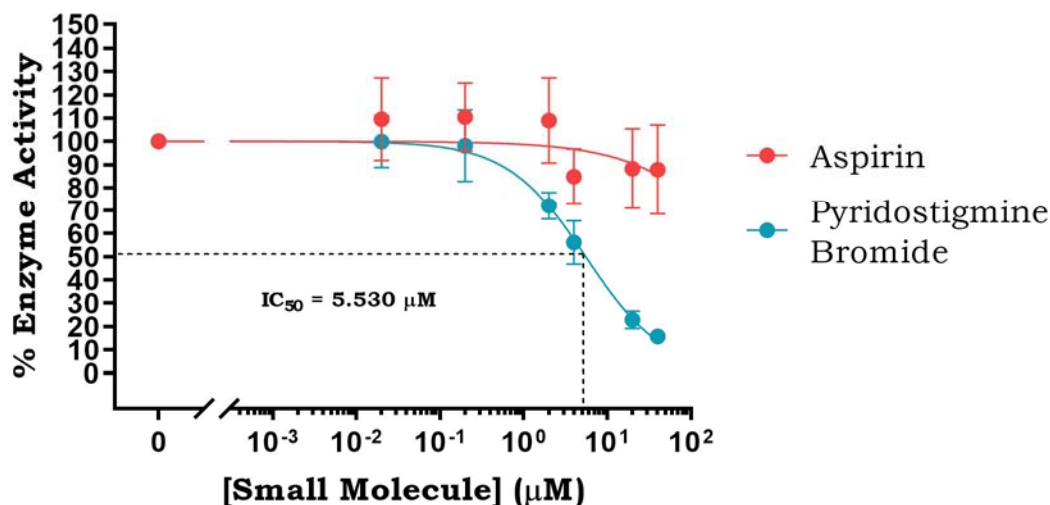


Figure 19. The Effect of Pyridostigmine Bromide on Acetylcholinesterase Activity.

The shift in percentage of in vitro acetylcholinesterase activity when the enzyme was separately exposed to different small molecules at increasing concentrations primarily by folds of ten, over a 30-min time span. Aspirin is a known non-inhibitor of acetylcholinesterase. Pyridostigmine bromide is a known inhibitor of acetylcholinesterase. Each data point on the graph represented the mean percentage value of acetylcholinesterase activity recorded for the treatment with one specific small molecule, and at one specific small molecule concentration. Each mean percentage value of acetylcholinesterase activity was averaged from three experimental replicates, corresponding to nine technical replicates (n = 9). Each set of upper and lower bars surrounding each data point on the graph represented the standard deviation of a mean percentage value of acetylcholinesterase activity. The IC₅₀ value represented the concentration of pyridostigmine bromide required to inhibit acetylcholinesterase activity by 50%.

In conclusion, the final results supported the hypothesis and demonstrated the reliability of the developed assay in this study. The evidence was the characteristic reverse S-shaped curve on the dosage-response graph, representing the sigmoidal decrease in enzyme activity with increasing inhibitor concentrations, primarily by a factor of ten. With two known acetylcholinesterase inhibitors examined, the results also provided insights into the potential range of inhibition strength

for an acetylcholinesterase inhibitor. This information would be useful for comparing the inhibition strength on acetylcholinesterase activity for the four small molecules SPOPP, NP6A, 534_1(6), and 534_2(7) against that of the two known acetylcholinesterase inhibitors, serving as positive controls, to assess the effects of the small molecules on acetylcholinesterase activity as described below.

2.4 Examination of the Effect of Small Molecules on Acetylcholinesterase Activity

The rationale for examining the effects of SPOPP, NP6A, 534_1(6) and 534_2(7) on acetylcholinesterase activity was already provided on pages 30 to 33 in Chapter 1.

2.4.1 Preparation of the Synthetic Small Molecules

2.4.1.1 Synthesis of SPOPP and NP6A

In two separate small weighing boats, 1.8200 g of acenaphthenequinone and 1.1500 g of L-proline in powder form were weighed on an analytical balance. Mass measurements were typically accurate to three decimal places, occasionally varying slightly at the fourth decimal place. After weighing, 200 mL of 100% high-performance liquid chromatography-grade methanol was measured and transferred to a 1000-mL round-bottom flask using a 500-mL graduated cylinder. The pre-weighed acenaphthenequinone and L-proline were also transferred to the same 1000-mL round-bottom flask. To ensure no powder was left behind in the weighing boats, the boats were rinsed with a small amount of 100% normal-grade methanol. The flask was then gently swirled by hand for 10 mins to thoroughly mix the acenaphthenequinone, which was only partially soluble, with the highly soluble L-proline in 100% normal-grade methanol.

Before preparing the reaction mixture, a water reflux apparatus was set up and maintained at a temperature of 35°C. After the 10-min swirl, a 25×7-mm magnetic stir bar was added to the flask. The flask was then placed under the water reflux apparatus. Through reflux, the reaction

mixture was continuously stirred at 280 rpm while being simmered at 35°C for precisely 3 h to synthesize SPOPP and NP6A (Figures 20-21). Concurrently, a rotary evaporator was set up at 30°C.

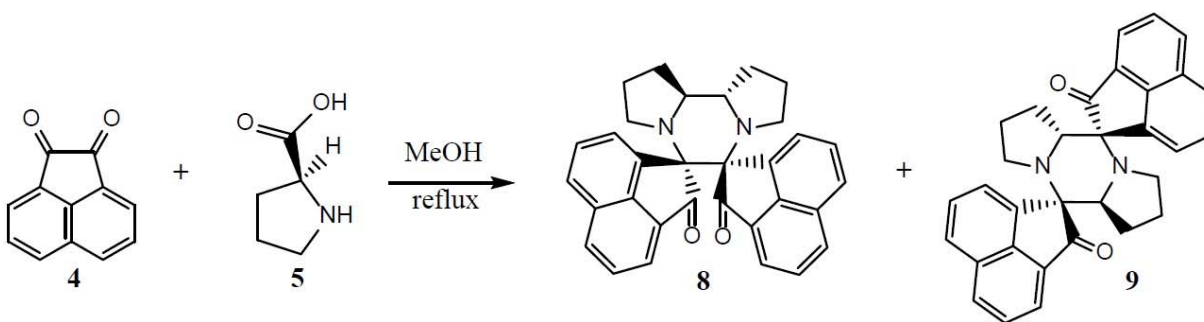


Figure 20. The Synthesis of SPOPP and NP6A.

Acenaphthenequinone (4) and L-proline (5) was dissolved in methanol, continuously stirred and warmed at 35°C for exactly three hours while being placed under reflux to synthesize SPOPP (8) and NP6A (9).²⁶



Figure 21. The Synthesis of SPOPP and NP6A.

A photo showing the completion of the reaction described in Figure 20.

Following the 3-h simmer, the flask was carefully removed quickly and attached to the rotary evaporator. During rotary evaporation, 100% methanol was evaporated from the reaction mixture at 30°C until no solvent remained and product solids began to reappear. After the solids reappeared, the flask was left under the same rotary evaporation conditions for an additional 3 h

to ensure thorough removal of any remaining residual methanol integrated within the solids. This step was crucial to prevent the solids from turning into sticky chunks of sludge.

Once the solids were completely dried, the magnetic stir bar was removed by tilting the flask to allow it to slide out naturally. The removed stir bar was rinsed in a small beaker with a small amount of 100% normal-grade methanol to redissolve any remaining adhering solids. A self-made fishing rod, equipped with a magnetic stir bar at its end, was used to pull the stir bar out through magnetism. After that, the solution from rinsing the stir bar was transferred back to the same round-bottom flask containing the bulk of the product solids.

The flask was then reattached to the rotary evaporator and left under the same rotary evaporation conditions for another 2 h to further dry the residual methanol used for rinsing (Figure 22). Finally, the product solids were scraped into a vial and stored at 4°C. The product solids were considered crude, containing various substances including SPOPP and NP6A, resulting in a dark green color (Figure 23).



Figure 22. Crude Product Solids From the Synthesis of SPOPP and NP6A.

A photo showing the crude product solids obtained after the reaction mixture shown in Figure 21 was completely evaporated through rotary evaporation.



Figure 23. Crude Product Solids From the Synthesis of SPOPP and NP6A.

A photo showing the dark green crude product solids after they were scraped into a vial from the 1000-mL round-bottom flask shown in Figure 22.

2.4.1.2 Preparation of Flash Column Chromatography

In two separate small weighing boats, 0.5000 g of the crude product, which included SPOPP and NP6A, and 4.00 g of silica in powder form, were weighed on an analytical balance and a top loading balance, respectively. Mass measurements were typically accurate to three decimal places, occasionally varying slightly at the fourth decimal place. After weighing, 500 mL of 100% high-performance liquid chromatography-grade methanol was measured and transferred to a 1000-mL round-bottom flask using the 500-mL graduated cylinder. The pre-weighed crude product and silica were then added to the same 1000-mL round-bottom flask. To ensure no material was left behind in the weighing boats, the boats were rinsed with a small amount of 100% normal-grade methanol to collect every speck of both materials into the flask. The flask was then gently swirled by hand for 10 mins to thoroughly mix the crude product and silica.

During this time, the rotary evaporator was set up at 30°C. After the 10-min swirl, the flask was attached to the rotary evaporator. Using rotary evaporation, 100% methanol was evaporated from the solution at 30°C until no solvent remained and solids began to reappear. After the solids reappeared, the flask was left under the same rotary evaporation conditions for an additional 5 mins to ensure the thorough removal of any remaining residual methanol integrated within the

solids. Given the extremely dry nature of the solids, 5 mins of drying was considered sufficient. Once the solids were completely dried, they were scraped into a vial and stored at 4°C. These solids consisted of the crude product adhering to silica particles, and were intended for the subsequent purification process using flash column chromatography. The whole sample's color had transformed from dark green to bright orange.

In a 1000-mL Erlenmeyer flask, 180.00 g of silica was weighed on a top loading balance. Mass measurements were typically accurate to three decimal places, occasionally varying slightly at the fourth decimal place. After weighing, 3 L of high-performance liquid chromatography-grade hexane, mixed with normal-grade ethyl acetate in a 9:1 ratio, was divided into smaller portions and distributed into a 600-mL beaker and two 1000-mL Erlenmeyer flasks. One of the Erlenmeyer flasks contained the pre-weighed 180.00 g of silica. The 1000-mL graduated cylinder was used to measure and transfer the solvent.

Next, the bottom of the glass column, the entire V-shaped zone, was entirely filled with sand. After filling the V-shaped zone, hexane-ethyl acetate was carefully pipetted down the side of the column in small drips, gradually raising the liquid level to a point where even significant disturbance, such as splashing large volumes of liquid, would not distort the sand layer's flat surface. Subsequently, a substantial volume of hexane-ethyl acetate was poured into the column, filling it to half of its total height. The silica solution from one of the two 1000-mL Erlenmeyer flasks was then introduced into the column. After transferring, the flask was rinsed with a small amount of hexane-ethyl acetate to ensure that any remaining residual silica was washed into the column.

With the aid of an air pump, the hexane-ethyl acetate solution in the column was rapidly drained. The combination of the solution's large volume and the air pressure released by the pump

compacted the silica layer tightly on top of the sand layer. Simultaneously, as the hexane-ethyl acetate solution was being drained, any residual silica particles adhering to the column's side were washed down by gently pipetting tiny streams of hexane-ethyl acetate alongside the column's wall. Since the silica particles were denser than the hexane-ethyl acetate solution, the silica layer sank faster and became compacted before the solution could follow. Once the level of the hexane-ethyl acetate solution descended to the top surface of the tightly packed silica layer, the drainage was immediately halted. The volume of hexane-ethyl acetate used to pack the silica layer was then recollected for reuse in the upcoming purification process.

Prepared and ready for sample loading, the previously acquired bright orange solids, which included the crude product adhering to silica particles, were gently sprinkled onto the top surface of the tightly packed silica layer. To ensure thorough distribution of the sample, small drips of hexane-ethyl acetate were carefully pipetted down along the column's wall, washing any residual solids onto the silica layer. This process continued until the solvent sufficiently covered the sample layer, without overflowing. The objective was to uniformly moisten and flatten the sample layer while preventing sample dilution.

Following this, an additional layer of sand was sprinkled on top of the sample layer. This second sand layer was intentionally made thicker than the first one located in the V-shaped zone at the base of the glass column. Its purpose was to create a thick barrier that would shield the evenly distributed sample layer from disturbances when the hexane-ethyl acetate was introduced to initiate the purification process. Once the sand layer was in place, more small drips of hexane-ethyl acetate were carefully pipetted down along the column's wall again, until the liquid reached a specific height where even intense disturbances, like splashing large volumes of liquid, would not distort the flat surface of the second sand layer. Finally, to complete this setup, a substantial

volume of hexane-ethyl acetate was transferred into the column until it was filled nearly to its total height.

2.4.1.3 Purification of SPOPP and NP6A

With the assistance of the air pump, the purification process was initiated and continuously maintained using hexane-ethyl acetate at a flow rate of 2 psi/min. Whenever the level of hexane-ethyl acetate dropped low near the second sand layer, the air pump was temporarily halted and removed to allow for the addition of more hexane-ethyl acetate. This was done without interrupting the drainage flow during the process.

As the sample layer separated into distinct bands while migrating through the silica layer, SPOPP in the orange band and NP6A in the yellow band were collected separately into two 100-mL round-bottom flasks (Figure 24). These flasks were then attached to the rotary evaporator. Through rotary evaporation at 30°C, the hexane-ethyl acetate eluent was evaporated until no solvent remained and purified solids began to reappear. After the solids reappeared, the flasks were left under the same rotary evaporation conditions for an additional 5 mins to ensure the complete removal of any remaining residual hexane-ethyl acetate. Subsequently, the flasks were removed and stored at 4°C. Upon evaluating the quality of the purification, the purified solids were redissolved in 100% acetonitrile before being subjected to high performance liquid chromatography.

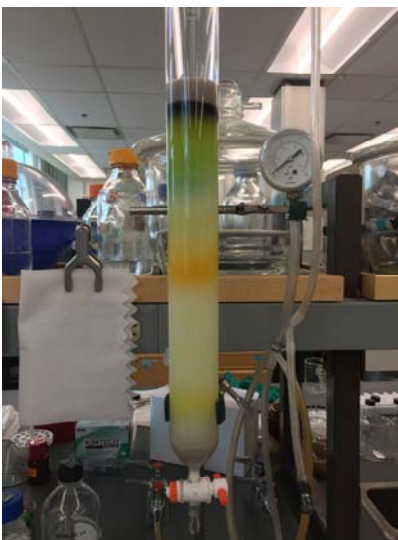


Figure 24. The Purification of SPOPP and NP6A.

SPOPP in the orange band and NP6A in the yellow band were isolated separately through flash column chromatography.

2.4.1.4 Synthesis of 534_1(6) and 534_2(7)

Both 534_1(6) and 534_2(7) were readily available and provided by Dr. Hooi Xian Lee, a former team member from the Lee research group.⁴⁹

2.4.2 Evaluation of the Effect of Small Molecules on Acetylcholinesterase Activity

2.4.2.1 Experimental Procedure

The experimental setup closely mirrored the one planned and established for the second performance test. Experiments were carried out using 96-well microtiter plates. In this test, all five components of the assay were included: sodium phosphate buffer, *Electrophorus electricus* acetylcholinesterase, acetylthiocholine iodide, DTNB, and a small molecule as the test sample. On the plate, each row was divided into four different control wells and six different treatment wells.

For the control wells, there were four different types: first negative control, second negative control, first positive control, and second positive control.

In the first negative control well, the following components were added: 180 μL of 0.1 M of sodium phosphate buffer at pH 8.0, 10 μL of 10 mM of DTNB, and 10 μL of 14 mM of acetylthiocholine iodide.

In the second negative control well, the following components were added: 170 μL of 0.1 M of sodium phosphate buffer at pH 8.0, 10 μL of 10 mM of DTNB, and 20 μL of 0.09 units/mL of acetylcholinesterase.

In the first positive control well, the following components were added: 160 μL of 0.1 M of sodium phosphate buffer at pH 8.0, 10 μL of 10 mM of DTNB, 20 μL of 0.09 units/mL of acetylcholinesterase, and 10 μL of 14 mM of acetylthiocholine iodide.

In the second positive control well, the following components were added: 140 μL of 0.1 M of sodium phosphate buffer at pH 8.0, 10 μL of 10 mM of DTNB, 20 μL of 0.09 units/mL of acetylcholinesterase, 20 μL of a specific concentration of a solvent used to dissolve the small molecule, and 10 μL of 14 mM of acetylthiocholine iodide.

In each treatment well, the following components were added: 140 μL of 0.1 M of sodium phosphate buffer at pH 8.0, 10 μL of 10 mM of DTNB, 20 μL of 0.09 units/mL of acetylcholinesterase, 20 μL of a specific concentration of a small molecule, and 10 μL of 14 mM of acetylthiocholine iodide. The concentration of the small molecule was divided into six increasing concentrations ordered from least to most concentrated: 0.02, 0.2, 2, 4, 20, and 40 μM . Once all concentrations of the small molecule were added to the treatment wells, the wells underwent a 15-min incubation period before acetylthiocholine iodide was introduced to initiate the assay.

There were three rows in total, each representing one technical replicate. The three technical replicates were combined to form one experimental replicate corresponding to a single

run. For each experimental replicate, the change in the absorbance of TNB^{2-} was detected at the wavelength of 412 nm and recorded every 2 mins for a total of 30 mins using the Synergy 2 plate reader machine. A total of three experimental replicates were performed for the known non-inhibitor aspirin, or each small molecule. A total of six experimental replicates were performed for each pair of aspirin and one of the small molecules, forming one experimental set. The only minor difference was a slight alteration in the order of component addition. To maintain the enzyme's freshness, acetylcholinesterase was introduced immediately after DTNB, before adding the sample and acetylthiocholine iodide.

2.4.2.2 Hypothesis and Predicted Outcomes

According to the hypothesis, if a small molecule acts as an acetylcholinesterase inhibitor, as its concentration increases, the linear rate of TNB^{2-} absorbance increase should slow down, leading to a smaller change in the absorbance. This gradual decrease would cause the initially steep incline, which starts at a certain degree, to flatten into a straight horizontal line.

On a dose-response graph where the percentage of enzyme activity is plotted against the concentration of small molecule, an increase in the concentration of the small molecule by factors of ten should result in a decrease in the percentage of enzyme activity. This decrease should follow a sigmoidal trend, producing a reverse S-shaped curve.

2.4.2.3 Observations and Analyses

Based on the mean data from three experimental replicates, a graph illustrating the percentage of enzyme activity versus the concentration of two different types of small molecules was generated. In all four experimental sets, where the effect of aspirin was compared to that of four small molecules: SPOPP, NP6A, 534_1(6), and 534_2(7), it was observed that as the concentration of aspirin increased, mainly by a factor of ten within the range of 0.02 to 40 μM , the

percentage of enzyme activity remained quite similar to the positive controls. In the presence of aspirin, the acetylcholinesterase activity did not significantly deviate from that observed in the positive controls. However, there were substantial variations in the data as indicated by the large standard deviations observed for the aspirin treatment. Disappointingly, both the trend and data variability were similarly observed for the other four small molecules as well (Figures 25-28).

***In Vitro* Acetylcholinesterase Activity in the Presence of SPOPP**

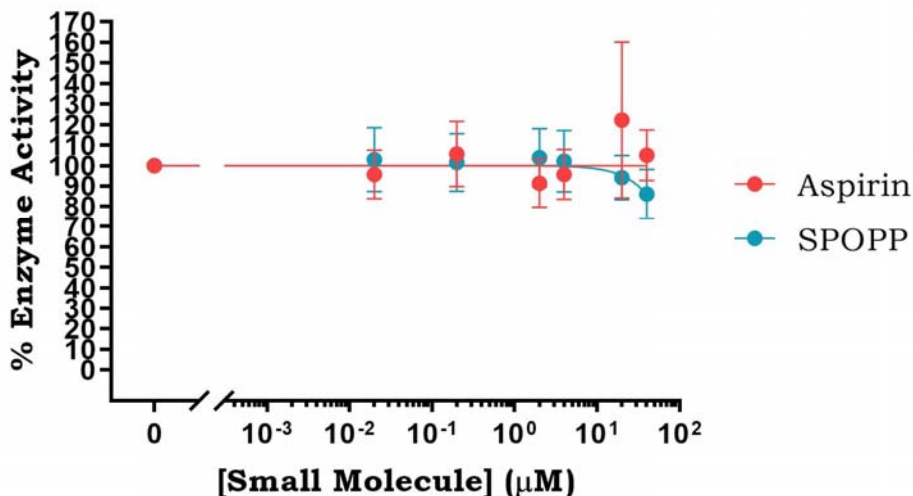


Figure 25. The Effect of SPOPP on Acetylcholinesterase Activity.

The shift in percentage of *in vitro* acetylcholinesterase activity when the enzyme was separately exposed to different small molecules at increasing concentrations primarily by factors of ten, over a 30-min time span. Aspirin is a known non-inhibitor of acetylcholinesterase. SPOPP is a small molecule that was used to test for an inhibitory effect on acetylcholinesterase activity. Each data point on the graph represented the mean percentage value of acetylcholinesterase activity recorded for the treatment with one specific small molecule, and at one specific small molecule concentration. Each mean percentage value of acetylcholinesterase activity was averaged from three experimental replicates, corresponding to nine technical replicates ($n = 9$). Each set of upper and lower bars surrounding each data point on the graph represented the standard deviation of a mean percentage value of acetylcholinesterase activity.

***In Vitro* Acetylcholinesterase Activity in the Presence of NP6A**

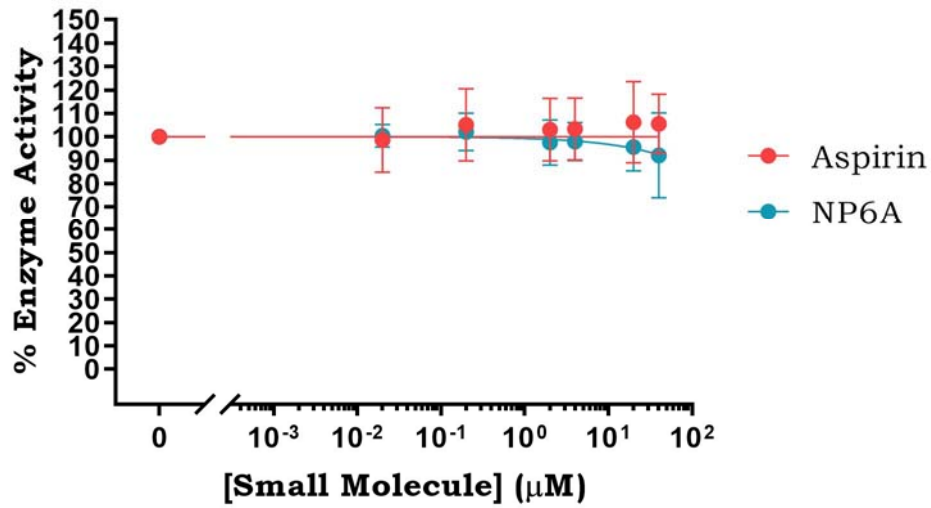


Figure 26. The Effect of NP6A on Acetylcholinesterase Activity.

The shift in percentage of *in vitro* acetylcholinesterase activity when the enzyme was separately exposed to different small molecules at increasing concentrations primarily by factors of ten, over a 30-min time span. Aspirin is a known non-inhibitor of acetylcholinesterase. NP6A is a small molecule that was used to test for an inhibitory effect on acetylcholinesterase activity. Each data point on the graph represented the mean percentage value of acetylcholinesterase activity recorded for the treatment with one specific small molecule, and at one specific small molecule concentration. Each mean percentage value of acetylcholinesterase activity was averaged from three experimental replicates, corresponding to nine technical replicates ($n = 9$). Each set of upper and lower bars surrounding each data point on the graph represented the standard deviation of a mean percentage value of acetylcholinesterase activity.

***In Vitro* Acetylcholinesterase Activity in the Presence of 534_1(6)**

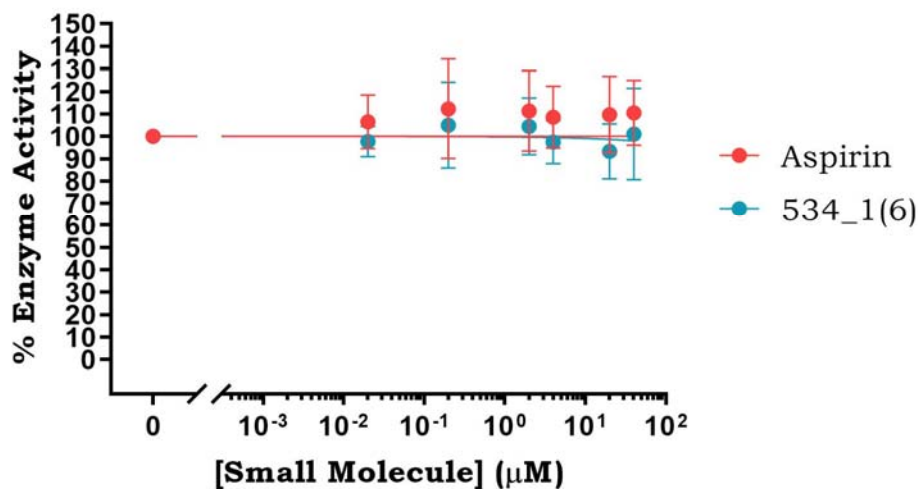


Figure 27. The Effect of 534_1(6) on Acetylcholinesterase Activity.

The shift in percentage of *in vitro* acetylcholinesterase activity when the enzyme was separately exposed to different small molecules at increasing concentrations primarily by factors of ten, over a 30-min time span. Aspirin is a known non-inhibitor of acetylcholinesterase. 534_1(6) is a small molecule that was used to test for an inhibitory effect on acetylcholinesterase activity. Each data point on the graph represented the mean percentage value of acetylcholinesterase activity recorded for the treatment with one specific small molecule, and at one specific small molecule concentration. Each mean percentage value of acetylcholinesterase activity was averaged from three experimental replicates, corresponding to nine technical replicates ($n = 9$). Each set of upper and lower bars surrounding each data point on the graph represented the standard deviation of a mean percentage value of acetylcholinesterase activity.

***In Vitro* Acetylcholinesterase Activity in the Presence of 534_2(7)**

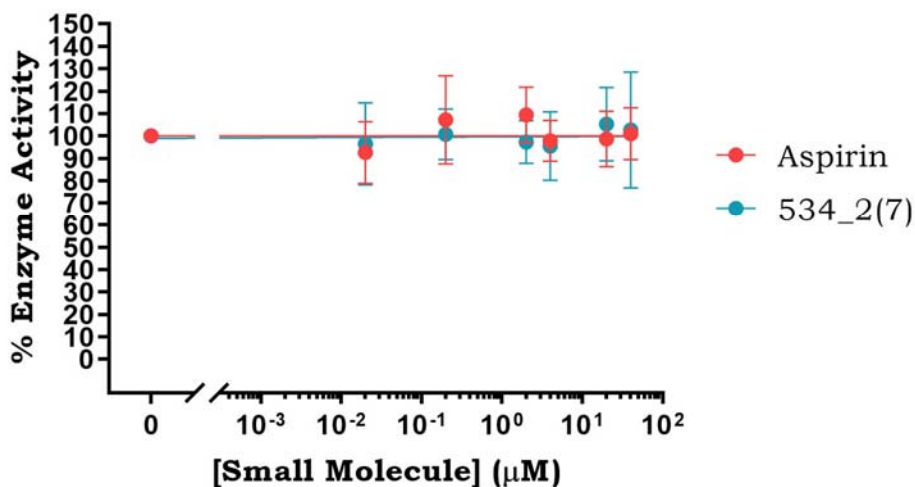


Figure 28. The Effect of 534_2(7) on Acetylcholinesterase Activity.

The shift in percentage of *in vitro* acetylcholinesterase activity when the enzyme was separately exposed to different small molecules at increasing concentrations primarily by factors of ten, over a 30-min time span. Aspirin is a known non-inhibitor of acetylcholinesterase. 534_2(7) is a small molecule that was used to test for an inhibitory effect on acetylcholinesterase activity. Each data point on the graph represented the mean percentage value of acetylcholinesterase activity recorded for the treatment with one specific small molecule, and at one specific small molecule concentration. Each mean percentage value of acetylcholinesterase activity was averaged from three experimental replicates, corresponding to nine technical replicates ($n = 9$). Each set of upper and lower bars surrounding each data point on the graph represented the standard deviation of a mean percentage value of acetylcholinesterase activity.

Although the treatments with SPOPP and NP6A showed a slight reduction in enzyme activity as the concentration of these small molecules increased from 20 µM onwards, there was substantial overlap between the standard deviations of the mean data at concentrations of 20 µM and 40 µM, making it difficult to conclude a true inhibition. Since none of the treatments with the four small molecules exhibited sufficient inhibition of enzyme activity, the determination of their IC_{50} values was not possible (Figures 25-28). In summary, the final results suggested that none of the four small molecules was able to inhibit acetylcholinesterase activity, as there were no noticeable signs of inhibition.

Chapter 3

Investigating the Effect of Mushroom Extracts on Acetylcholinesterase Activity

3.1 Introduction

The rationale for examining the effects of the following mushroom extracts on acetylcholinesterase activity was already provided on pages 34 to 38 in Chapter 1: *Agaricus subrufescens* 295E1-E3, *Amanita muscaria* 243E1-E3, *Ganoderma applanatum* M5E1-E3, *Hericium erinaceus* 288E1 and E3, *Inonotus obliquus* 285E1-E3, *Phellinus igniarius* PIE1-E3, *Phellinus pini* 91E1-E3, *Pleurotus ostreatus* 68E1 and E2.

3.2 Materials and Methods

3.2.1 Preparation of the Mushroom Extracts

3.2.1.1 Extraction of the Mushroom Extracts

All mushroom extracts, available in powder form, were provided by members of the Lee research group. The crude extracts were prepared using the following procedure.

Before the extraction commenced, all mushroom specimens were manually ground into fine powder. Subsequently, for one specimen, approximately 1 g of powder was extracted with 10 mL of 80% ethanol at 65°C for 3 h while being continuously stirred in a small beaker. The resulting solution was filtered through gravity filtration and labeled as E1.

The unfiltered residues remaining from the first extraction were subjected to a second extraction with 10 mL of 50% methanol at 65°C for 3 h, also with continuous stirring. Afterwards, this solution was filtered through gravity filtration again and labeled as E2.

Following the same procedure, the unfiltered residues remaining from the second extraction were subjected to a third extraction with 10 mL of autoclaved water at 65°C for 3 h

while being continuously stirred. Afterwards, this solution was filtered through gravity filtration again and labeled as E3.

Subsequently, all three types of solutions were subjected to rotary evaporation to remove the solvents. The remaining substances were further dried to form crude extracts through lyophilization with a Labconco freeze dryer. Finally, the crude extracts of all mushroom specimens were individually resuspended in different solvents, as outlined in the table below (Table 7).⁵⁰

Mushroom Species	Extract	Solvent Used to Extract
<i>Agaricus subrufescens</i>	295E1	80% Ethanol
	295E2	50% Methanol
	295E3	Water
<i>Amanita muscaria</i>	243E1	80% Ethanol
	243E2	50% Methanol
	243E3	Water
<i>Ganoderma applanatum</i>	M5E1	80% Ethanol
	M5E2	50% Methanol
	M5E3	Water
<i>Hericium erinaceus</i>	288E1	80% Ethanol
	288E3	Water
<i>Inonotus obliquus</i>	285E1	80% Ethanol
	285E2	50% Methanol
	285E3	Water
<i>Phellinus igniarius</i>	PIE1	80% Ethanol
	PIE2	50% Methanol
	PIE3	Water
<i>Phellinus pini</i>	91E1	80% Ethanol
	91E2	50% Methanol
	91E3	Water
<i>Pleurotus ostreatus</i>	68E1	80% Ethanol
	68E2	50% Methanol

Table 7. Summary of the Preparation of the Mushroom Extracts.

The crude extracts of all mushroom specimens were resuspended in different solvents as indicated.

3.3 Results and Discussion

3.3.1 Evaluation of the Effect of Crude Mushroom Extracts on Acetylcholinesterase

Activity

3.3.1.1 Experimental Procedure

The experiment setup was similar to what was previously planned and setup for the experimentation with the small molecules, as described in Chapter 2, with a few minor adjustments. Experiments were carried out using 96-well microtiter plates. In this test, all five components of the assay were included: sodium phosphate buffer, *Electrophorus electricus* acetylcholinesterase, acetylthiocholine iodide, DTNB, and a mushroom extract as the test sample. On the plate, each row was divided into four different control wells and five different treatment wells.

For the control wells, there were four different types: first negative control, second negative control, first positive control, and second positive control.

In the first negative control well, the following components were added: 180 μL of 0.1 M of sodium phosphate buffer at pH 8.0, 10 μL of 10 mM of DTNB, and 10 μL of 14 mM of acetylthiocholine iodide.

In the second negative control well, the following components were added: 170 μL of 0.1 M of sodium phosphate buffer at pH 8.0, 10 μL of 10 mM of DTNB, and 20 μL of 0.09 units/mL of acetylcholinesterase.

In the first positive control well, the following components were added: 160 μL of 0.1 M of sodium phosphate buffer at pH 8.0, 10 μL of 10 mM of DTNB, 20 μL of 0.09 units/mL of acetylcholinesterase, and 10 μL of 14 mM of acetylthiocholine iodide.

In the second positive control well, the following components were added: 140 μL of 0.1 M of sodium phosphate buffer at pH 8.0, 10 μL of 10 mM of DTNB, 20 μL of 0.09 units/mL of

acetylcholinesterase, 20 μL of a specific concentration of a solvent used to resuspend the powder of the mushroom extract, and 10 μL of 14 mM of acetylthiocholine iodide.

In each treatment well, the following components were added: 140 μL of 0.1 M of sodium phosphate buffer at pH 8.0, 10 μL of 10 mM of DTNB, 20 μL of 0.09 units/mL of acetylcholinesterase, 20 μL of a specific concentration of a mushroom extract, and 10 μL of 14 mM of acetylthiocholine iodide. The concentration of the crude mushroom extract was divided into five increasing concentrations ordered from least to most concentrated: 0.1875, 0.375, 0.75, 1.5, and 3.0 mg/mL. Once all concentrations of the mushroom extract were added to the treatment wells, the wells underwent a 15-min incubation period before acetylthiocholine iodide was introduced to initiate the assay.

There were three rows in total, each representing one technical replicate. The three technical replicates were combined to form one experimental replicate corresponding to a single run. For each experimental replicate, the change in the absorbance of TNB^{2-} was detected at the 412-nm wavelength and recorded every 2 mins for a total of 30 mins using the Synergy 2 plate reader machine. A total of two experimental replicates were performed for each of two mushroom extracts, one known to inhibit acetylcholinesterase activity and another extract from the group under investigation. A total of four experimental replicates were performed, pairing one extract known to inhibit acetylcholinesterase activity and another extract from the group under investigation, forming one experimental set.

3.3.1.2 Hypothesis and Predicted Outcomes

According to the hypothesis, if a mushroom extract contains any substance that acts as an acetylcholinesterase inhibitor, as the extract concentration increases, the linear rate of TNB^{2-} absorbance increase should slow down, leading to a smaller change in the absorbance. This gradual

decrease would cause the initially steep incline, which starts at a certain degree, to flatten into a straight horizontal line.

On a dose-response graph where the percentage of enzyme activity is plotted against the concentration of mushroom extract, an increase in the concentration of the mushroom extract by factors of ten should result in a decrease in the percentage of enzyme activity. This decrease should follow a sigmoidal trend, producing a reverse S-shaped curve.

3.3.1.3 Observations and Analyses

With the current limited knowledge of the *in vitro* bioactivity of mushroom extracts on acetylcholinesterase activity, the range of extract concentration used in this experimentation initially ranged from 0.0937 mg/mL to 1.5 mg/mL. This choice was based on a common observation that various mushroom species, which have previously been studied, contain natural substances primarily extracted using either methanol or water. These substances typically exhibit an inhibition of acetylcholinesterase activity in the range of approximately 10% to 30% when their concentration is around 0.2 mg/mL. Utilizing this critical information as a reference point, a reasonable and appropriate extrapolation was made in both directions to establish a concentration range from 0.0937 mg/mL to 1.5 mg/mL.

After determining this range, it was applied to conduct the experimentation on the following crude mushroom extracts: *Phellinus igniarius* PIE3, *Phellinus igniarius* PIE2, *Ganoderma applanatum* M5E3, and *Ganoderma applanatum* M5E1. Furthermore, considering that only *Pleurotus ostreatus* has been extensively studied as possessing an inhibitory effect on acetylcholinesterase activity, the *Pleurotus ostreatus* 68E1 extract was used as the control in the initial phase of the experimentation.³¹

Based on the mean data from two experimental replicates, a graph showing the percentage of enzyme activity plotted against concentration for two different mushroom extracts was created. In each experimental set, the potential inhibitory effect of the *Pleurotus ostreatus* 68E1 extract was used as the positive control to establish a relative standard for determining the inhibition strength on acetylcholinesterase activity for the four mushroom extracts mentioned earlier, should any of them inhibit the enzyme activity.

Throughout the four experimental sets, despite a successive increase in the concentration of the *Pleurotus ostreatus* 68E1 extract by a factor of two, ranging from 0.0937 mg/mL to 1.5 mg/mL, the percentage of enzyme activity was reduced by at most approximately 15% (Figures 29-32). Considering the low data variability, as indicated by the relatively small standard deviation bars around each mean data point, it was evident that the extent of acetylcholinesterase activity inhibition upon treatment with the *Pleurotus ostreatus* 68E1 extract was consistent with the common 13% inhibition value reported in the current literature when acetylcholinesterase was treated with the methanol extract of *Pleurotus ostreatus* at a concentration exceeding 0.2 mg/mL (Figures 29-32).³¹

Unlike the control *Pleurotus ostreatus* 68E1, there appeared to be no inhibition of acetylcholinesterase activity upon treatment with the *Phellinus igniarius* PIE3, *Phellinus igniarius* PIE2, nor *Ganoderma applanatum* M5E3 extract (Figures 29-31). Surprisingly, there was a sudden and consistent increase in the percentage of enzyme activity when acetylcholinesterase was treated individually with any of the three extracts. This abnormality was accompanied by high data variability, indicated by slightly broader standard deviation bars around each mean data point, raising questions about the legitimacy of the observed trend (Figures 29-31). Even if it were the case, it remained unclear what could be causing this seemingly stimulatory effect on

acetylcholinesterase activity, as no further conclusive evidences were obtained from subsequent experimentation. Nonetheless, within the scope of this study, these three mushroom extracts of *Phellinus igniarius* PIE3, *Phellinus igniarius* PIE2, and *Ganoderma applanatum* M5E3 were ruled out as potential candidates for acetylcholinesterase inhibition.

***In Vitro* Acetylcholinesterase Activity in the Presence of *Phellinus igniarius* PIE3 Extract**

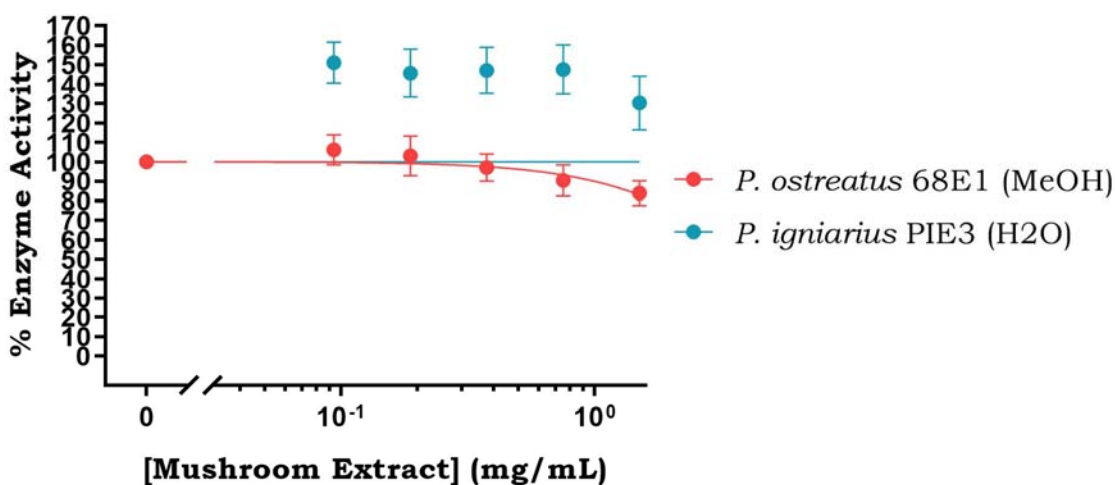


Figure 29. The Effect of *Phellinus igniarius* PIE3 on Acetylcholinesterase Activity at Low Extract Concentrations.

The shift in percentage of *in vitro* acetylcholinesterase activity when the enzyme was separately exposed to increasing concentrations of mushroom extracts, ranging from 0.0937 mg/mL to 1.5 mg/mL, over a 30-min time span. *Pleurotus ostreatatus* 68E1 is a mushroom extract known to inhibit acetylcholinesterase. *Phellinus igniarius* PIE3 is a mushroom extract that was used to test for an inhibitory effect on acetylcholinesterase activity. Each data point on the graph represented the mean percentage value of acetylcholinesterase activity recorded for the treatment with one specific mushroom extract, and at one specific extract concentration. Each mean percentage value of acetylcholinesterase activity was averaged from two experimental replicates, corresponding to six technical replicates (n = 6). Each set of upper and lower bars surrounding each data point on the graph represented the standard deviation of a mean percentage value of acetylcholinesterase activity.

On a side note, regarding the two missing mean data points at the higher extract concentration end of the *Phellinus igniarius* PIE2 data, they were excluded due to the solution's opaqueness in the treatment wells of the last two highest extract concentrations. This opaqueness

resulted in an extremely high background level, far exceeding the upper limit of the plate reader machine's absorbance detection range. Theoretically, at this level of intensity, even the background absorbance, excluding the true absorbance from TNB^{2-} as a product of the reduction of DTNB, could not be accurately measured as a numerical value. This is because the designated wavelength, which is supposed to pass through the solution after being emitted from the plate reader machine, may barely penetrate the solution, leading the machine to mistakenly determine that the solution has an infinitely high absorbance. Therefore, with careful consideration, these two missing mean data points representing the outcome of the treatment of acetylcholinesterase with either 0.75 mg/mL or 1.5 mg/mL of the *Phellinus igniarius* PIE2 extract were disregarded (Figure 30).

***In Vitro* Acetylcholinesterase Activity
in the Presence of *Phellinus igniarius* PIE2 Extract**

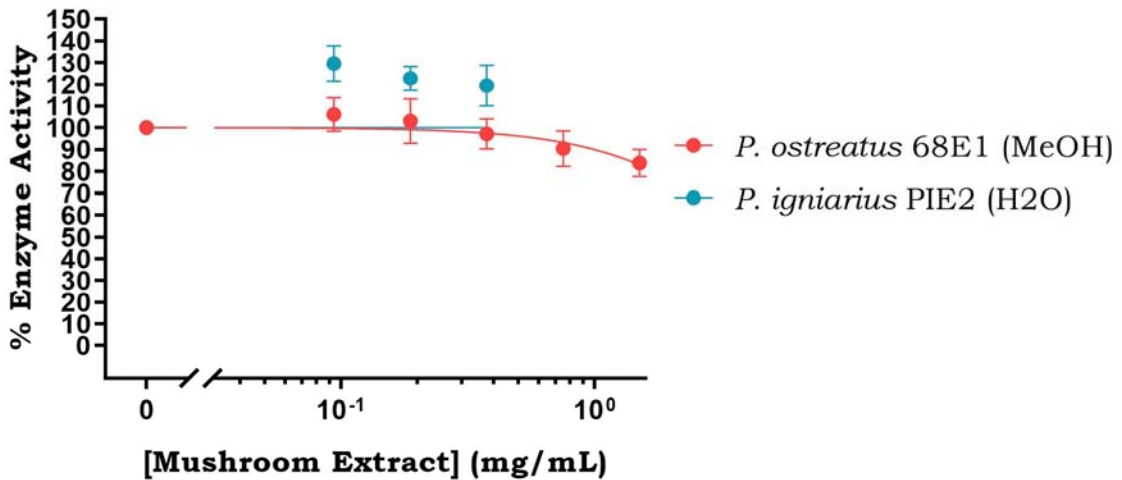


Figure 30. The Effect of *Phellinus igniarius* PIE2 on Acetylcholinesterase Activity at Low Extract Concentrations.

The shift in percentage of *in vitro* acetylcholinesterase activity when the enzyme was separately exposed to increasing concentrations of mushroom extracts, ranging from 0.0937 mg/mL to 1.5 mg/mL, over a 30-min time span. *Pleurotus ostreatus* 68E1 is a mushroom extract known to inhibit acetylcholinesterase. *Phellinus igniarius* PIE2 is a mushroom extract that was used to test for an inhibitory effect on acetylcholinesterase activity. Each data point on the graph represented the mean percentage value of acetylcholinesterase activity recorded for the treatment with one specific mushroom extract, and at one specific extract concentration. Each mean percentage value of acetylcholinesterase activity was averaged from two experimental replicates, corresponding to six technical replicates (n = 6). Each set of upper and lower bars surrounding each data point on the graph represented the standard deviation of a mean percentage value of acetylcholinesterase activity.

***In Vitro* Acetylcholinesterase Activity in the Presence of *Ganoderma applanatum* M5E3 Extract**

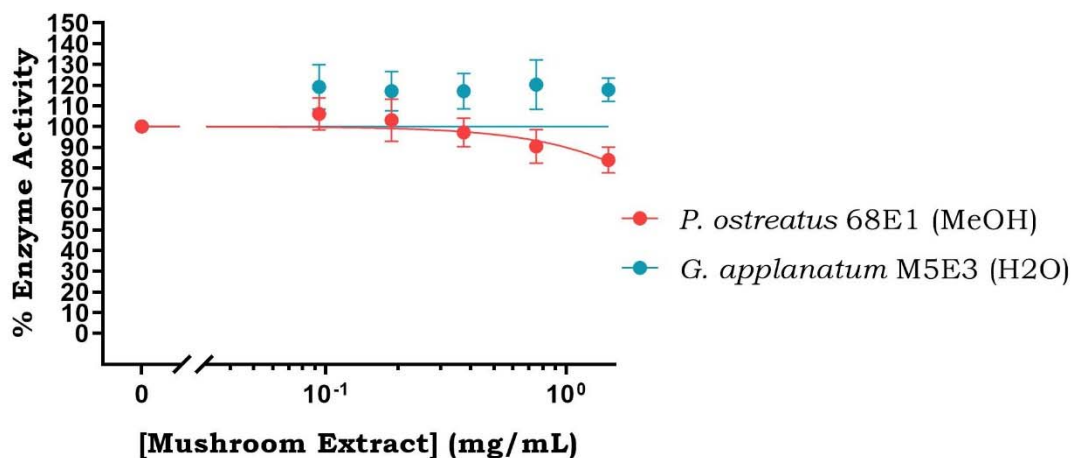


Figure 31. The Effect of *Ganoderma applanatum* M5E3 on Acetylcholinesterase Activity at Low Extract Concentrations.

The shift in percentage of *in vitro* acetylcholinesterase activity when the enzyme was separately exposed to increasing concentrations of mushroom extracts, ranging from 0.0937 mg/mL to 1.5 mg/mL, over a 30-min time span. *Pleurotus ostreatus* 68E1 is a mushroom extract known to inhibit acetylcholinesterase. *Ganoderma applanatum* M5E3 is a mushroom extract that was used to test for an inhibitory effect on acetylcholinesterase activity. Each data point on the graph represented the mean percentage value of acetylcholinesterase activity recorded for the treatment with one specific mushroom extract, and at one specific extract concentration. Each mean percentage value of acetylcholinesterase activity was averaged from two experimental replicates, corresponding to six technical replicates (n = 6). Each set of upper and lower bars surrounding each data point on the graph represented the standard deviation of a mean percentage value of acetylcholinesterase activity.

Among the four mushroom extracts experimented in the initial phase, only the *Ganoderma applanatum* M5E1 extract exhibited an inhibition of acetylcholinesterase activity. When comparing the inhibition strength displayed by the *Pleurotus ostreatus* 68E1 extract, there was a similarity in strength when the enzyme was treated individually with either of the extracts at concentrations ranging from 0.0937 mg/mL to 0.375 mg/mL. However, this similarity gradually diverged as the extract concentration increased beyond 0.375 mg/mL.

During the transition from 0.375 mg/mL to 1.5 mg/mL, the *Pleurotus ostreatus* 68E1 extract actually exhibited a slightly greater inhibition strength than the *Ganoderma applanatum*

M5E1 extract. This trend continued until the extract concentration approached very close to 1.5 mg/mL, at which point there was a sharp decline in the percentage of acetylcholinesterase activity observed for the treatment with the *Ganoderma applanatum* M5E1 extract. This decline allowed the inhibition strength exerted by the *Ganoderma applanatum* M5E1 extract to surpass that of the *Pleurotus ostreatus* 68E1 extract.

Visualizing the data at the intersection point between the *Pleurotus ostreatus* 68E1 and the *Ganoderma applanatum* M5E1 data, assuming there was an imaginary line perpendicular to the trendline of the *Pleurotus ostreatus* 68E1 data passing through the intersection point, it could be observed that the sharp decline in the trendline of the *Ganoderma applanatum* M5E1 data near the 1.5 mg/mL-concentration mark deviated almost 45° degrees as it surpassed away from the trendline of the *Pleurotus ostreatus* 68E1 data. At 1.5 mg/mL, exceeding the approximate 15% inhibition strength exerted by the *Pleurotus ostreatus* 68E1 extract, the *Ganoderma applanatum* M5E1 extract exhibited an approximate inhibition strength of 21% (Figure 32).

Based on this observation, it was postulated that the *Ganoderma applanatum* M5E1 data may hold promise as the most potent candidate for acetylcholinesterase inhibition in the initial phase of the experimentation. Consequently, it was decided that a higher concentration range from 0.375 mg/mL to 5.0 mg/mL of *Ganoderma applanatum* M5E1 should be further investigated.

***In Vitro* Acetylcholinesterase Activity in the Presence of *Ganoderma applanatum* M5E1 Extract**

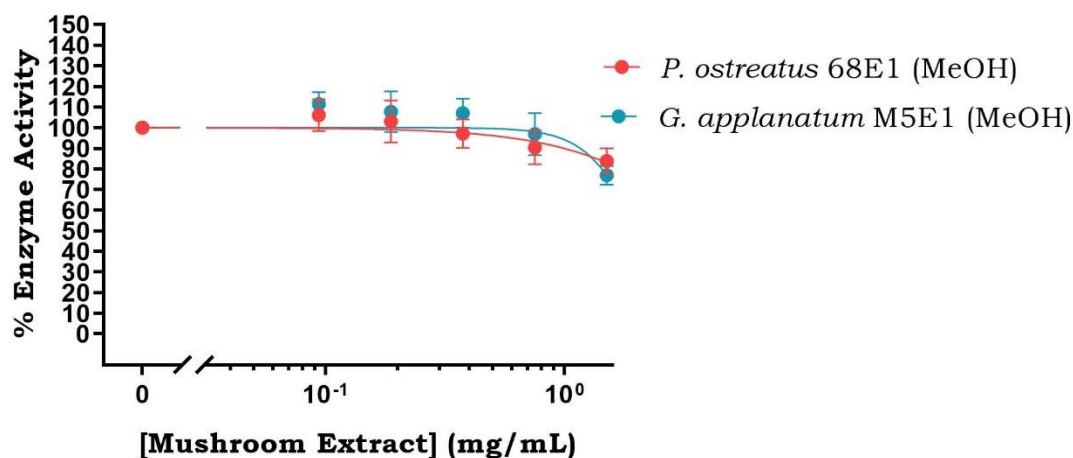


Figure 32. The Effect of *Ganoderma applanatum* M5E1 on Acetylcholinesterase Activity at Low Extract Concentrations.

The shift in percentage of *in vitro* acetylcholinesterase activity when the enzyme was separately exposed to increasing concentrations of mushroom extracts, ranging from 0.0937 mg/mL to 1.5 mg/mL, over a 30-min time span. *Pleurotus ostreatus* 68E1 is a mushroom extract known to inhibit acetylcholinesterase. *Ganoderma applanatum* M5E1 is a mushroom extract that was used to test for an inhibitory effect on acetylcholinesterase activity. Each data point on the graph represented the mean percentage value of acetylcholinesterase activity recorded for the treatment with one specific mushroom extract, and at one specific extract concentration. Each mean percentage value of acetylcholinesterase activity was averaged from two experimental replicates, corresponding to six technical replicates ($n = 6$). Each set of upper and lower bars surrounding each data point on the graph represented the standard deviation of a mean percentage value of acetylcholinesterase activity.

Utilizing the established null results of the *Phellinus igniarius* PIE3, *Phellinus igniarius* PIE2, and *Ganoderma applanatum* M5E3 data to an advantage, one of these three extracts was selected to be the negative control and paired with the *Ganoderma applanatum* M5E1 data in the second phase of the experimentation. That chosen extract was the *Ganoderma applanatum* M5E3 extract. In terms of the experimental results, there was no particularly significant detail that favored the selection of the *Ganoderma applanatum* M5E3 extract as the negative control over the other two. The choice was based on one of the fundamental principles of scientific experimentation.

When applying the scientific method to any experiment, apart from varying levels of one or more independent variable of interest, all other variables should be tightly controlled to maintain their constant state. This is done to ensure that the influence exerted by the independent variable(s) on the subject of interest is directly responsible for the observed outcome measured by the dependent variable with an intrinsic connection to the subject of interest. In this experimentation, there were two independent variables: the concentration of a mushroom extract and the type of mushroom extract. Regarding the type of extract, as there were different mushroom species, and each species had different extracts extracted using different solvents or solvent combinations, it was preferable to have a relative comparison between two types of extract derived from the same species on a graph whenever possible. This approach helped maintain consistency and aesthetics in presenting the experimental results.

By extending the extract concentration range to a higher level, the inhibitory effect on acetylcholinesterase activity exerted by the *Ganoderma applanatum* M5E1 extract became more apparent (Figure 33). At 1.5 mg/mL, the approximate inhibition strength was 31%. With a standard deviation of approximately 10%, the mean data point closely matched the approximate inhibition strength of 21% observed in the *Ganoderma applanatum* M5E1 data during its participation in the initial phase of the experimentation. At 3.0 mg/mL, the approximate inhibition strength further increased to 62%, which was twice the strength observed for the previous mean data point. Although the standard deviation of the mean data point at 3.0 mg/mL had slightly more variation than the one at 1.5 mg/mL, there was no overlap between the two mean data points, indicating that the robust increase in inhibition strength was authentic. Unfortunately, similar to the previous case of the two missing mean data points for the last two highest extract concentrations of the *Phellinus igniarius* PIE2 data, the solution at 5.0 mg/mL was too opaque, resulting in an extremely high

background absorbance beyond the detection capability of the plate reader machine. As a result, the mean data point at 5.0 mg/mL of the *Ganoderma applanatum* M5E1 data was also disregarded. Nonetheless, the approximate inhibition strength exerted by the extract at 5.0 mg/mL could still be estimated to be around 80% through trendline extrapolation. Despite these challenges, the entire *Ganoderma applanatum* M5E1 dataset was sufficient to determine an IC₅₀ value of 2.320 mg/mL (Figure 33).

***In Vitro* Acetylcholinesterase Activity in the Presence of *Ganoderma applanatum* Extracts**

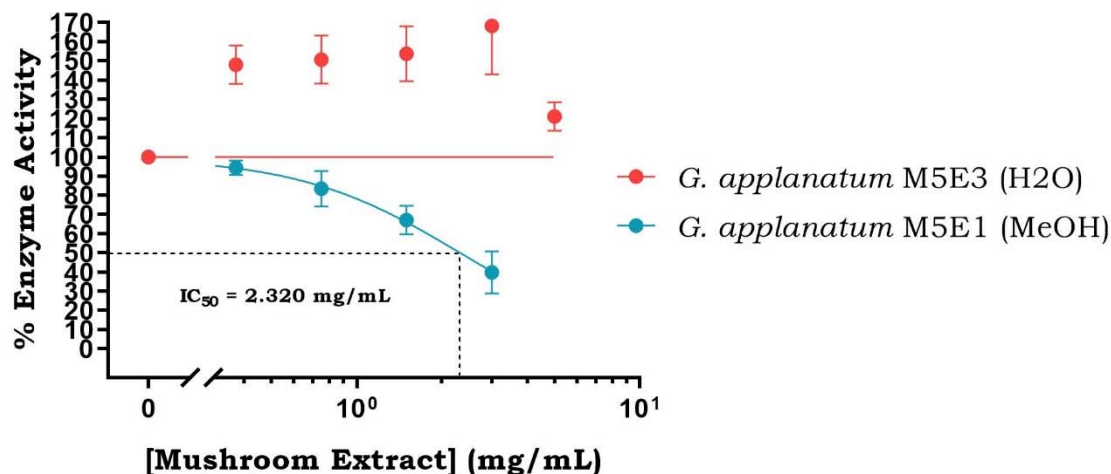


Figure 33. The Effect of *Ganoderma applanatum* M5E1 on Acetylcholinesterase Activity at High Extract Concentrations.

The shift in percentage of *in vitro* acetylcholinesterase activity when the enzyme was separately exposed to increasing concentrations of mushroom extracts, ranging from 0.1875 mg/mL to 3.0 mg/mL, over a 30-min time span. *Ganoderma applanatum* M5E3 is a mushroom extract used as the negative control. *Ganoderma applanatum* M5E1 is a mushroom extract that was used to test for an inhibitory effect on acetylcholinesterase activity. Each data point on the graph represented the mean percentage value of acetylcholinesterase activity recorded for the treatment with one specific mushroom extract, and at one specific extract concentration. Each mean percentage value of acetylcholinesterase activity was averaged from two experimental replicates, corresponding to six technical replicates (n = 6). Each set of upper and lower bars surrounding each data point on the graph represented the standard deviation of a mean percentage value of acetylcholinesterase activity. The IC₅₀ value represented the concentration of *Ganoderma applanatum* M5E1 required to inhibit acetylcholinesterase activity by 50%.

In contrast to the *Ganoderma applanatum* M5E1 data, the *Ganoderma applanatum* M5E3 data exhibited a significant spike in the percentage of enzyme activity when acetylcholinesterase was treated with the extract. Furthermore, when compared to the *Ganoderma applanatum* M5E3 data from its previous experimental set during the initial phase of the experimentation, the percentage of enzyme activity for all mean data points, except the one at 5.0 mg/mL, increased by approximately 30%, and even as high as 50% for the one at 3.0 mg/mL. This spike in activity was also in line with the previous results seen in the *Phellinus igniarius* PIE3 data. As previously mentioned, whether this apparent stimulatory effect on acetylcholinesterase activity induced by the *Ganoderma applanatum* M5E3 extract was real or not would require further experimentation to obtain more conclusive evidences. However, at the moment, based solely on the inconsistency in the data between the four experimental replicates and the fairly large overlapping standard deviation among most of the mean data points, it appeared that there may not be any significant biochemical effect on acetylcholinesterase activity exerted by the *Ganoderma applanatum* M5E3 extract.

Overall, with the data gathered from the second phase of the experimentation, it was confirmed that the *Ganoderma applanatum* M5E1 extract did indeed inhibit acetylcholinesterase activity, and this inhibitory effect was significant. Additionally, as there was a potential issue with solutions containing a mushroom extract at the concentration of 5.0 mg/mL being too opaque for their absorbance to be measured by the plate reader machine, the extract concentration range was subsequently adjusted to range from 0.1875 mg/mL to 3.0 mg/mL. This range was then used to experiment with the remaining mushroom extracts to assess their potential inhibitory effects on acetylcholinesterase activity in the final phase of the experimentation (Figure 33).

In many ways, the third phase of the experimentation resembled the initial phase. The only change made was in the choice of the control. Instead of using *Pleurotus ostreatus* 68E1, the *Ganoderma applanatum* M5E1 extract was employed as the positive control. This decision was based on the fact that the *Ganoderma applanatum* M5E1 extract exhibited a stronger inhibitory effect on acetylcholinesterase activity, making it a more suitable relative standard for evaluating the inhibition strength of the remaining mushroom extracts, should any of them exhibit a significant inhibitory effect.

Out of the remaining extracts, an additional seven were found to inhibit acetylcholinesterase. These extracts, along with the *Ganoderma applanatum* M5E1 extract, were ranked in the following order from the weakest to the strongest inhibition strength, as indicated by their IC₅₀ values, from highest to lowest: *Hericium erinaceus* 288E3 with an IC₅₀ value of 3.866 mg/mL, *Ganoderma applanatum* M5E2 with an IC₅₀ value of 3.038 mg/mL, *Ganoderma applanatum* M5E1 with an IC₅₀ value of 2.320 mg/mL, *Amanita muscaria* 243E1 with an IC₅₀ value of 1.380 mg/mL, *Agaricus subrufescens* 295E1 with an IC₅₀ value of 1.230 mg/mL, *Agaricus subrufescens* 295E2 with an IC₅₀ value of 1.110 mg/mL, *Hericium erinaceus* 288E1 with an IC₅₀ value of 1.060 mg/mL, and *Inonotus obliquus* 285E1 with an IC₅₀ value of 0.980 mg/mL (Table 8 and Figures 34-40).

Mushroom Species	Extract	IC₅₀ [mg/mL]	Maximum Inhibition
<i>Agaricus subrufescens</i>	295E1	1.230	83.00% at 3.000 mg/mL
	295E2	1.110	87.00% at 3.000 mg/mL
<i>Amanita muscaria</i>	243E1	1.380	67.00% at 3.000 mg/mL
<i>Ganoderma applanatum</i>	M5E1	2.320	62.00% at 3.000 mg/mL
	M5E2	3.038	48.00% at 3.000 mg/mL
<i>Hericium erinaceus</i>	288E1	1.060	78.00% at 3.000 mg/mL
	288E3	3.866	39.00% at 3.000 mg/mL
<i>Inonotus obliquus</i>	285E1	0.980	91.00% at 3.000 mg/mL
<i>Pleurotus ostreatus</i>	68E1	N/A	16.00% at 1.500 mg/mL

Table 8. Summary of Mushroom Extracts that Inhibited Acetylcholinesterase Activity.

A list of mushroom extracts found to inhibit the *in vitro* acetylcholinesterase activity in this study. The IC₅₀ value represented the concentration of a mushroom extract required to inhibit acetylcholinesterase activity by 50%. The maximum inhibition represented a mushroom extract's highest level of inhibition on acetylcholinesterase activity, based on observations recorded from the conducted experiments.

Although the ranking of the inhibition strength followed this order, the ranking of the approximate maximum inhibition strength at 3.0 mg/mL, the highest extract concentration tested in the third phase of the experimentation, did not necessarily align with the same order. It was ranked from the weakest to the strongest approximate maximum inhibition strength, as indicated by the percentage of acetylcholinesterase activity inhibited: *Hericium erinaceus* 288E3 at 39%, *Ganoderma applanatum* M5E2 at 48%, *Ganoderma applanatum* M5E1 at 62%, *Amanita muscaria* 243E1 at 67%, *Hericium erinaceus* 288E1 at 78%, *Agaricus subrufescens* 295E1 at 83%, *Agaricus subrufescens* 295E2 at 87%, and *Inonotus obliquus* 285E1 at 91% (Table 8 and Figures 34-40).

Aside from the inhibition strength, the determination of the inhibition range for these mushroom extracts also took into consideration three key characteristics of the sigmoidal dosage-response curve: the breadth of the curve during the initial transition before it starts to climb or dive, the steepness of the linear segment around the inflection point, and the total length of the linear segment before the curve levels off.

Starting with *Hericium erinaceus* 288E3, its inhibition range was estimated to be from 0.75 mg/mL to 3.0 mg/mL. Despite having a fairly broad initial dive, and a moderately steep linear segment at the inflection point, its inhibition range was mostly limited by a very short total length of the linear segment, which quickly leveled off after 1.5 mg/mL to 3.0 mg/mL (Figure 34).

***In Vitro* Acetylcholinesterase Activity in the Presence of *Hericium erinaceus* 288E3 Extract**

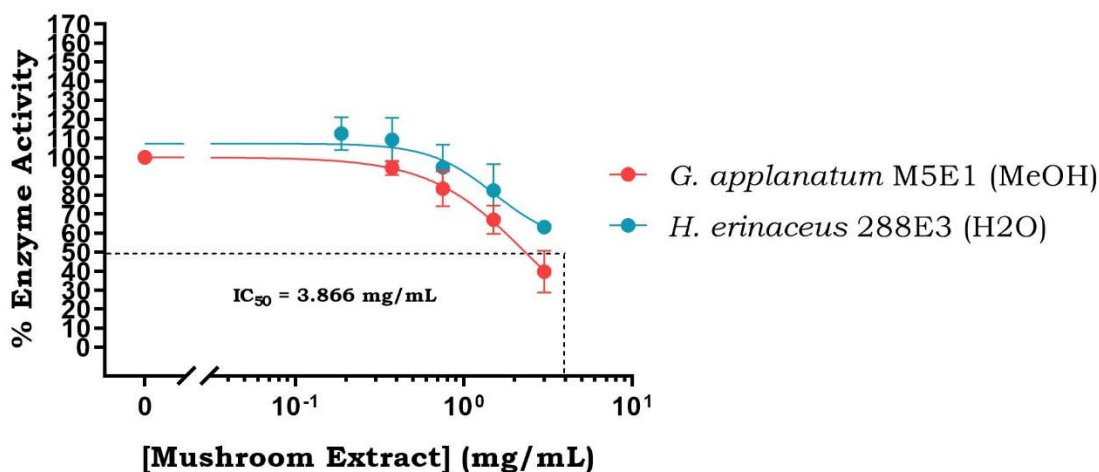


Figure 34. The Effect of *Hericium erinaceus* 288E3 on Acetylcholinesterase Activity at High Extract Concentrations.

The shift in percentage of *in vitro* acetylcholinesterase activity when the enzyme was separately exposed to increasing concentrations of mushroom extracts, ranging from 0.1875 mg/mL to 3.0 mg/mL, over a 30-min time span. *Ganoderma applanatum* M5E1 is a mushroom extract used as a controlled reference for comparison. *Hericium erinaceus* 288E3 is a mushroom extract that was used to test for an inhibitory effect on acetylcholinesterase activity. Each data point on the graph represented the mean percentage value of acetylcholinesterase activity recorded for the treatment with one specific mushroom extract, and at one specific extract concentration. Each mean percentage value of acetylcholinesterase activity was averaged from two experimental replicates, corresponding to six technical replicates (n = 6). Each set of upper and lower bars surrounding each data point on the graph represented the standard deviation of a mean percentage value of acetylcholinesterase activity. The IC₅₀ value represented the concentration of *Hericium erinaceus* 288E3 required to inhibit acetylcholinesterase activity by 50%.

Moving to *Ganoderma applanatum* M5E2, its inhibition range was estimated to be from 2.75 mg/mL to 3.5 mg/mL. In contrast to *Hericium erinaceus* 288E3, its inhibition range was very

restricted due to an acute initial dive, resulting in an extremely steep and extended linear plunge at the inflection point (Figure 35).

***In Vitro* Acetylcholinesterase Activity in the Presence of *Ganoderma applanatum* M5E2 Extract**

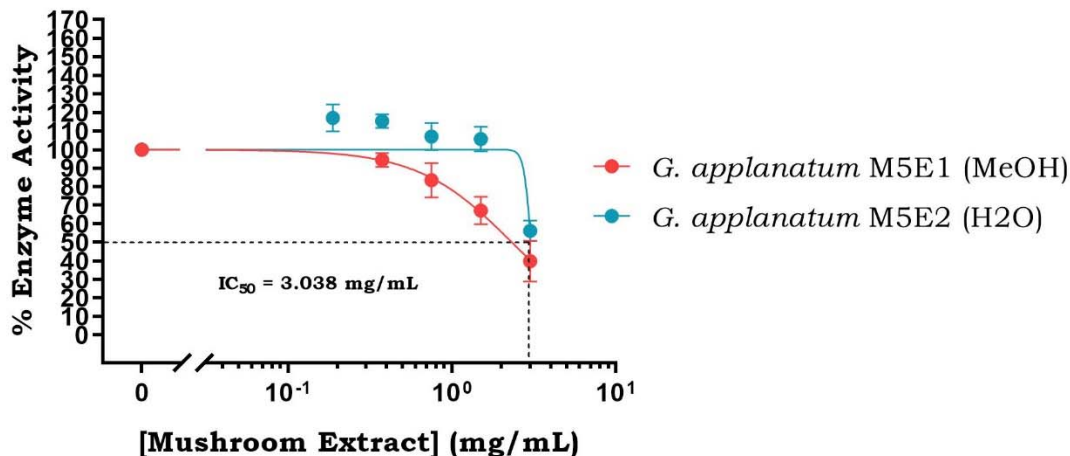


Figure 35. The Effect of *Ganoderma applanatum* M5E2 on Acetylcholinesterase Activity at High Extract Concentrations.

The shift in percentage of *in vitro* acetylcholinesterase activity when the enzyme was separately exposed to increasing concentrations of mushroom extracts, ranging from 0.1875 mg/mL to 3.0 mg/mL, over a 30-min time span. *Ganoderma applanatum* M5E1 is a mushroom extract used as a controlled reference for comparison. *Ganoderma applanatum* M5E2 is a mushroom extract that was used to test for an inhibitory effect on acetylcholinesterase activity. Each data point on the graph represented the mean percentage value of acetylcholinesterase activity recorded for the treatment with one specific mushroom extract, and at one specific extract concentration. Each mean percentage value of acetylcholinesterase activity was averaged from two experimental replicates, corresponding to six technical replicates (n = 6). Each set of upper and lower bars surrounding each data point on the graph represented the standard deviation of a mean percentage value of acetylcholinesterase activity. The IC₅₀ value represented the concentration of *Ganoderma applanatum* M5E2 required to inhibit acetylcholinesterase activity by 50%.

Amanita muscaria 243E1 had an estimated inhibition range from 0.375 mg/mL to 4.0 mg/mL. Similar to *Hericium erinaceus* 288E3, but with a broader initial dive, and a slightly steeper and longer total length of the linear segment at the inflection point, this allowed it to have an inhibition range generally wider than *Hericium erinaceus* 288E3 (Figure 36).

***In Vitro* Acetylcholinesterase Activity in the Presence of *Amanita muscaria* 243E1 Extract**

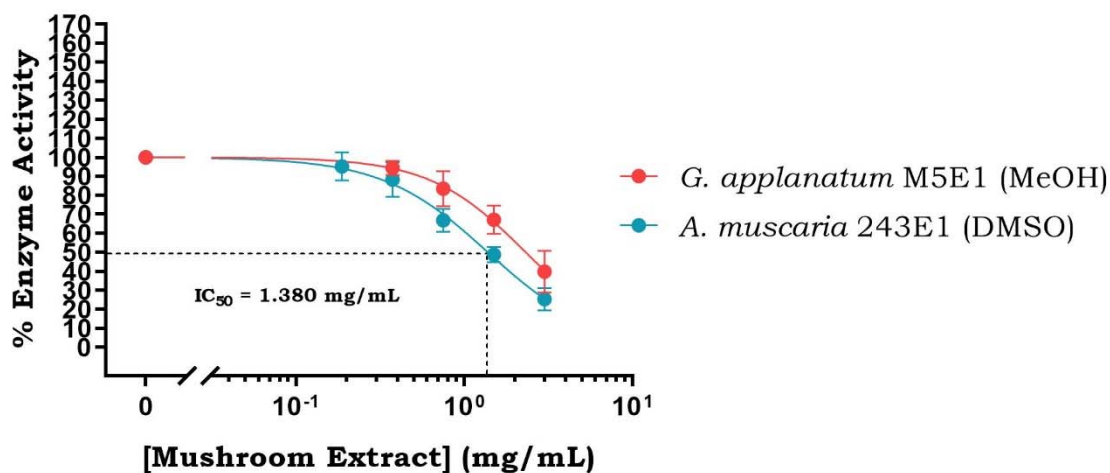


Figure 36. The Effect of *Amanita muscaria* 243E1 on Acetylcholinesterase Activity at High Extract Concentrations.

The shift in percentage of *in vitro* acetylcholinesterase activity when the enzyme was separately exposed to increasing concentrations of mushroom extracts, ranging from 0.1875 mg/mL to 3.0 mg/mL, over a 30-min time span. *Ganoderma applanatum* M5E1 is a mushroom extract used as a controlled reference for comparison. *Amanita muscaria* 243E1 is a mushroom extract that was used to test for an inhibitory effect on acetylcholinesterase activity. Each data point on the graph represented the mean percentage value of acetylcholinesterase activity recorded for the treatment with one specific mushroom extract, and at one specific extract concentration. Each mean percentage value of acetylcholinesterase activity was averaged from two experimental replicates, corresponding to six technical replicates (n = 6). Each set of upper and lower bars surrounding each data point on the graph represented the standard deviation of a mean percentage value of acetylcholinesterase activity. The IC₅₀ value represented the concentration of *Amanita muscaria* 243E1 required to inhibit acetylcholinesterase activity by 50%.

Remarkably, the sigmoidal dosage-response curves of *Agaricus subrufescens* 295E1 and *Agaricus subrufescens* 295E2 closely resembled that of *Amanita muscaria* 243E1. They all displayed nearly identical broad initial dives and similarly matched total lengths of the linear segment at the inflection point which also leveled off just after 3.0 mg/mL. The only difference was the steepness of the linear segment at the inflection point, with *Agaricus subrufescens* 295E2 being the steepest, and *Agaricus subrufescens* 295E1 and *Amanita muscaria* 243E1 being somewhat less steep but similar. As a result, both *Agaricus subrufescens* 295E1 and *Agaricus*

subrufescens 295E2 had an estimated inhibition range from 0.375 mg/mL to 4.0 mg/mL (Figures 37-38).

***In Vitro* Acetylcholinesterase Activity in the Presence of *Agaricus subrufescens* 295E1 Extract**

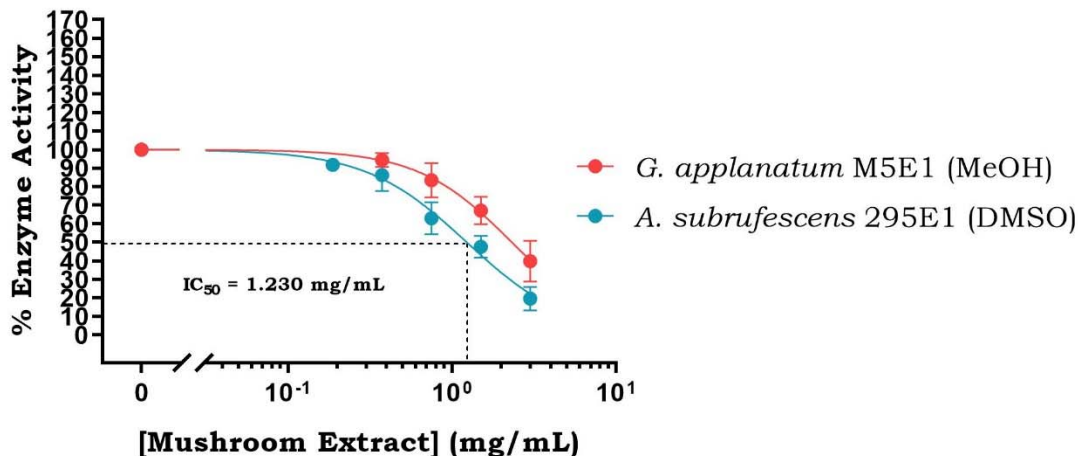


Figure 37. The Effect of *Agaricus subrufescens* 295E1 on Acetylcholinesterase Activity at High Extract Concentrations.

The shift in percentage of *in vitro* acetylcholinesterase activity when the enzyme was separately exposed to increasing concentrations of mushroom extracts, ranging from 0.1875 mg/mL to 3.0 mg/mL, over a 30-min time span. *Ganoderma applanatum* M5E1 is a mushroom extract used as a controlled reference for comparison. *Agaricus subrufescens* 295E1 is a mushroom extract that was used to test for an inhibitory effect on acetylcholinesterase activity. Each data point on the graph represented the mean percentage value of acetylcholinesterase activity recorded for the treatment with one specific mushroom extract, and at one specific extract concentration. Each mean percentage value of acetylcholinesterase activity was averaged from two experimental replicates, corresponding to six technical replicates (n = 6). Each set of upper and lower bars surrounding each data point on the graph represented the standard deviation of a mean percentage value of acetylcholinesterase activity. The IC₅₀ value represented the concentration of *Agaricus subrufescens* 295E1 required to inhibit acetylcholinesterase activity by 50%.

***In Vitro* Acetylcholinesterase Activity in the Presence of *Agaricus subrufescens* 295E2 Extract**

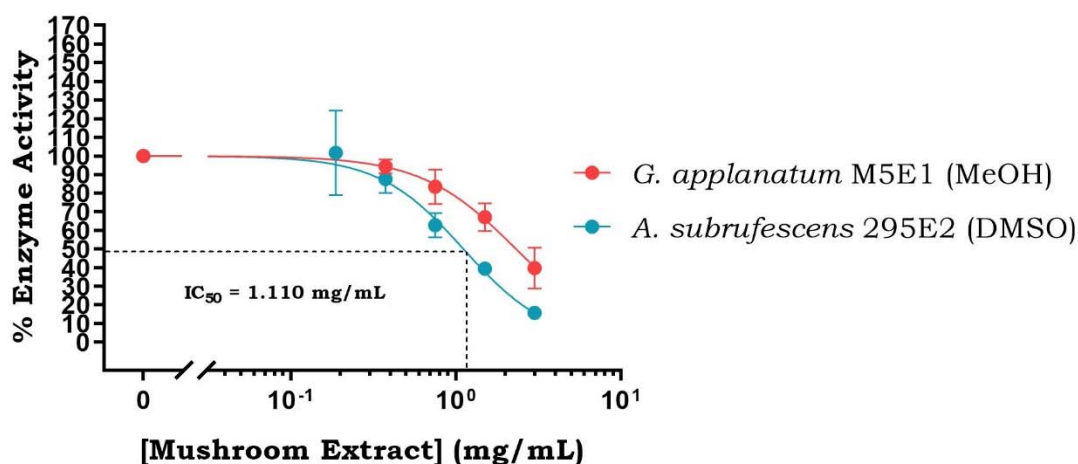


Figure 38. The Effect of *Agaricus subrufescens* 295E2 on Acetylcholinesterase Activity at High Extract Concentrations.

The shift in percentage of *in vitro* acetylcholinesterase activity when the enzyme was separately exposed to increasing concentrations of mushroom extracts, ranging from 0.1875 mg/mL to 3.0 mg/mL, over a 30-min time span. *Ganoderma applanatum* M5E1 is a mushroom extract used as a controlled reference for comparison. *Agaricus subrufescens* 295E2 is a mushroom extract that was used to test for an inhibitory effect on acetylcholinesterase activity. Each data point on the graph represented the mean percentage value of acetylcholinesterase activity recorded for the treatment with one specific mushroom extract, and at one specific extract concentration. Each mean percentage value of acetylcholinesterase activity was averaged from two experimental replicates, corresponding to six technical replicates ($n = 6$). Each set of upper and lower bars surrounding each data point on the graph represented the standard deviation of a mean percentage value of acetylcholinesterase activity. The IC_{50} value represented the concentration of *Agaricus subrufescens* 295E2 required to inhibit acetylcholinesterase activity by 50%.

Moving to *Hericium erinaceus* 288E1, its sigmoidal dosage-response curve resembled that of *Hericium erinaceus* 288E3 in terms of the steepness of the linear segment at the inflection point. However, the initial dive was much broader, even more extensive than that of *Amanita muscaria* 243E1, *Agaricus subrufescens* 295E1, and *Agaricus subrufescens* 295E2. Additionally, the total length of the linear segment of the curve extended to the degree where the point the curve began leveling off was beyond clear sight. This combination of characteristics led to an estimated inhibition range for *Hericium erinaceus* 288E1 from 0.0937 mg/mL to 5.0 mg/mL (Figure 39).

***In Vitro* Acetylcholinesterase Activity in the Presence of *Hericiium erinaceus* 288E1 Extract**

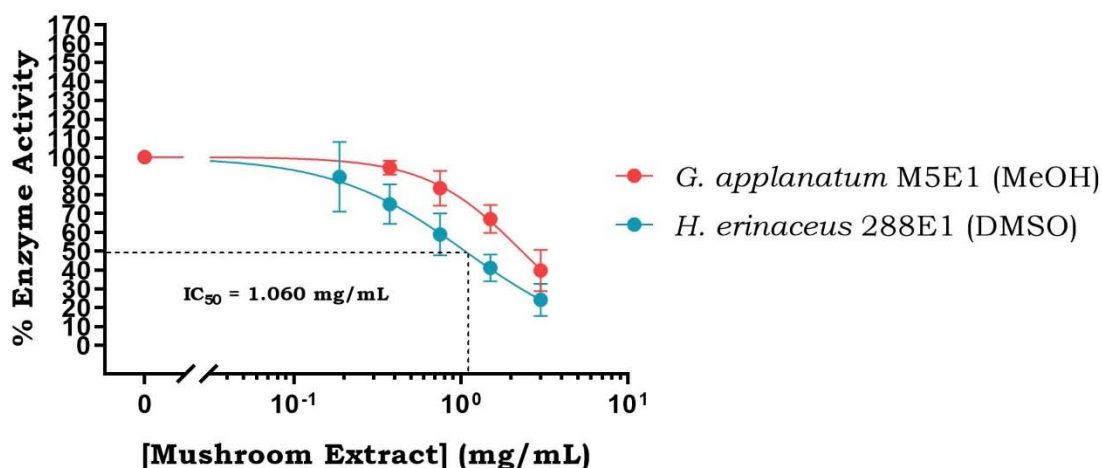


Figure 39. The Effect of *Hericiium erinaceus* 288E1 on Acetylcholinesterase Activity at High Extract Concentrations.

The shift in percentage of *in vitro* acetylcholinesterase activity when the enzyme was separately exposed to increasing concentrations of mushroom extracts, ranging from 0.1875 mg/mL to 3.0 mg/mL, over a 30-min time span. *Ganoderma applanatum* M5E1 is a mushroom extract used as a controlled reference for comparison. *Hericiium erinaceus* 288E1 is a mushroom extract that was used to test for an inhibitory effect on acetylcholinesterase activity. Each data point on the graph represented the mean percentage value of acetylcholinesterase activity recorded for the treatment with one specific mushroom extract, and at one specific extract concentration. Each mean percentage value of acetylcholinesterase activity was averaged from two experimental replicates, corresponding to six technical replicates (n = 6). Each set of upper and lower bars surrounding each data point on the graph represented the standard deviation of a mean percentage value of acetylcholinesterase activity. The IC₅₀ value represented the concentration of *Hericiium erinaceus* 288E1 required to inhibit acetylcholinesterase activity by 50%.

Lastly, the sigmoidal dosage-response curve of *Inonotus obliquus* 285E1 closely resembled that of *Hericiium erinaceus* 288E1 in every aspect, except for the steepness of the linear segment at the inflection point, where it was the steepest among all eight extracts exhibiting acetylcholinesterase inhibition. Consequently, the inhibition range of *Inonotus obliquus* 285E1 was estimated to be from 0.0937 mg/mL to 6.0 mg/mL (Figure 40).

***In Vitro* Acetylcholinesterase Activity in the Presence of *Inonotus obliquus* 285E1 Extract**

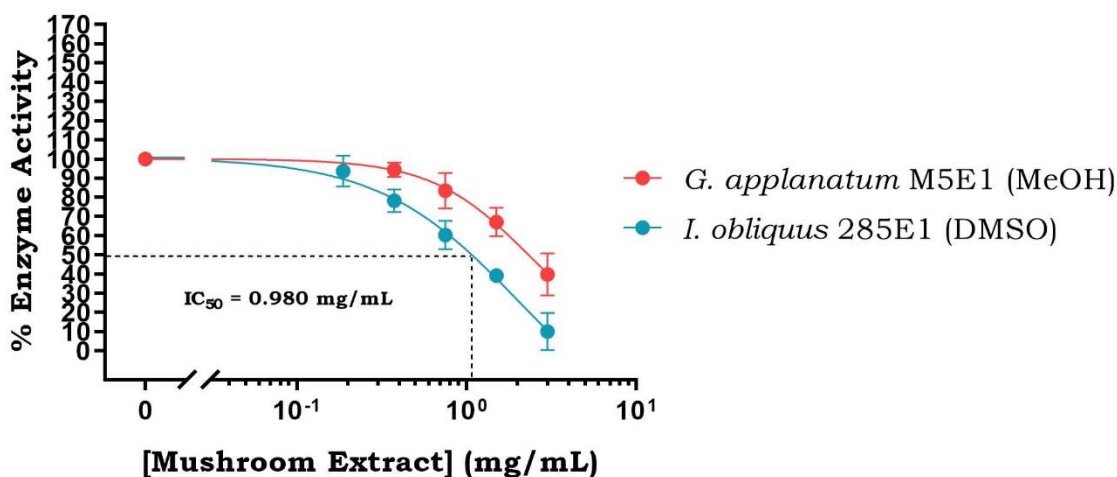


Figure 40. The Effect of *Inonotus obliquus* 285E1 on Acetylcholinesterase Activity at High Extract Concentrations.

The shift in percentage of *in vitro* acetylcholinesterase activity when the enzyme was separately exposed to increasing concentrations of mushroom extracts, ranging from 0.1875 mg/mL to 3.0 mg/mL, over a 30-min time span. *Ganoderma applanatum* M5E1 is a mushroom extract used as a controlled reference for comparison. *Inonotus obliquus* 285E1 is a mushroom extract that was used to test for an inhibitory effect on acetylcholinesterase activity. Each data point on the graph represented the mean percentage value of acetylcholinesterase activity recorded for the treatment with one specific mushroom extract, and at one specific extract concentration. Each mean percentage value of acetylcholinesterase activity was averaged from two experimental replicates, corresponding to six technical replicates (n = 6). Each set of upper and lower bars surrounding each data point on the graph represented the standard deviation of a mean percentage value of acetylcholinesterase activity. The IC₅₀ value represented the concentration of *Inonotus obliquus* 285E1 required to inhibit acetylcholinesterase activity by 50%.

Returning to *Ganoderma applanatum* M5E1, its initial dive was the broadest and most gradual of all mushroom extract datasets showing acetylcholinesterase inhibition. Combined with a steady decline in the percentage of acetylcholinesterase activity along its sigmoidal dosage-response curve, the inhibition range for *Ganoderma applanatum* M5E1 could potentially be extrapolated from 0.375 mg/mL up to 10.0 mg/mL (Figure 33).

In summary, the estimated acetylcholinesterase inhibition ranges for all eight mushroom extracts exhibiting acetylcholinesterase inhibition were ranked in the following order from the smallest to the largest range: *Ganoderma applanatum* M5E2 with a projected range from 2.75

mg/mL to 3.5 mg/mL, *Hericium erinaceus* 288E3 with a projected range from 0.75 mg/mL to 3.0 mg/mL, *Amanita muscaria* 243E1 and *Agaricus subrufescens* 295E1 and *Agaricus subrufescens* 295E2 with a projected range from 0.375 mg/mL to 4.0 mg/mL, *Hericium erinaceus* 288E1 with a projected range from 0.0937 mg/mL to 5.0 mg/mL, *Inonotus obliquus* 285E1 with a projected range from 0.0937 mg/mL to 6.0 mg/mL, and *Ganoderma applanatum* M5E1 with a projected range from 0.375 mg/mL to 10.0 mg/mL (Figures 33-40).

Regarding the mushroom extracts that did not inhibit acetylcholinesterase activity, their presence resulted in a higher percentage of acetylcholinesterase activity compared to the control wells lacking these extracts (Table 9 and Figures 41-50).

Mushroom Species	Extract	Solvent Used to Extract
<i>Agaricus subrufescens</i>	295E3	Water
<i>Amanita muscaria</i>	243E2	50% Methanol
	243E3	Water
<i>Ganoderma applanatum</i>	M5E3	Water
<i>Inonotus obliquus</i>	285E2	50% Methanol
	285E3	Water
<i>Phellinus igniarius</i>	PIE1	80% Ethanol
	PIE2	50% Methanol
	PIE3	Water
<i>Phellinus pini</i>	91E1	80% Ethanol
	91E2	50% Methanol
	91E3	Water
<i>Pleurotus ostreatus</i>	68E2	50% Methanol

Table 9. Summary of Mushroom Extracts that Were Negative for Acetylcholinesterase Activity Inhibition.

A list of mushroom extracts that did not inhibit the *in vitro* acetylcholinesterase activity in this study.

For some of these extracts, the increase in acetylcholinesterase activity compared to the standard controls was moderate, with a small standard deviation that was consistent across the extract concentration range, increasing successively by factors of two from 0.1875 mg/mL to 3.0 mg/mL. These extracts included *Amanita muscaria* 243E2, *Amanita muscaria* 243E3, *Agaricus*

subrufescens 295E3, *Inonotus obliquus* 285E2, *Inonotus obliquus* 285E3, and *Pleurotus ostreatus* 68E2 (Figures 41-46).

***In Vitro* Acetylcholinesterase Activity in the Presence of *Amanita muscaria* 243E2 Extract**

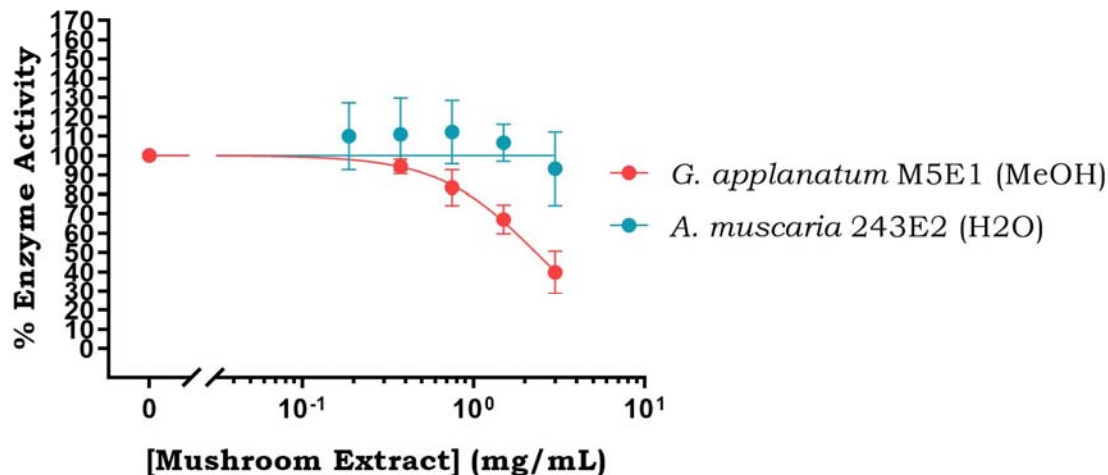


Figure 41. The Effect of *Amanita muscaria* 243E2 on Acetylcholinesterase Activity at High Extract Concentrations.

The shift in percentage of *in vitro* acetylcholinesterase activity when the enzyme was separately exposed to increasing concentrations of mushroom extracts, ranging from 0.1875 mg/mL to 3.0 mg/mL, over a 30-min time span. *Ganoderma applanatum* M5E1 is a mushroom extract used as a controlled reference for comparison. *Amanita muscaria* 243E2 is a mushroom extract that was used to test for an inhibitory effect on acetylcholinesterase activity. Each data point on the graph represented the mean percentage value of acetylcholinesterase activity recorded for the treatment with one specific mushroom extract, and at one specific extract concentration. Each mean percentage value of acetylcholinesterase activity was averaged from two experimental replicates, corresponding to six technical replicates ($n = 6$). Each set of upper and lower bars surrounding each data point on the graph represented the standard deviation of a mean percentage value of acetylcholinesterase activity.

***In Vitro* Acetylcholinesterase Activity
in the Presence of *Amanita muscaria* 243E3 Extract**

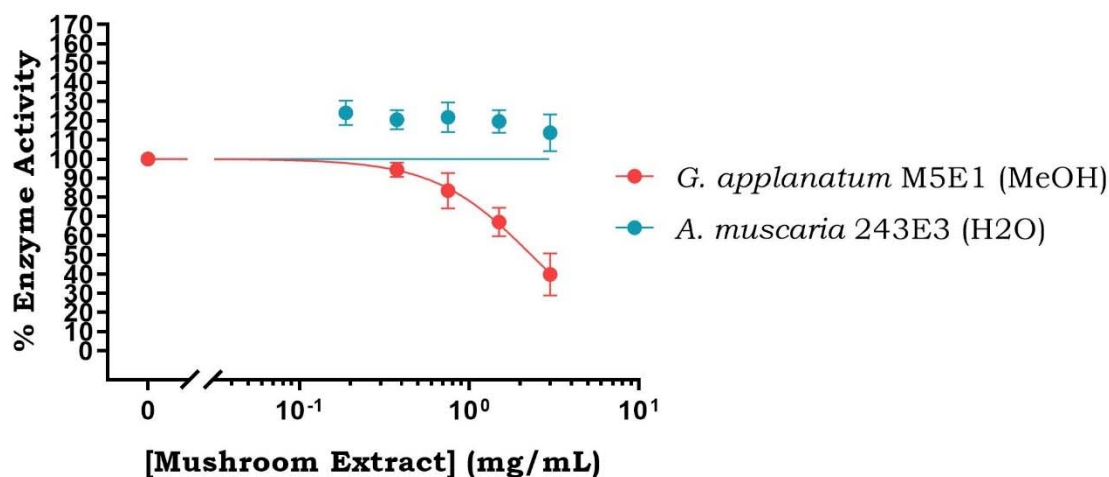


Figure 42. The Effect of *Amanita muscaria* 243E3 on Acetylcholinesterase Activity at High Extract Concentrations.

The shift in percentage of *in vitro* acetylcholinesterase activity when the enzyme was separately exposed to increasing concentrations of mushroom extracts, ranging from 0.1875 mg/mL to 3.0 mg/mL, over a 30-min time span. *Ganoderma applanatum* M5E1 is a mushroom extract used as a controlled reference for comparison. *Amanita muscaria* 243E3 is a mushroom extract that was used to test for an inhibitory effect on acetylcholinesterase activity. Each data point on the graph represented the mean percentage value of acetylcholinesterase activity recorded for the treatment with one specific mushroom extract, and at one specific extract concentration. Each mean percentage value of acetylcholinesterase activity was averaged from two experimental replicates, corresponding to six technical replicates (n = 6). Each set of upper and lower bars surrounding each data point on the graph represented the standard deviation of a mean percentage value of acetylcholinesterase activity.

***In Vitro* Acetylcholinesterase Activity in the Presence of *Agaricus subrufescens* 295E3 Extract**

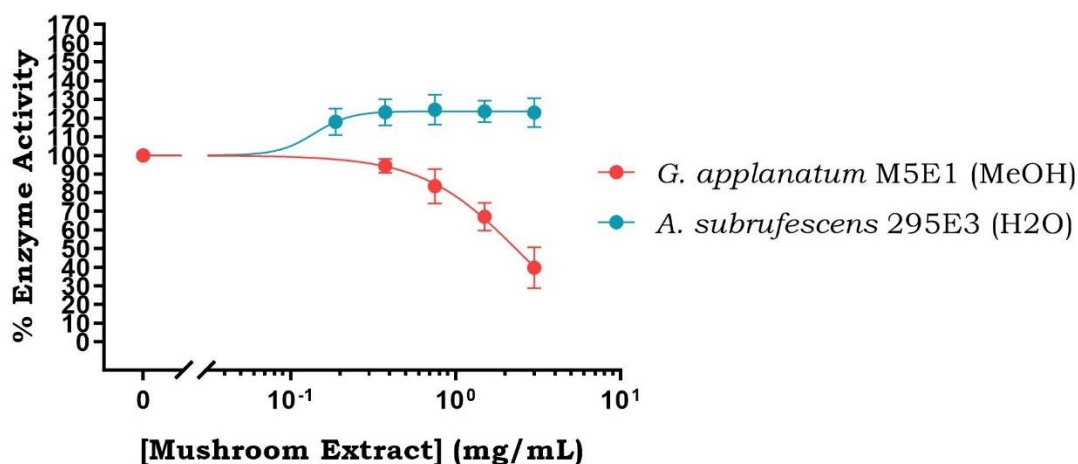


Figure 43. The Effect of *Agaricus subrufescens* 295E3 on Acetylcholinesterase Activity at High Extract Concentrations.

The shift in percentage of *in vitro* acetylcholinesterase activity when the enzyme was separately exposed to increasing concentrations of mushroom extracts, ranging from 0.1875 mg/mL to 3.0 mg/mL, over a 30-min time span. *Ganoderma applanatum* M5E1 is a mushroom extract used as a controlled reference for comparison. *Agaricus subrufescens* 295E3 is a mushroom extract that was used to test for an inhibitory effect on acetylcholinesterase activity. Each data point on the graph represented the mean percentage value of acetylcholinesterase activity recorded for the treatment with one specific mushroom extract, and at one specific extract concentration. Each mean percentage value of acetylcholinesterase activity was averaged from two experimental replicates, corresponding to six technical replicates (n = 6). Each set of upper and lower bars surrounding each data point on the graph represented the standard deviation of a mean percentage value of acetylcholinesterase activity.

***In Vitro* Acetylcholinesterase Activity
in the Presence of *Inonotus obliquus* 285E2 Extract**

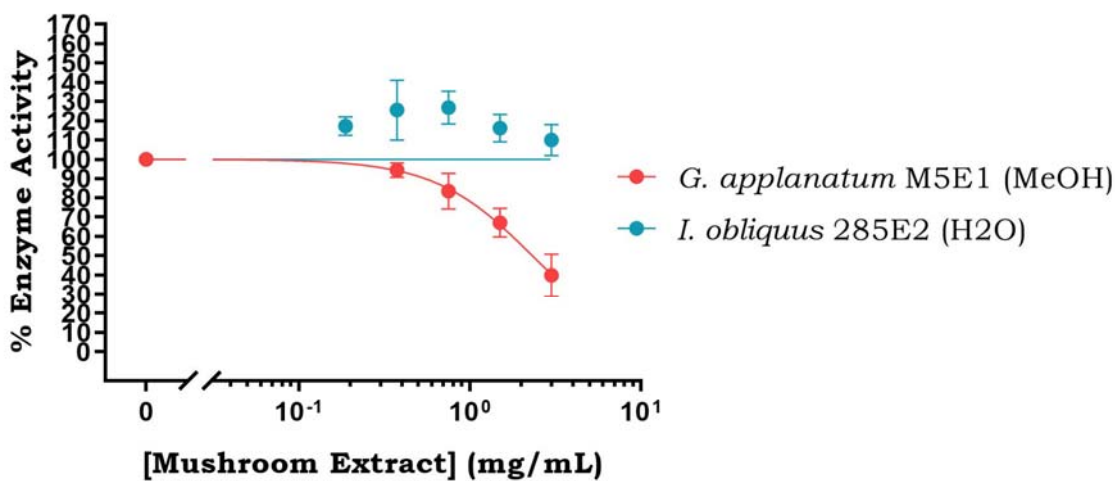


Figure 44. The Effect of *Inonotus obliquus* 285E2 on Acetylcholinesterase Activity at High Extract Concentrations.

The shift in percentage of *in vitro* acetylcholinesterase activity when the enzyme was separately exposed to increasing concentrations of mushroom extracts, ranging from 0.1875 mg/mL to 3.0 mg/mL, over a 30-min time span. *Ganoderma applanatum* M5E1 is a mushroom extract used as a controlled reference for comparison. *Inonotus obliquus* 285E2 is a mushroom extract that was used to test for an inhibitory effect on acetylcholinesterase activity. Each data point on the graph represented the mean percentage value of acetylcholinesterase activity recorded for the treatment with one specific mushroom extract, and at one specific extract concentration. Each mean percentage value of acetylcholinesterase activity was averaged from two experimental replicates, corresponding to six technical replicates (n = 6). Each set of upper and lower bars surrounding each data point on the graph represented the standard deviation of a mean percentage value of acetylcholinesterase activity.

***In Vitro* Acetylcholinesterase Activity
in the Presence of *Inonotus obliquus* 285E3 Extract**

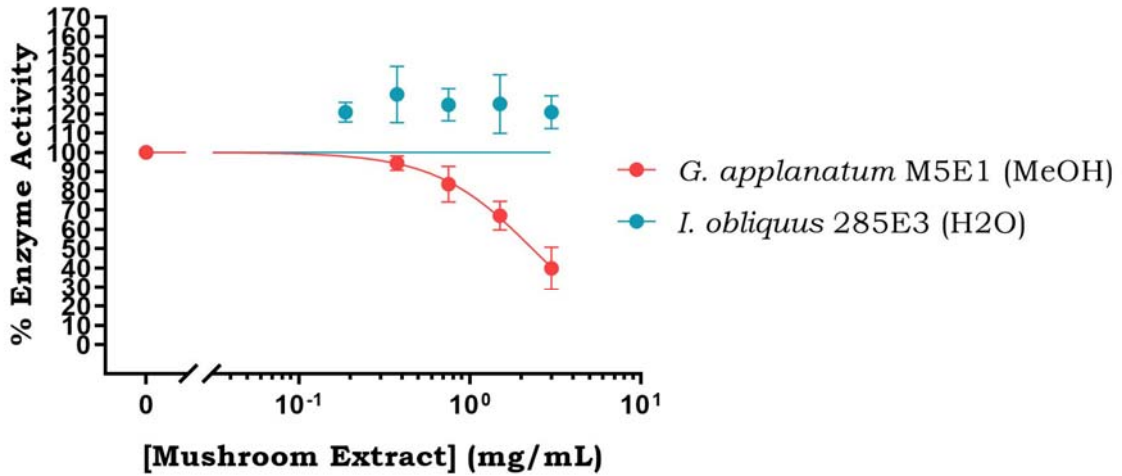


Figure 45. The Effect of *Inonotus obliquus* 285E3 on Acetylcholinesterase Activity at High Extract Concentrations.

The shift in percentage of *in vitro* acetylcholinesterase activity when the enzyme was separately exposed to increasing concentrations of mushroom extracts, ranging from 0.1875 mg/mL to 3.0 mg/mL, over a 30-min time span. *Ganoderma applanatum* M5E1 is a mushroom extract used as a controlled reference for comparison. *Inonotus obliquus* 285E3 is a mushroom extract that was used to test for an inhibitory effect on acetylcholinesterase activity. Each data point on the graph represented the mean percentage value of acetylcholinesterase activity recorded for the treatment with one specific mushroom extract, and at one specific extract concentration. Each mean percentage value of acetylcholinesterase activity was averaged from two experimental replicates, corresponding to six technical replicates (n = 6). Each set of upper and lower bars surrounding each data point on the graph represented the standard deviation of a mean percentage value of acetylcholinesterase activity.

***In Vitro* Acetylcholinesterase Activity
in the Presence of *Pleurotus ostreatus* 68E2 Extract**

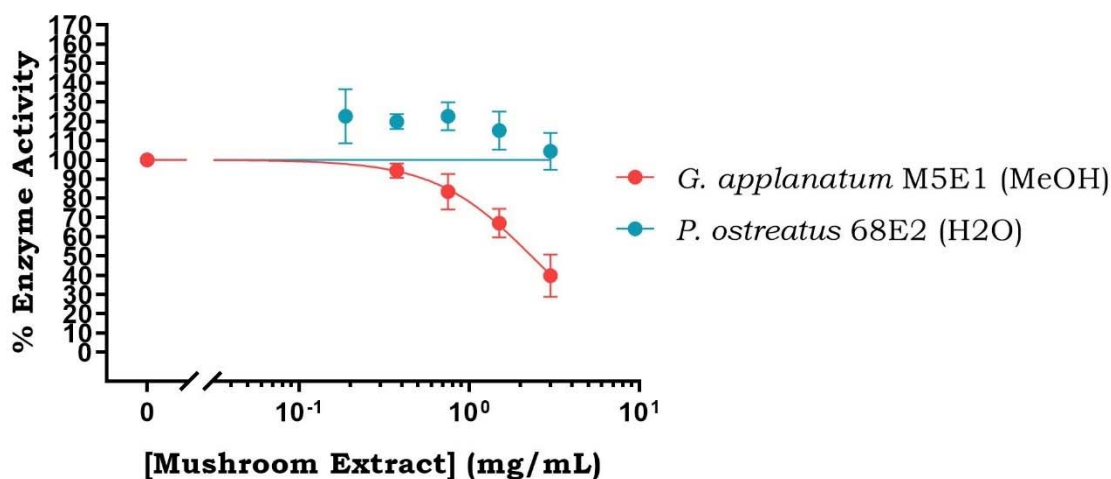


Figure 46. The Effect of *Pleurotus ostreatus* 68E2 on Acetylcholinesterase Activity at High Extract Concentrations.

The shift in percentage of *in vitro* acetylcholinesterase activity when the enzyme was separately exposed to increasing concentrations of mushroom extracts, ranging from 0.1875 mg/mL to 3.0 mg/mL, over a 30-min time span. *Ganoderma applanatum* M5E1 is a mushroom extract used as a controlled reference for comparison. *Pleurotus ostreatus* 68E2 is a mushroom extract that was used to test for an inhibitory effect on acetylcholinesterase activity. Each data point on the graph represented the mean percentage value of acetylcholinesterase activity recorded for the treatment with one specific mushroom extract, and at one specific extract concentration. Each mean percentage value of acetylcholinesterase activity was averaged from two experimental replicates, corresponding to six technical replicates (n = 6). Each set of upper and lower bars surrounding each data point on the graph represented the standard deviation of a mean percentage value of acetylcholinesterase activity.

However, for some other extracts, the increase in acetylcholinesterase activity was abnormally high, accompanied by a large standard deviation that fluctuated tremendously across the same extract concentration range (Figures 47-50).

***In Vitro* Acetylcholinesterase Activity
in the Presence of *Phellinus pini* 91E1 Extract**

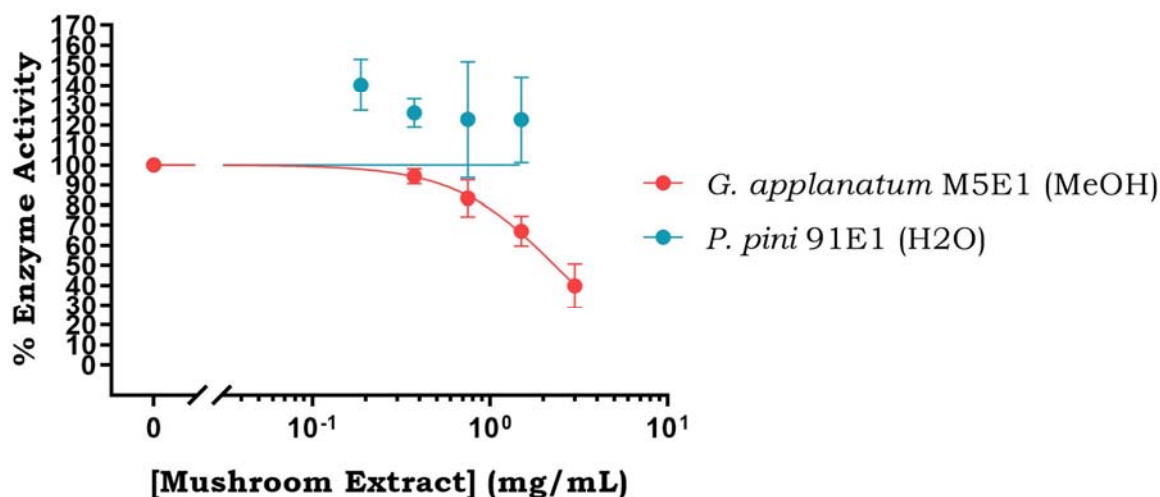


Figure 47. The Effect of *Phellinus pini* 91E1 on Acetylcholinesterase Activity at High Extract Concentrations.

The shift in percentage of *in vitro* acetylcholinesterase activity when the enzyme was separately exposed to increasing concentrations of mushroom extracts, ranging from 0.1875 mg/mL to 3.0 mg/mL, over a 30-min time span. *Ganoderma applanatum* M5E1 is a mushroom extract used as a controlled reference for comparison. *Phellinus pini* 91E1 is a mushroom extract that was used to test for an inhibitory effect on acetylcholinesterase activity. Each data point on the graph represented the mean percentage value of acetylcholinesterase activity recorded for the treatment with one specific mushroom extract, and at one specific extract concentration. Each mean percentage value of acetylcholinesterase activity was averaged from two experimental replicates, corresponding to six technical replicates (n = 6). Each set of upper and lower bars surrounding each data point on the graph represented the standard deviation of a mean percentage value of acetylcholinesterase activity.

***In Vitro* Acetylcholinesterase Activity in the Presence of *Phellinus igniarius* PIE1 Extract**

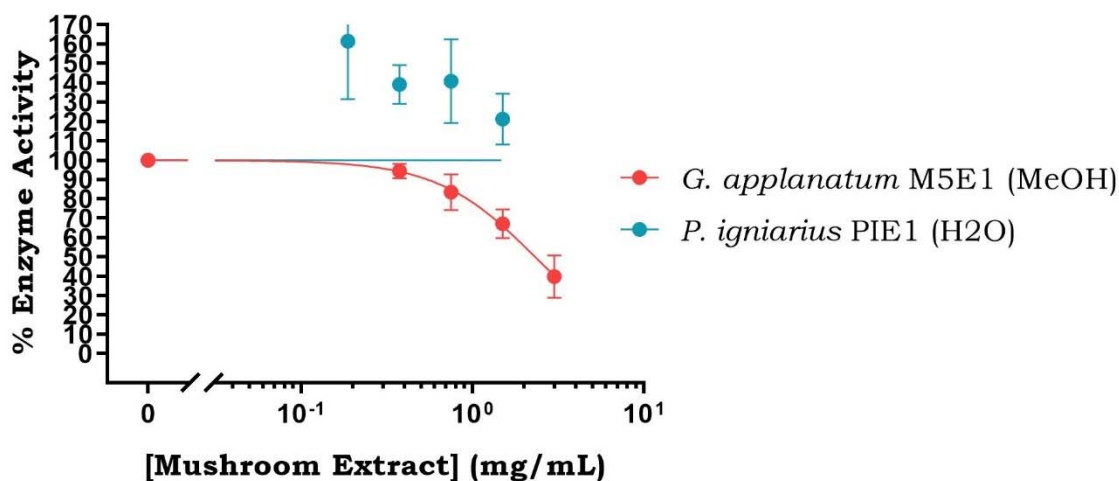


Figure 48. The Effect of *Phellinus igniarius* PIE1 on Acetylcholinesterase Activity at High Extract Concentrations.

The shift in percentage of *in vitro* acetylcholinesterase activity when the enzyme was separately exposed to increasing concentrations of mushroom extracts, ranging from 0.1875 mg/mL to 3.0 mg/mL, over a 30-min time span. *Ganoderma applanatum* M5E1 is a mushroom extract used as a controlled reference for comparison. *Phellinus igniarius* PIE1 is a mushroom extract that was used to test for an inhibitory effect on acetylcholinesterase activity. Each data point on the graph represented the mean percentage value of acetylcholinesterase activity recorded for the treatment with one specific mushroom extract, and at one specific extract concentration. Each mean percentage value of acetylcholinesterase activity was averaged from two experimental replicates, corresponding to six technical replicates (n = 6). Each set of upper and lower bars surrounding each data point on the graph represented the standard deviation of a mean percentage value of acetylcholinesterase activity.

Notably, *Phellinus pini* 91E2 and *Phellinus pini* 91E3 displayed instability that even led to a much lower percentage of acetylcholinesterase activity at higher extract concentrations compared to the standard controls. This peculiar trend, where the acetylcholinesterase activity was much higher at lower extract concentrations, and then rapidly decreased to a significantly lower percentage of enzyme activity at higher extract concentrations, raised questions about its credibility as a true acetylcholinesterase inhibition event (Figures 49 and 50). As to what in these extracts may induce this strange anomaly remained largely undetermined.

***In Vitro* Acetylcholinesterase Activity
in the Presence of *Phellinus pini* 91E2 Extract**

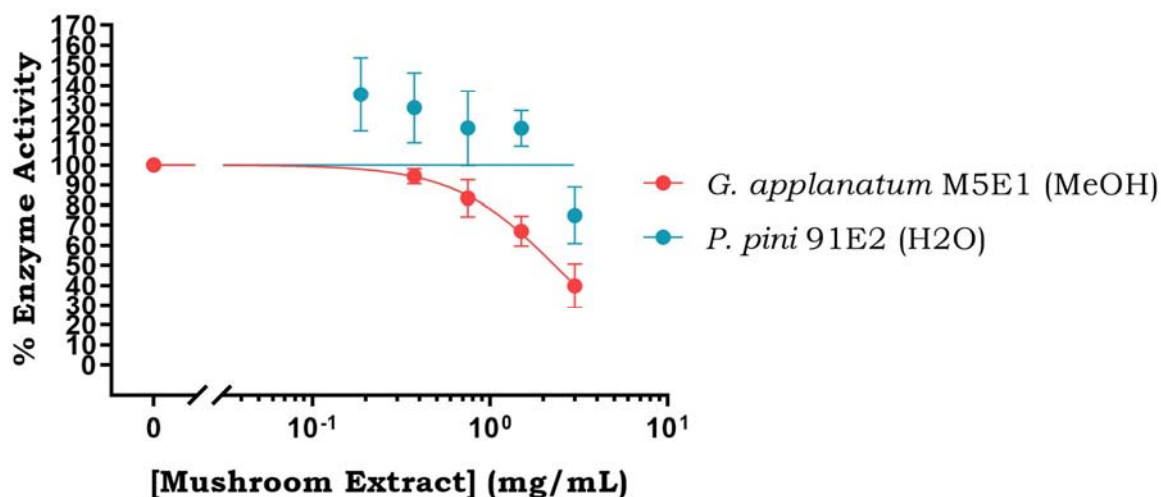


Figure 49. The Effect of *Phellinus pini* 91E2 on Acetylcholinesterase Activity at High Extract Concentrations.

The shift in percentage of *in vitro* acetylcholinesterase activity when the enzyme was separately exposed to increasing concentrations of mushroom extracts, ranging from 0.1875 mg/mL to 3.0 mg/mL, over a 30-min time span. *Ganoderma applanatum* M5E1 is a mushroom extract used as a controlled reference for comparison. *Phellinus pini* 91E2 is a mushroom extract that was used to test for an inhibitory effect on acetylcholinesterase activity. Each data point on the graph represented the mean percentage value of acetylcholinesterase activity recorded for the treatment with one specific mushroom extract, and at one specific extract concentration. Each mean percentage value of acetylcholinesterase activity was averaged from two experimental replicates, corresponding to six technical replicates (n = 6). Each set of upper and lower bars surrounding each data point on the graph represented the standard deviation of a mean percentage value of acetylcholinesterase activity.

***In Vitro* Acetylcholinesterase Activity in the Presence of *Phellinus pini* 91E3 Extract**

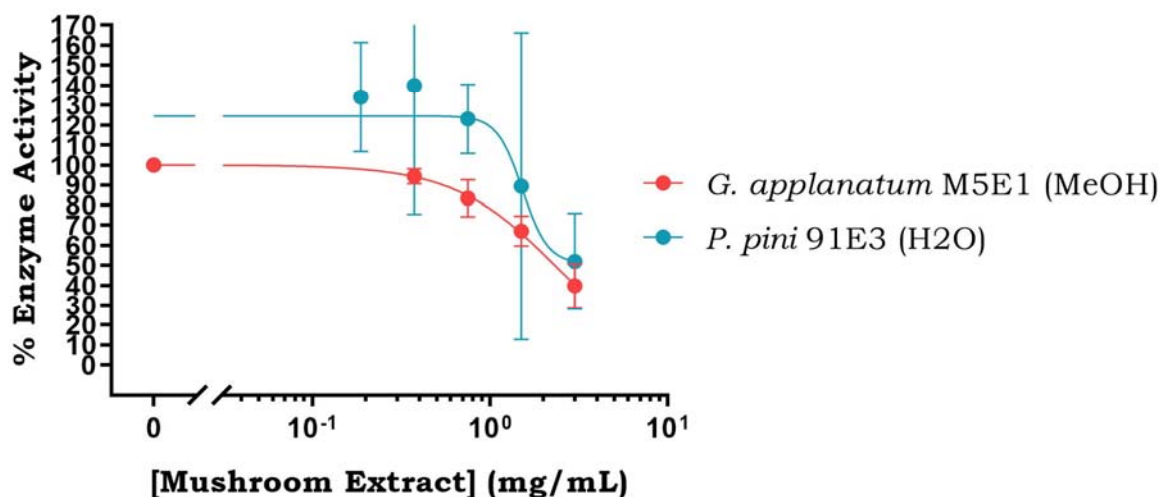


Figure 50. The Effect of *Phellinus pini* 91E3 on Acetylcholinesterase Activity at High Extract Concentrations.

The shift in percentage of *in vitro* acetylcholinesterase activity when the enzyme was separately exposed to increasing concentrations of mushroom extracts, ranging from 0.1875 mg/mL to 3.0 mg/mL, over a 30-min time span. *Ganoderma applanatum* M5E1 is a mushroom extract used as a controlled reference for comparison. *Phellinus pini* 91E3 is a mushroom extract that was used to test for an inhibitory effect on acetylcholinesterase activity. Each data point on the graph represented the mean percentage value of acetylcholinesterase activity recorded for the treatment with one specific mushroom extract, and at one specific extract concentration. Each mean percentage value of acetylcholinesterase activity was averaged from two experimental replicates, corresponding to six technical replicates (n = 6). Each set of upper and lower bars surrounding each data point on the graph represented the standard deviation of a mean percentage value of acetylcholinesterase activity.

Due to the abnormal trend observed with *Phellinus pini* 91E2 and *Phellinus pini* 91E3, it was challenging to definitively determine whether these extracts had a genuine acetylcholinesterase inhibition effect. Therefore, further future experimentation through alternative biochemical analysis methods would be necessary to provide more conclusive answers to this mystery.

Chapter 4

General Discussion

4.1 General Remarks

This study successfully achieved its original research objectives within a reasonable timeframe yielding some new findings. The primary research objectives of this study were to investigate four small molecules and mushroom extracts from eight different mushroom species to screen for their potential inhibitory effects on acetylcholinesterase activity *in vitro*. Throughout the experimentation process, none of the small molecules exhibited inhibition, but eight mushroom extracts were identified as inhibitors of acetylcholinesterase activity. Notably, the strength of inhibition on the enzyme activity was substantial, with approximate maximum inhibition strengths ranging from 39% to 91%. Furthermore, these significant inhibitory effects were achieved with relatively small quantities, as indicated by IC₅₀ values ranging from 4.0 mg/mL to slightly less than 1.0 mg/mL. The eight mushroom extracts that demonstrated inhibition were as follows: *Agaricus subrufescens* 295E1, *Agaricus subrufescens* 295E2, *Amanita muscaria* 243E1, *Ganoderma applanatum* M5E1, *Ganoderma applanatum* M5E2, *Hericium erinaceus* 288E1, *Hericium erinaceus* 288E3, and *Inonotus obliquus* 285E1.

4.2 Establishment of the Acetylcholinesterase Assay

In order to successfully perform the screening and achieve the presented results, the acetylcholinesterase assay was used. The assay was designed based on five main components: sodium phosphate buffer, *Electrophorus electricus* acetylcholinesterase, acetylthiocholine iodide, a small molecule or a mushroom extract as the test sample, and DTNB. Together, they allow the assay to specifically quantify the level of enzyme activity of acetylcholinesterase through the absorbance of TNB²⁻, the reduced counterpart of DTNB after its reduction by one of the byproducts

produced from the hydrolysis of acetylthiocholine iodide by acetylcholinesterase. In the order of the reaction sequence, acetylcholinesterase first hydrolyzes acetylthiocholine into acetic acid and thiocholine. Next, thiocholine acts as a reducing agent and reduces DTNB into TNB²⁻ by severing the disulfide linkage of DTNB. As a compound reflecting one shade of yellow, a colorimetric detection of TNB²⁻ can be translated into absorbance at the wavelength of 412 nm. Thus, the more TNB²⁻ there is, the greater the absorbance will be, reflecting a higher level of acetylcholinesterase activity, and vice versa.

First, the sodium phosphate buffer was made to 0.1 M at pH 8.0. The pH was adjusted to 8.0 to minimize the protonation of TNB²⁻, as the ionized form is the only form capable of reflecting the yellow color. It was also adjusted to maintain the thiocholine in its deprotonated form, allowing it to readily attack the disulfide linkage of DTNB by the free thiol group. Furthermore, the pH falls within the optimal range for *Electrophorus electricus* acetylcholinesterase activity. The choice of a 0.1 M concentration was made to maintain a balanced ionic strength that does not interfere with the π -cation interaction between the positively charged nitrogen atom of acetylthiocholine and the electron-rich aromatic rings of the side chain of tryptophan residues within the peripheral anionic site of acetylcholinesterase in the case of excessively high ionic strength, nor cause aggregation of the side chains of charged residues of the enzyme in the case of excessively low ionic strength.

Secondly, *Electrophorus electricus* acetylcholinesterase was selected due to its cost-effectiveness compared to the *Homo sapiens* orthologue. There was not much concern with the enzyme performance based on the chosen orthologue, as the amino acid sequence of its active site is highly conserved across species, giving rise to activity redundancy. Thirdly, the acetylthiocholine iodide was chosen for its special free thiol group that readily reduces DTNB once hydrolyzed by acetylcholinesterase. Lastly, DTNB was selected as a reagent for thiol

quantification because it does not react non-specifically with non-thiols, and the TNB²⁻ absorbance outside of the UV range eliminates the need for expensive experimental tools for UV detection.

Once the assay design was established and all necessary materials were prepared, the assay was initially tested to ensure proper functionality without any test sample added. Then, the assay was tested with five different concentrations of acetylcholinesterase to determine one appropriate concentration that could produce a sufficiently steep linear increase in TNB²⁻ absorbance over time, making it easier to detect the inhibition of acetylcholinesterase activity in the presence of a potential novel inhibitor. Following this, the assay was tested with known inhibitors of acetylcholinesterase to verify that inhibition would occur in the presence of a true inhibitor. Simultaneously, the results from the experiments with the known inhibitors were used as a point of reference for comparing the acetylcholinesterase inhibition strength with other potential novel inhibitors that may be discovered in this study. Only after the results from these four testing procedures were satisfactory that it was officially qualified for testing with the small molecules and mushroom extracts.

4.3 The Effects of the Selective Small Molecules on Acetylcholinesterase Activity

Previously, SPOPP, 534_1(6), and 534_2(7) were known for their *in vitro* anticancer properties. Using the web-based ligand-centric computational program for small molecule target prediction called MolTarPred, acetylcholinesterase was identified as the top target for binding by SPOPP and NP6A. Since dispiropyrrrolizidine derivatives have molecular structures closely related to SPOPP and NP6A, it was predicted that 534_1(6) and 534_2(7) may also bind to acetylcholinesterase. However, this study firmly established that none of these small molecules possesses an inhibitory effect against acetylcholinesterase activity.

Although the results were negative, they provided a confident conclusion that these small molecules do not exhibit inhibitory effects on acetylcholinesterase activity. These findings also raised questions about the reliability of small molecule target prediction programs, such as MolTarPred. These programs should generally only be used as supportive tools to assist in experimental design, but should not be solely relied upon to draw decisive conclusions in research studies without supporting experimental evidences, as demonstrated in this study.

4.4 The Effects of the Selective Mushroom Extracts on Acetylcholinesterase Activity

Contrary to the small molecules, this study extensively established, and was the first to report eight novel mushroom extracts with significant inhibition of acetylcholinesterase activity. These extracts exhibited a maximum inhibition strength ranging from 39% to 91% at relatively low concentrations, with IC₅₀ values ranging from 4.0 mg/mL to slightly less than 1.0 mg/mL. In comparison to the IC₅₀ value range of the example mushroom species reported for *in vitro* inhibition of acetylcholinesterase activity in Table 2, the IC₅₀ values of mushroom extracts shown to inhibit acetylcholinesterase activity in this study were relatively low. This indicated that their inhibition strength on acetylcholinesterase activity was relatively moderate to strong. However, until further isolation and purification of substances from these extracts were done, it should be carefully noted that these IC₅₀ values represented an extract as a whole, rather than an individual small molecule. Therefore, an effective comparison between the efficacy of acetylcholinesterase inhibition of an extract versus that of a purified molecule would deem to be difficult to achieve.

Supposedly there are a few existing novel small molecules responsible for the inhibitory effect seen in these extracts, whether or not the potency of these small molecules falls within the average IC₅₀ range from as low as 0.02 μM to as high as 25 μM observed for acetylcholinesterase inhibitors,²⁵ or even falling below the lower end of the average range, and whether or not they are

any more effective than the current inhibitors in any way, remained tentative for further investigation in future *in vitro* and *in vivo* studies.

As any biological extract is a complex mixture of numerous known and unknown small molecules, achieving consistent inhibition of acetylcholinesterase activity across a wide concentration range in six technical replicates suggests that there may be one or multiple inhibitors present in each extract, possibly in significant quantities. Alternatively, there could be one or more highly abundant components that suppress one or multiple enhancers promoting acetylcholinesterase activity. If these findings are consistently replicated in future studies, further analyses of the content within each of these eight mushroom extracts could be conducted to identify the specific small molecule or group of small molecules responsible for the observed inhibition of acetylcholinesterase activity in this study.

One potential approach for future analyses of the extracts could be through the application of chromatography, one of the well-established biochemical laboratory techniques that the Lee lab at the University of Northern British Columbia is proficient at. With various types of chromatography to be utilized, one way to approach the analyses could involve a combination of size-exclusion chromatography and high-performance liquid chromatography. The process would begin with size-exclusion chromatography to fractionate the content of each extract based on size. Subsequently, each fraction collected could be further subdivided into smaller sub-fractions using high-performance liquid chromatography, employing a gradient mobile phase to optimize separation based on solubility. Rather than relying on a single solvent, a gradient comprising a mixture of two or more solvents could be used to continuously alter the solubility condition over time in a dynamic fashion. This approach would provide a limitless range of solubility conditions confined within the gradient for the small molecules within each fraction to dissolve into. Finally,

each collected sub-fraction containing a single small molecule could be separately tested *in vitro* to assess its impact on acetylcholinesterase activity. If the molecule demonstrates significant inhibitory activity, further analyses, including kinetics and structural analysis could be further conducted to elucidate its mode of inhibition on the enzyme activity and determine its chemical identity.

In addition to the points mentioned earlier, the new findings provided further evidences and reaffirmed the therapeutic potential of several mushroom species with medicinal properties to combat against neurodegenerative diseases. These properties have been well-documented in numerous past and recent research studies, particularly in the cases of *Hericium erinaceus* and *Inonotus obliquus*. Previous research has mainly focused on the 80% methanol,⁵¹ and 70% ethanol extracts of the two species, which contain substances demonstrating strong antioxidative properties.⁵² The antioxidant properties exhibited by these extracts were mostly found targeting and upregulating the nuclear factor erythroid 2-related factor 2 signaling pathway. This pathway assists cells in resisting the harmful effects of reactive oxygen species during the cells' response to oxidative stress. This role of antioxidative properties is crucial in the context of neurodegeneration, as oxidative stress-induced apoptosis, leading to the loss of neurons, is another common pathological event in various neurodegenerative diseases.⁵¹ Nonetheless, given that acetylcholinesterase specializes in the regulation of cholinergic neurotransmission within neurons, as opposed to the more general cellular response to oxidative stress observed across all cell types, the new findings presented in this study possibly marked the first emphasis on the therapeutic role of *Hericium erinaceus* and *Inonotus obliquus*, directed towards an enzyme with a highly localized function exclusive to a distinct cell type, playing a more direct and substantial role in the development of neurodegenerative diseases.

As for *Agaricus subrufescens*, *Amanita muscaria*, and *Ganoderma applanatum*, it appears that there have been no prior reports nor extensive research conducted on their potential roles in the treatment of neurodegenerative diseases. Any specific biological targets that these mushrooms may inhibit in this context have also not been reported. Therefore, the findings presented in this study were the first to highlight and comprehensively establish the novel medicinal properties of these three mushrooms, particularly their targeting of acetylcholinesterase as a potential therapeutic approach for neurodegenerative diseases.

Beside being the first to report the acetylcholinesterase inhibitory property possessed by a few mushroom species, these findings also contained important observations worth mentioning as well. In consistent with the 80% methanol and 70% ethanol extracts of *Hericium erinaceus* and *Inonotus obliquus* reported to demonstrate strong oxidative properties in previous research, almost all mushroom extracts reported to inhibit acetylcholinesterase activity in this study were also extracted using methanol and ethanol. The only difference was the percentage of methanol and ethanol used to extract, which were 50% methanol for the E2 extracts and 80% ethanol for the E1 extracts. With respect to the E1 and E2 mushroom extracts used in this study, the substances contained within these extracts were previously predicted to be small molecules, in contrast to the E3 extracts that were predicted to contain macromolecules such as polysaccharides.⁵⁰ In comparison to known acetylcholinesterase inhibitors such as rivastigmine, galanthamine, and donepezil, the small molecules contained within the E1 extracts may likely have a similar solubility, as all are soluble in ethanol to various degrees. Taken altogether, these observations suggested that mushroom extracts derived from methanol and ethanol extractions may contain more substances that possess an inhibitory property on acetylcholinesterase activity. Nevertheless, until these substances are isolated, purified, and further analyzed according to the approach suggested above,

their identity and the degree to which they inhibit acetylcholinesterase activity in comparison to the current acetylcholinesterase inhibitors remains tentative.

Regarding the mushroom extracts that enhanced acetylcholinesterase activity, this elevated enzyme activity level was of particular interest because it may indicate neurotoxicity in the context of neurodegeneration. For instance, Melo et al. (2003) conducted an *in vitro* study demonstrating how amyloid plaques contribute to an increased acetylcholinesterase activity in Alzheimer's disease using a retinal cell-based model. Their study showed that cells incubated with amyloid beta-peptides alone for 24 h exhibited an enhanced enzyme activity level beyond that observed in the control group without amyloid beta-peptides. This enhanced level of enzyme activity was consistently observed to be between 120% to 130%, similar to the moderate increase in the percentage of acetylcholinesterase activity seen in response to the individual treatments with the following nine mushroom extracts in this study: *Amanita muscaria* 243E2, *Amanita muscaria* 243E3, *Agaricus subrufescens* 295E3, *Ganoderma applanatum* M5E3, *Inonotus obliquus* 285E2, *Inonotus obliquus* 285E3, *Phellinus igniarius* PIE2, *Phellinus igniarius* PIE3, and *Pleurotus ostreatus* 68E2.⁵³

Most notably, cases involving extracts from natural products other than mushrooms enhancing acetylcholinesterase activity have also been documented.⁵⁴ Unlike the eight mushroom extracts that displayed a significant inhibitory effect on the acetylcholinesterase activity, these particular extracts were hypothesized to potentially contain enhancers of acetylcholinesterase. These enhancers could act as toxins exacerbating the detrimental effects associated with neurodegeneration.

Likewise, a similar reasoning could be inferred for the following remaining four mushroom extracts: *Phellinus igniarius* PIE1, *Phellinus pini* 91E1, *Phellinus pini* 91E2, and *Phellinus pini*

91E3. The only more surprising exception was that these extracts not only induced an unusually high percentage of acetylcholinesterase activity, but also exhibited a moderate to drastic decline in enzyme activity as the extract concentration increased progressively from 0.1875 mg/mL to 3.0 mg/mL. As peculiar as the trend was, it was not unique and have been observed in several other related studies. For instance, Akbari et al. (2022) reported an *in vivo* study on how vitamin B12 administration prevents ethanol-induced learning and memory impairment. A comparative analysis showed the hippocampal acetylcholinesterase activity of mice fed with water containing 20% ethanol throughout their adolescence intensified to over 200% of the normal enzyme activity level observed in the untreated group. On top of the ethanol treatment, further administration of vitamin B12, starting with a dosage from 0.5 mg/kg to 1.5 mg/kg in the murine hippocampus already displaying intensified hippocampal acetylcholinesterase activity level induced by 20% ethanol, and subsequently, administration of vitamin B12 alone at a dosage of 1.5 mg/kg to the murine hippocampus with normal hippocampal acetylcholinesterase activity level, gradually mitigated the level of hippocampal acetylcholinesterase activity, to the extension where the enzyme activity level was reduced to 60% of the normal enzyme activity level observed in the control with no treatment of 20% ethanol and vitamin B12.⁵⁵

Based on the observed pattern in the *in vivo* study, it was hypothesized that the peculiar pattern of acetylcholinesterase activity in response to the increasing dosages of either the *Phellinus igniarius* PIE1, *Phellinus pini* 91E1, *Phellinus pini* 91E2, or *Phellinus pini* 91E3 extract may also result from a similar circumstance. It was hypothesized that within each of these four extracts, there may be one or more acetylcholinesterase enhancers in extremely great abundance to the point of saturation, making their enhancing effects on acetylcholinesterase activity nearly completely dosage-independent. Conversely, within each of these same extracts again, there may be one or

more acetylcholinesterase inhibitors in scarcity compared to the enhancers, making their inhibitory effects on acetylcholinesterase activity lean more towards being dosage-dependent instead. Then at some point forward, there may come a point where the concentration of the inhibitors may become sufficient to reverse the enhancing effects of the enhancers on acetylcholinesterase activity, leading to a drastic decline after reaching elevated levels beyond the norm. This hypothesis was reminiscent of the peculiar response of acetylcholinesterase activity to the increasing dosages of these four extracts.

Considering both hypotheses above, the enhanced acetylcholinesterase activity observed in response to the separate treatments with *Amanita muscaria* 243E2, *Amanita muscaria* 243E3, *Agaricus subrufescens* 295E3, *Ganoderma applanatum* M5E3, *Inonotus obliquus* 285E2, *Inonotus obliquus* 285E3, *Phellinus igniarius* PIE1, *Phellinus igniarius* PIE2, *Phellinus igniarius* PIE3, *Phellinus pini* 91E1, *Phellinus pini* 91E2, *Phellinus pini* 91E3, and *Pleurotus ostreatus* 68E2 all pointed towards the existence of one or more acetylcholinesterase enhancers in extreme abundance within each of these thirteen extracts. If this holds true, then there should also exist an extremely narrow concentration range between zero and the point of saturation for the enhancers, where their enhancing effects on acetylcholinesterase activity briefly become dosage-dependent. If this is the case, the extremely narrow concentration range should exist somewhere below 0.1875 mg/mL.

Further testing was conducted under the same experiment setup, extending into an ultra-low concentration range from 9.37×10^{-6} mg/mL to 9.37×10^{-2} mg/mL, specifically for the *Agaricus subrufescens* 295E3 and *Inonotus obliquus* 285E3 extracts. The results revealed a concentration range between 0.01 mg/mL and 0.1 mg/mL where the enhancing effects of these two extracts on acetylcholinesterase activity became dosage-dependent. Thus, to some extent, the hypotheses were supported, although the existence of one or more acetylcholinesterase enhancers

in extreme abundance may not hold true for the remaining eleven extracts. Consequently, these test results should be considered preliminary, and further studies would be required to conduct. Moreover, a bioactivity-guided approach should be employed to isolate compounds with inhibitory or stimulatory activity on acetylcholinesterase.

Considering that the mushroom extracts enhancing acetylcholinesterase activity to be detrimental to the process of neurodegeneration, utilizing them in research for the therapeutics of neurodegenerative diseases may be risky and ineffective. However, it is worth noting that an enhanced acetylcholinesterase activity level may not necessarily be an undesirable biological effect in cell types other than neurons. In addition to its major role in neurotransmission regulation, it has been reported that the acetylcholinesterase enzyme can also act as a mediator promoting cell proliferation and regeneration. There are substantial evidences of its involvement in a cell's life cycle in various studies using invertebrate and vertebrate models, such as sea slugs, octopuses, and salamanders.

For example, in a study by Fossati et al. (2013) on limb regeneration in octopuses, the acetylcholinesterase activity was shown to increase and become most active when a small hook sprouted from an amputated tentacle between day 17 to day 28. Afterwards, the enzyme activity level gradually dissipated as the full functional structure was completely regrown. Most notably, acetylcholinesterase was mobilized from the nervous system to participate in the limb regeneration process.⁵⁶ This suggests that the process of regeneration is nerve-dependent, and implies that acetylcholinesterase can serve as a dual mediator with both inhibitory and enhancing effects on the enzyme that can be beneficial for the development of diverse life functionalities and disease treatments under the right conditions and circumstances. Therefore, even though deviating from the original research objectives, the discovery of these acetylcholinesterase activity-enhancing

mushroom extracts in this study could still prove to be useful in future studies related to cellular regeneration.

4.5 Concluding Remarks and Future Directions

In conclusion, this study found that none of the four small molecules inhibited acetylcholinesterase activity, but eight mushroom extracts did. While the negative results with the small molecules were not particularly exciting, they still provided valuable additional knowledge contributing to the understanding of the medicinal properties of dispiropiperazine and dispiropyrrrolizidine derivatives. Moreover, these results paved way for future studies to shift focus onto exploring other potential medicinal properties of these molecules. Additionally, this study highlighted the need for caution when using small molecule target prediction programs like MolTarPred.

Moving forward, this study has made a significant contribution by identifying eight novel mushroom extracts that showed inhibition of acetylcholinesterase activity. These extracts, from *Hericium erinaceus* and *Inonotus obliquus*, were found to exhibit an inhibitory effect against acetylcholinesterase activity for the first time. Simultaneously, the study was the first to report extracts from *Agaricus subrufescens*, *Amanita muscaria*, and *Ganoderma applanatum* as having potential beneficial medicinal properties against neurodegeneration. Collectively, these extracts may provide new sources of compounds for potential drug development in the treatment of neurodegenerative diseases.

Even for the extracts that were found to enhance acetylcholinesterase activity, they may prove useful as biological tools for understanding tissue development, or as sources of compounds for drug development to treat other types of diseases. Nonetheless, the discovery of the inhibitory properties against acetylcholinesterase activity in the mentioned eight novel mushroom extracts in

this study served as a reminder of the latent medicinal potentials of mushrooms as medicines for the treatment of a wide range of diseases. Given the vast number of mushroom species, many of which contain undiscovered compounds, future studies should be encouraged to conduct further research in this area.

References

1. Massoulie, J., Anselmet, A., Bon, S., Krejci, E., Legay, C., Morel, N., and Simon, S. (1998). Acetylcholinesterase: C-Terminal Domains, Molecular Forms, and Functional Localization. *Journal of Physiology Paris* *92*, 183-190.
2. Camp, S., Zhang, L., Marquez, M., Torre, B., Long, J.M., Bucht, G., and Taylor, P. (2005). Acetylcholinesterase (AChE) gene modification in transgenic animals: Functional consequences of selected exon and regulatory region deletion. *Chemico-Biological Interactions* *157-158*, 79-86.
3. Rotundo, R.L. (2017). Biogenesis, assembly and trafficking of acetylcholinesterase. *Journal of Neurochemistry* *142*, 52-58.
4. Cortes-Gomez, M.A., Barbera, V.M., Alom, J., Saez-Valero, J., and Garcia-Ayllon, M.S. (2023). Presenilin 1 Modulates Acetylcholinesterase Trafficking and Maturation. *International Journal of Molecular Sciences* *24*, 1437.
5. Perrier, A.L., Massoulie, J., and Krejci, E. (2002). PRiMA: The Membrane Anchor of Acetylcholinesterase in the Brain. *Neuron* *33*, 275-285.
6. Ruiz, C.A., Rossi, S.G., and Rotundo, R.L. (2015). Rescue and stabilization of acetylcholinesterase in skeletal muscle by N-terminal peptides derived from the non-catalytic subunits. *Journal of Biological Chemistry* *290*, 20774-20781.
7. Rosenberry, T.L., Brazzolotto, X., Macdonald, I.R., Wandhammer, M., Trovaslet-Leroy, M., Darvesh, S., and Nachon, F. (2017). Comparison of the Binding Reversible Inhibitors to Human Butyrylcholinesterase and Acetylcholinesterase: A Crystallographic, Kinetic and Calorimetric Study. *Molecules* *22*, 2098.
8. Zhou, Y., Wang, S., and Zhang, Y. (2010). Catalytic Reaction Mechanism of Acetylcholinesterase Determined by Born-Oppenheimer Ab Initio QM/MM Molecular Dynamics Simulations. *The Journal of Physical Chemistry B* *114*, 8817-8825.
9. Picciotto, M.R., Higley, M.J., and Mineur, Y.S. (2012). Acetylcholine as a neuromodulator: cholinergic signaling shapes nervous system function and behavior. *Neuron* *76*, 116-129.
10. Muramatsu, I., Masuoka, T., Uwada, J., Yoshiki, H., Yazama, T., Lee, K.S., Sada, K., Nishio, M., Ishibashi, T., and Taniguchi, T. (2018). Nicotinic Acetylcholine Receptor Signaling in Neuroprotection. Springer, Singapore. 45-58.
11. Volpicelli-Daley, L.A., Duysen, E.G., Lockridge, O., and Levey, A.I. (2003). Altered Hippocampal Muscarinic Receptors in Acetylcholinesterase-Deficient Mice. *Annals of Neurology* *53*, 788-796.

12. Bernard, V., Brana, C., Liste, I., Lockridge, O., and Bloch, B. (2003). Dramatic depletion of cell surface m2 muscarinic receptor due to limited delivery from intracytoplasmic stores in neurons of acetylcholinesterase-deficient mice. *Molecular and Cellular Neuroscience* 23, 121-133.
13. Muramatsu, I., Masuoka, T., Uwada, J., Yoshiki, H., Lee, K.S., Sada, K., Nishio, M., Ishibashi, T., and Taniguchi, T. (2017). Regulation of synaptic acetylcholine concentrations by acetylcholine transport in rat striatal cholinergic transmission. *Journal of Neurochemistry* 143, 76-86.
14. Shaltiel, G., Hanan, M., Wolf, Y., Barbash, S., Kovalev, E., Shoham, S., and Soreq, H. (2012). Hippocampal microRNA-132 mediates stress-inducible cognitive deficits through its acetylcholinesterase target. *Brain Structure and Function* 218, 59-72.
15. Simchovitz, A., Heneka, M.T., and Soreq, H. (2016). Personalized genetics of the cholinergic blockade of neuroinflammation. *Journal of Neurochemistry* 142, 178-187.
16. Paul, R., and Borah, A. (2017). Global loss of acetylcholinesterase activity with mitochondrial complexes inhibition and inflammation in brain of hypercholesterolemic mice. *Scientific Reports* 7, 17922.
17. Fried, G.H., and Hademenos, G.J. (2013). *Schaum's outlines of Biology (Fourth Edition)*. McGraw-Hill Education, United States of America. 303-320.
18. Jeitner, T.M., Voloshyna, I., and Reiss, A.B. (2011). Oxysterol Derivatives of Cholesterol in Neurodegenerative Disorders. *Current Medicinal Chemistry* 18, 1515-1525.
19. Ulrich, J., Meier-Ruge, W., Probst, A., Meier, E., and Ipsen, S. (1990). Senile Plaques: Staining for Acetylcholinesterase and A4 Protein: A Comparative Study in the Hippocampus and Entorhinal Cortex. *Acta Neuropathologica* 80, 624-628.
20. Alvarez, A., Alarcon, R., Opazo, C., Campos, E.O., Munoz, F.J., Calderon, F.H., Dajas, F., Gentry, M.K., Doctor, B.P., Mello, F.G.D., and Inestrosa, N.C. (1998). Stable Complexes Involving Acetylcholinesterase and Amyloid- β Peptide Change the Biochemical Properties of the Enzyme and Increase the Neurotoxicity of Alzheimer's Fibrils. *The Journal of Neuroscience* 18, 3213-3223.
21. Alvarez, A., Opazo, C., Alarcon, R., Garrido, J., and Inestrosa, N.C. (1997). Acetylcholinesterase Promotes the Aggregation of Amyloid- β Peptide Fragments by Forming a Complex with the Growing Fibrils. *Journal of Molecular Biology* 272, 348-361.
22. Alvarez, A., Bronfman, F., Perez, C.A., Vicente, M., Garrido, J., and Inestrosa, N.C. (1995). Acetylcholinesterase, a Senile Plaque Component, Affects the Fibrillogenesis of Amyloid- β Peptides. *Neuroscience Letters* 201, 49-52.

23. Walczak-Nowicka, L.J., and Herbet, M. (2021). Acetylcholinesterase Inhibitors in the Treatment of Neurodegenerative Diseases and the Role of Acetylcholinesterase in their Pathogenesis. *International Journal of Molecular Sciences* 22, 9290.
24. Colovic, M.B., Krstic, D.Z., Lazarevic-Pasti, T.D., Bondzic, A.M., Vasic, V.M. (2013). Acetylcholinesterase Inhibitors: Pharmacology and Toxicology. *Current Neuropharmacology* 11, 315-335.
25. ChEMBL. (2022). IC₅₀ of Acetylcholinesterase Inhibitors. (EMBL-EBI European Molecular Biology Laboratory-European Bioinformatics Institute).
26. Liu, V.P., Li, W.M., Lofroth, J., Zeb, M., Patrick, B.O., Bott, T.M., and Lee, C.H. (2023). A specific dispiropiperazine derivative that arrests cell cycle, induces apoptosis, necrosis and DNA damage. *Scientific Reports* 13, 8674.
27. Lee, H.X., Li, W.M., Ang, C.W., Reimer, K., Liu, V., Patrick, B.O., Yeong, K.Y., and Lee, C.H. (2022). Regio- and stereoselective synthesis of dispiropyrrrolizidines through 1,3-dipolar cycloaddition reaction: Inhibition of KRAS expression. *Journal of Molecular Structure* 1263, 133177.
28. Bell, V., Silva, C.R.P.G., Guina, J., and Fernandes, T.H. (2022). Mushrooms as future generation healthy foods. *Frontiers in Nutrition* 9, 1050099.
29. Arshadi, N., Nouri, H., and Moghimi, H. (2023). Increasing the production of the bioactive compounds in medicinal mushrooms: an omics perspective. *Microbial Cell Factories* 22, 11.
30. Jiang, X., Li, S., Feng, X., Li, L., Hao, J., Wang, D., and Wang, Q. (2022). Mushroom Polysaccharides as Potential Candidates for Alleviating Neurodegenerative Diseases. *Nutrients* 14, 4833.
31. Tel, G., Ozturk, M., Duru, M.E., and Turkoglu, A. (2015). Antioxidant and anticholinesterase activities of five wild mushroom species with total bioactive contents. *Pharmaceutical Biology* 53, 824-830.
32. Deveci, E., Cayan, F., Tel-Cayan, G., and Duru, M.E. (2019). Structural characterization and determination of biological activities for different polysaccharides extracted from tree mushroom species. *Journal of Food Biochemistry* 43, 1-13.
33. Giridharan, V.V., Thandavarayan, R.A., and Konishi, T. (2011). Amelioration of scopolamine induced cognitive dysfunction and oxidative stress by *Inonotus obliquus* – a medicinal mushroom. *Food & Function* 2, 320.
34. Ozturk, M., Duru, M.E., Kivrak, S., Mercan-Dogan, N., Turkoglu, A., and Ozler, M.A. (2011). *In vitro* antioxidant, anticholinesterase and antimicrobial activity studies on three

Agaricus species with fatty acid compositions and iron contents: A comparative study on the three most edible mushrooms. *Food and Chemical Toxicology* 49, 1353-1360.

35. Hasnat, M.A., Pervin, M., and Lim, B.O. (2013). Acetylcholinesterase Inhibition and *in Vitro* and *in Vivo* Antioxidant Activities of *Ganoderma lucidum* Grown on Germinated Brown Rice. *Molecules* 18, 6663-6678.
36. Tel, G., Ozturk, M., Duru, M.E., and Turkoglu, A. (2015). Antioxidant and anticholinesterase activities of five wild mushroom species with total bioactive contents. *Pharmaceutical Biology* 53, 824-830.
37. Kaur, R., Singh, V., and Shri, R. (2017). Anti-amnesic effects of *Ganoderma* species: A possible cholinergic and antioxidant mechanism. *Biomedicine & Pharmacotherapy* 92, 1055-1061.
38. Deveci, E., Cayan, F., Tel-Cayan, G., and Duru, M.E. (2019). Structural characterization and determination of biological activities for different polysaccharides extracted from tree mushroom species. *Journal of Food Biochemistry* 43, 12965.
39. Chen, Z., Bishop, K.S., Tanambell, H., Buchanan, P., and Quek, S.Y. (2019). Assessment of In Vitro Bioactivities of Polysaccharides Isolated from *Hericium Novae-Zelandiae*. *Antioxidants* 8, 211.
40. Giridharan, V.V., Thandavarayan, R.A., and Konishi, T. (2011). Amelioration of scopolamine induced cognitive dysfunction and oxidative stress by *Inonotus obliquus* – a medicinal mushroom. *Food & Function* 2, 320.
41. Nguyen, T.K., Im, K.H., Choi, J., Shin, P.G., and Lee, T.S. (2016). Evaluation of Antioxidant, Anti-cholinesterase, and Anti-inflammatory Effects of Culinary Mushroom *Pleurotus pulmonarius*. *Mycobiology* 44, 291-301.
42. Li, S., Li, A.J., Zhao, J., Santillo, M.F., and Xia, M. (2022). Acetylcholinesterase Inhibition Assays for High-Throughput Screening. *High-Throughput Screening Assays in Toxicology* 2474, 47-58.
43. Owusu-Apenten, R. (2005). Colorimetric Analysis of Protein Sulfhydryl Groups in Milk: Applications and Processing Effects. *Food Science and Nutrition* 45, 1-23.
44. Winther, J.R., and Thorpe, C. (2014). Quantification of Thiols and Disulfides. *Biochimica et Biophysica Acta* 1840, 838-846.
45. Wiesner, J., Kriz, Z., Kuca, K., Jun, D., and Koca, J. (2007). Acetylcholinesterases – the structural similarities and differences. *Journal of Enzyme Inhibition and Medicinal Chemistry* 22, 417-424.

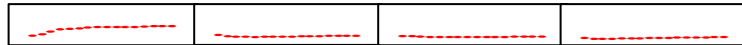
46. Kasteel, E.E.J., Nijmeijer, S.M., Darney, K., Lautz, L.S., Dorne, J.L.C.M., Kramer, N.I., and Westerink, R.H.S. (2020). Acetylcholinesterase inhibition in electric eel and human donor blood: an in vitro approach to investigate interspecies differences and human variability in toxicodynamics. *Archives of Toxicology* *94*, 4055-4065.
47. Brenda. (2022). Information on EC 3.1.1.7 – acetylcholinesterase and Organism(s) *Electrophorus electricus*. (BRENDA The Comprehensive Enzyme Information System).
48. ChEMBL. (2022). IC₅₀ of Galanthamine Hydrobromide. (EMBL-EBI European Molecular Biology Laboratory-European Bioinformatics Institute).
49. Lee, H.X., Li, W.M., Khatra, J., Xia, Z., Sannikov, O., Ling, Y., Zhu, H., and Lee, C.H. (2022). Antiproliferative Fatty Acids Isolated from the Polypore Fungus *Onnia tomentosa*. *Journal of Fungi* *8*, 1-21.
50. Smith, A., Javed, S., Barad, A., Myhre, V., Li, W.M., Reimer, K., Massicotte, H.B., Tackaberry, L.E., Payne, G.W., Egger, K.N., and Lee, C.H. (2017). Growth-Inhibitory and Immunomodulatory Activities of Wild Mushrooms from North-Central British Columbia. *International Journal of Medicinal Mushrooms* *19*, 485-497.
51. Gunjima, K., Tomiyama, R., Takakura, K., Yamada, T., Hashida, K., Nakamura, Y., Konishi, T., Matsugo, S., and Hori, O. (2014). 3,4-Dihydroxybenzalacetone Protects Against Parkinson's Disease-Related Neurotoxin 6-OHDA Through Akt/Nrf2/Glutathione Pathway. *Journal of Cellular Biochemistry* *115*, 151-160.
52. Roda, E., Luca, F.D., Ratto, D., Priori, E.C., Savino, E., Bottone, M.G., and Rossi, P. (2023). Cognitive Healthy Aging in Mice: Boosting Memory by an Ergothioneine-Rich *Hericium erinaceus* Primordium Extract. *Biology* *12*, 196.
53. Melo, J.B., Agostinho, P., and Oliveira, C.R. (2003). Involvement of oxidative stress in the enhancement of acetylcholinesterase activity induced by amyloid beta-peptide. *Neuroscience Research* *45*, 117-127.
54. Youssef, B., Ramadan, K.S., ElShebiny, S., and Ibrahim, E.A. (2022). Antidepressant-like effects of aqueous extracts of miswak (*Salvadora persica*) and date palm (*Phoenix dactylifera*) on depression-like behaviors using CUMS model in male rats. *Journal of Food Biochemistry* *46*, 14164.
55. Akbari, E., Hossaini, D., Amiry, G.Y., Ansari, M., Haidary, M., Beheshti, F., and Ahmadi-Soleimani, S.M. (2022). Vitamin B12 administration prevents ethanol-induced learning and memory impairment through re-establishment of the brain oxidant/antioxidant balance, enhancement of BDNF and suppression of GFAP. *Behavioural Brain Research* *438*, 114156.

56. Fossati, S.M., Carella, F., Vico, G.D., Benfenati, F., and Zullo, L. (2013). Octopus Arm Regeneration: Role of Acetylcholinesterase During Morphological Modification. *Journal of Experimental Marine Biology and Ecology* 447, 93-99.
57. Marsh, G., Whalley, K., Wright, R., Yates, D., Silva, K.D., Vallis, J., Przedborski, S., and Dawson, V. "Understanding Parkinson's disease". *YouTube*, uploaded by nature video, 16 December 2019, https://www.youtube.com/watch?v=ckn9zybpYZ8&list=PLpnKz0nS88jq_74XhBv4EAfNTYDI48ljQ&index=23.
58. Bates, G.P., Dorsey, R., Gusella, J.F., Hayden, M.R., Kay, C., Leavitt, B.R., Nance, M., Ross, C.A., Scahill, R.I., Wetzel, R., Wild, E.J., and Tabrizi, S.J. (2015). Huntington disease. *Nature Reviews Disease Primers* 1, 15005.
59. UniProt. (2023). *Electrophorus electricus* Acetylcholinesterase. (EMBL-EBI European Molecular Biology Laboratory-European Bioinformatics Institute).
60. Ganeshpurkar, A., Singh, R., Shivhare, S., Divya, Kumar, D., Gutti, G., Singh, R., Kumar, A., and Singh, S.K. (2021). Improved machine learning scoring functions for identification of *Electrophorus electricus*'s acetylcholinesterase inhibitors. *Molecular Diversity* 3, 1455-1479.
61. Figure 1 from © Camp, S., Zhang, L., Marquez, M., Torre, B., Long, J.M., Bucht, G., and Taylor, P. (2005). Acetylcholinesterase (AChE) gene modification in transgenic animals: Functional consequences of selected exon and regulatory region deletion. *Chemico-Biological Interactions* 157-158, 79-86. Page 82. Adapted with permission from publisher.
62. Figure 2 from © Perrier, A.L., Massoulie, J., and Krejci, E. (2002). PRiMA: The Membrane Anchor of Acetylcholinesterase in the Brain. *Neuron* 33, 275-285. Page 281. Adapted with permission from publisher.
63. Figure 3 from © Dvir, H., Silman, I., Harel, M., Rosenberry, T.L., and Sussman, J.L. (2010). Acetylcholinesterase: From 3D Structure to Function. *Chemico-Biological Interactions* 187, 10-22. Page 22. Adapted with permission from publisher.
64. Figure 20 from © Liu, V. (2019). Spiropyrrrolizidine and Piperazine Derivatives: Synthesis and Evaluation on KRAS Expression Levels in Human Colon Cancer Cells. University of Northern British Columbia, 32. Page 32. By permission from author.

Supplementary Data

Replicate 1

	[unit/mL]	0.0	0.009	0.09	0.9
Minutes					
0		0.216	0.212	0.204	0.161
2		0.239	0.179	0.206	0.141
4		0.305	0.169	0.194	0.137
6		0.354	0.166	0.186	0.143
8		0.366	0.165	0.181	0.146
10		0.376	0.170	0.181	0.149
12		0.398	0.173	0.179	0.152
14		0.407	0.174	0.179	0.157
16		0.408	0.176	0.180	0.160
18		0.404	0.179	0.182	0.163
20		0.407	0.182	0.184	0.166
22		0.413	0.184	0.185	0.169
24		0.421	0.187	0.187	0.172
26		0.425	0.189	0.189	0.175
28		0.428	0.192	0.191	0.178
30		0.431	0.194	0.193	0.181



Replicate 2

	[unit/mL]	0.0	0.009	0.09	0.9
Minutes					
0		0.502	0.256	0.231	0.225
2		0.626	0.258	0.235	0.234
4		0.704	0.259	0.190	0.225
6		0.744	0.260	0.181	0.212
8		0.778	0.261	0.203	0.206
10		0.802	0.261	0.260	0.205
12		0.814	0.260	0.353	0.206
14		0.822	0.260	0.531	0.208
16		0.827	0.258	0.631	0.211
18		0.834	0.256	0.654	0.214
20		0.834	0.255	0.666	0.217
22		0.839	0.253	0.670	0.219
24		0.843	0.252	0.665	0.222
26		0.848	0.250	0.670	0.224

28		0.849	0.249	0.673	0.227
30		0.852	0.248	0.671	0.229



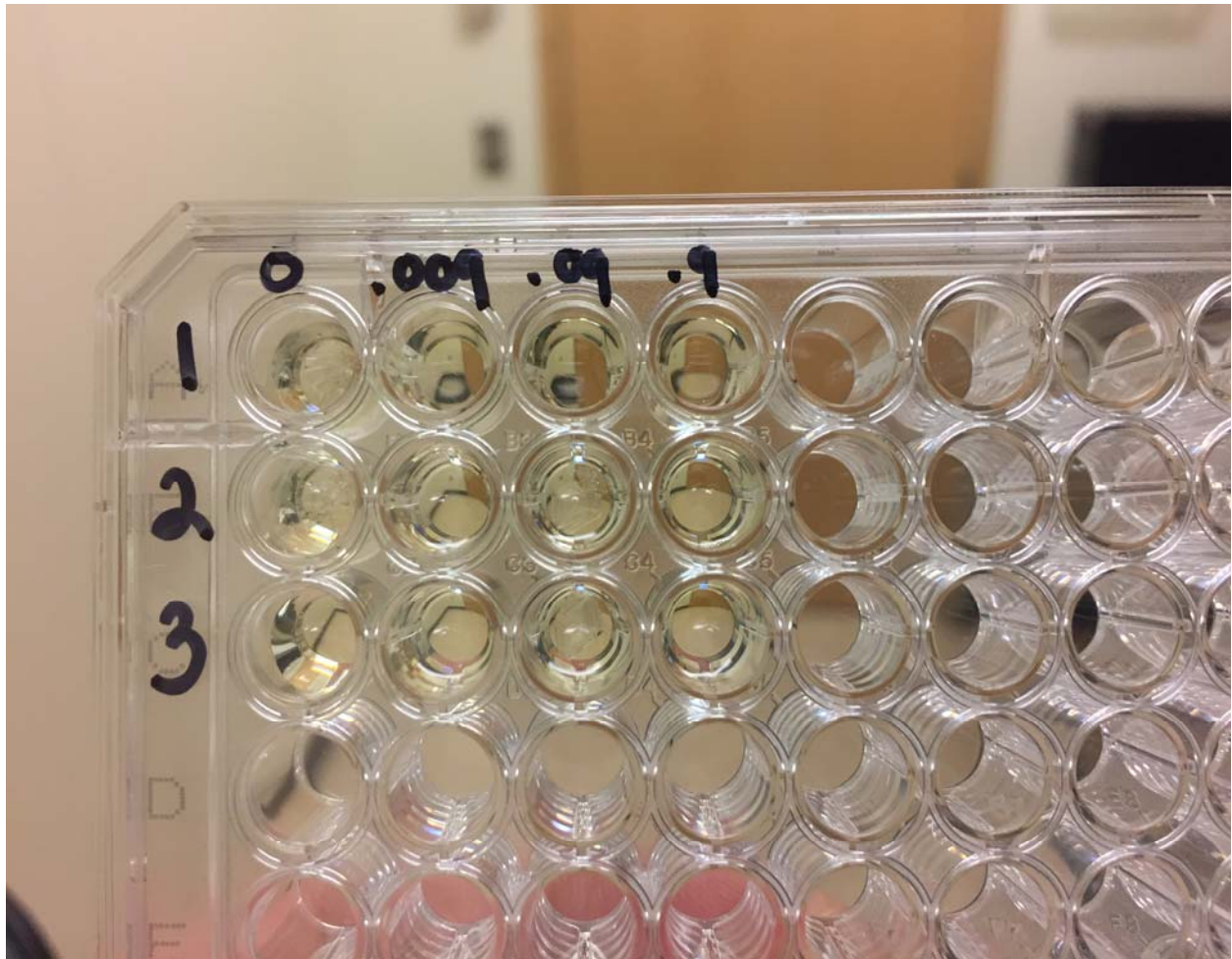
Replicate 3

	[unit/mL]	0.0	0.009	0.09	0.9
Minutes					
0		0.200	0.227	0.221	0.136
2		0.186	0.227	0.218	0.146
4		0.189	0.222	0.190	0.154
6		0.191	0.218	0.148	0.160
8		0.192	0.214	0.145	0.164
10		0.192	0.211	0.161	0.167
12		0.193	0.208	0.175	0.171
14		0.194	0.206	0.205	0.175
16		0.194	0.204	0.250	0.179
18		0.194	0.203	0.507	0.183
20		0.196	0.203	0.704	0.186
22		0.198	0.203	0.604	0.189
24		0.201	0.204	0.549	0.192
26		0.204	0.205	0.494	0.195
28		0.209	0.206	0.490	0.198
30		0.215	0.208	0.489	0.201



Supplementary Table 1. Evaluating the Assay with Different Concentrations of Acetylcholinesterase: The First Performance Test, Run 2.

The test aimed to assess the assay's ability to generate appropriate absorbance readings in response to increasing concentrations of acetylcholinesterase. It analyzed the rate of TNB²⁻ absorbance increase over a 30-min time span as acetylcholinesterase increased. The lower panels of graphs depicted the changes in TNB²⁻ absorbance in response to increasing concentrations of acetylcholinesterase over the course of 30 mins. The experiment was repeated three times (n = 3).



Supplementary Figure 1. Evaluating the Assay with Different Concentrations of Acetylcholinesterase: The First Performance Test, Run 2.

A photo of the microtiter plate used for the run was also attached to illustrate the unexpected results.

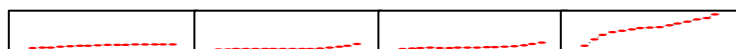
Replicate 1

	[unit/mL]	0.0	0.009	0.09	0.9
Minutes					
0		0.172	0.174	0.177	0.490
2		0.181	0.178	0.220	0.984
4		0.395	0.182	0.245	1.375
6		0.489	0.187	0.246	1.566
8		0.503	0.191	0.291	1.725
10		0.514	0.196	0.386	1.881
12		0.520	0.201	0.455	2.044
14		0.542	0.206	0.479	2.157
16		0.571	0.211	0.493	2.266
18		0.583	0.216	0.499	2.346
20		0.591	0.220	0.525	2.404
22		0.596	0.225	0.536	2.454
24		0.602	0.229	0.533	2.502
26		0.606	0.233	0.554	2.531
28		0.607	0.235	0.645	2.572
30		0.605	0.238	0.652	2.492



Replicate 2

	[unit/mL]	0.0	0.009	0.09	0.9
Minutes					
0		0.259	0.146	0.193	0.472
2		0.317	0.157	0.223	1.038
4		0.290	0.172	0.262	1.423
6		0.388	0.176	0.282	1.679
8		0.424	0.175	0.281	1.809
10		0.448	0.177	0.281	1.895
12		0.469	0.179	0.289	2.023
14		0.491	0.182	0.300	2.063
16		0.548	0.183	0.309	2.127
18		0.554	0.188	0.329	2.258
20		0.557	0.201	0.354	2.421
22		0.564	0.238	0.384	2.605
24		0.567	0.298	0.418	2.796
26		0.574	0.392	0.516	2.924
28		0.576	0.444	0.637	3.226
30		0.579	0.629	0.759	OVRFLW



Replicate 3

	[unit/mL]	0.0	0.009	0.09	0.9
Minutes					
0		0.158	0.182	0.155	0.394
2		0.161	0.182	0.172	0.932
4		0.165	0.184	0.190	1.338
6		0.169	0.187	0.207	1.604
8		0.172	0.190	0.225	1.788
10		0.175	0.192	0.242	1.926
12		0.178	0.195	0.260	2.048
14		0.18	0.197	0.277	2.148
16		0.183	0.200	0.294	2.222
18		0.186	0.202	0.311	2.298
20		0.189	0.205	0.328	2.362
22		0.193	0.208	0.345	2.428
24		0.197	0.212	0.361	2.479
26		0.200	0.216	0.377	2.509
28		0.205	0.220	0.394	2.525
30		0.209	0.224	0.411	2.551



Supplementary Table 2. Evaluating the Assay with Different Concentrations of Acetylcholinesterase: The First Performance Test, Run 3.

The test aimed to assess the assay's ability to generate appropriate absorbance readings in response to increasing concentrations of acetylcholinesterase. It analyzed the rate of TNB²⁻ absorbance increase over a 30-min time span as acetylcholinesterase concentration increased. The term "OVRFLW", or "Overflow", denoted absorbance readings that exceeded the upper limit of the Synergy 2 plate reader machine's detection range and could not be measured. Black highlighted sections in the tables represented unusual data where absorbance readings resulting from treatments with lower enzyme concentrations were higher than those from treatments with higher enzyme concentrations. The lower panels of graphs depicted the changes in TNB²⁻ absorbance in response to increasing concentrations of acetylcholinesterase over the course of 30 mins. The experiment was repeated three times (n = 3).

Replicate 1

	[unit/mL]	0.0	0.009	0.09	0.9
Minutes					
0		0.578	0.319	0.296	1.010
2		0.645	0.320	0.327	1.431
4		0.677	0.319	0.357	1.745
6		0.679	0.319	0.385	1.937
8		0.679	0.318	0.412	2.055
10		0.691	0.318	0.437	2.155
12		0.711	0.317	0.463	2.216
14		0.719	0.317	0.488	2.248
16		0.730	0.317	0.512	2.274
18		0.730	0.317	0.535	2.295
20		0.735	0.317	0.558	2.276
22		0.737	0.317	0.580	2.279
24		0.740	0.317	0.602	2.297
26		0.738	0.317	0.625	2.314
28		0.738	0.318	0.649	2.353
30		0.734	0.319	0.673	2.363



Replicate 2

	[unit/mL]	0.0	0.009	0.09	0.9
Minutes					
0		0.235	0.302	0.265	0.571
2		0.227	0.312	0.291	0.810
4		0.244	0.323	0.313	0.950
6		0.267	0.329	0.333	1.029
8		0.287	0.333	0.354	1.093
10		0.312	0.336	0.375	1.151
12		0.341	0.337	0.396	1.203
14		0.369	0.337	0.416	1.256
16		0.395	0.337	0.437	1.305
18		0.415	0.337	0.457	1.351
20		0.435	0.336	0.476	1.392
22		0.447	0.337	0.496	1.436
24		0.464	0.336	0.516	1.478
26		0.474	0.336	0.535	1.520
28		0.492	0.336	0.555	1.557
30		0.502	0.337	0.576	1.598



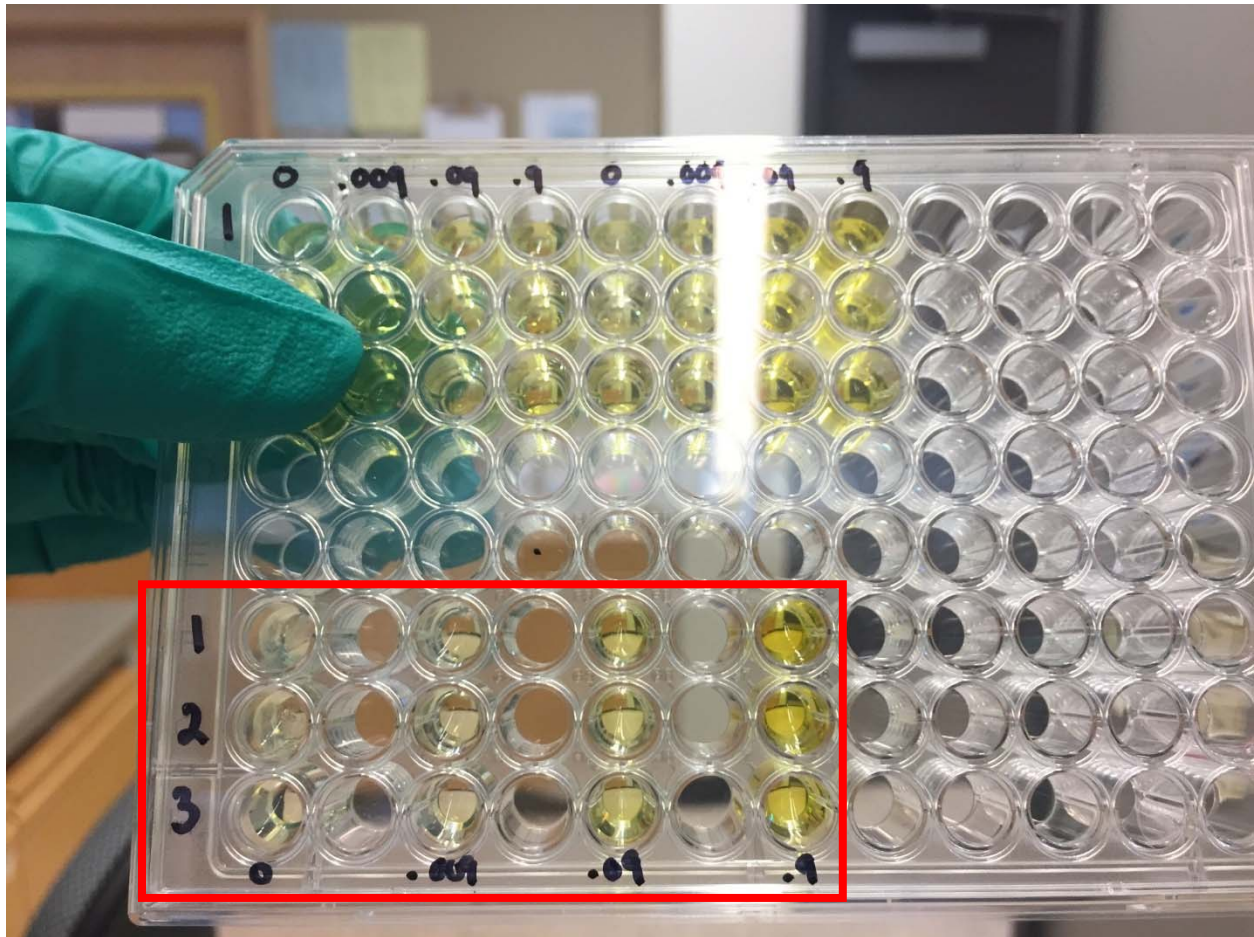
Replicate 3

	[unit/mL]	0.0	0.009	0.09	0.9
Minutes					
0		0.238	0.316	0.315	0.298
2		0.245	0.318	0.344	0.359
4		0.249	0.318	0.366	0.397
6		0.255	0.318	0.384	0.432
8		0.261	0.318	0.401	0.470
10		0.267	0.318	0.418	0.509
12		0.272	0.318	0.434	0.548
14		0.276	0.318	0.452	0.587
16		0.279	0.318	0.469	0.626
18		0.282	0.319	0.486	0.666
20		0.285	0.319	0.504	0.707
22		0.287	0.320	0.521	0.749
24		0.290	0.322	0.540	0.796
26		0.292	0.322	0.558	0.845
28		0.294	0.323	0.577	0.897
30		0.296	0.325	0.596	0.952



Supplementary Table 3. Evaluating the Assay with Different Concentrations of Acetylcholinesterase: The First Performance Test, Run 4.

The test aimed to assess the assay’s ability to generate appropriate absorbance readings in response to increasing concentrations of acetylcholinesterase. It analyzed the rate of TNB²⁻ absorbance increase over a 30-min time span as acetylcholinesterase concentration increased. Black highlighted sections in the tables represented unusual data where absorbance readings resulting from treatments with lower enzyme concentrations were higher than those from treatments with higher enzyme concentrations. The lower panels of graphs depicted the changes in TNB²⁻ absorbance in response to increasing concentrations of acetylcholinesterase over the course of 30 mins. The experiment was repeated three times (n = 3).



Supplementary Figure 2. Evaluating the Assay with Different Concentrations of Acetylcholinesterase: The First Performance Test Run 4.

A photo of the microtiter plate (the third 4x3 set at the bottom within the red box) used for the run was also attached to illustrate the crystal formation that likely contributed to the higher absorbance readings and the greater fluctuations along the absorbance readings of the two wells from replicates 1 and 2, which were both treated with the same enzyme concentration of 0 units/mL.

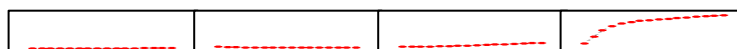
Replicate 1

	[unit/mL]	0.0	0.009	0.09	0.9
Minutes					
0		0.256	0.313	0.315	0.562
2		0.252	0.287	0.334	1.111
4		0.240	0.274	0.349	1.472
6		0.239	0.271	0.368	1.615
8		0.236	0.274	0.391	1.728
10		0.241	0.277	0.416	1.831
12		0.243	0.279	0.441	1.932
14		0.243	0.282	0.466	2.017
16		0.245	0.285	0.492	2.094
18		0.249	0.288	0.517	2.157
20		0.250	0.290	0.544	2.225
22		0.253	0.293	0.570	2.285
24		0.255	0.295	0.597	2.337
26		0.257	0.297	0.624	2.389
28		0.259	0.300	0.652	2.437
30		0.261	0.302	0.680	2.486



Replicate 2

	[unit/mL]	0.0	0.009	0.09	0.9
Minutes					
0		0.221	0.363	0.388	0.660
2		0.218	0.344	0.388	1.264
4		0.212	0.328	0.385	1.818
6		0.211	0.316	0.396	2.201
8		0.215	0.308	0.410	2.426
10		0.219	0.301	0.432	2.563
12		0.223	0.297	0.457	2.663
14		0.227	0.296	0.481	2.732
16		0.232	0.294	0.510	2.812
18		0.234	0.293	0.537	2.846
20		0.237	0.293	0.566	2.913
22		0.241	0.294	0.595	2.947
24		0.245	0.295	0.626	3.021
26		0.249	0.296	0.658	3.071
28		0.253	0.298	0.689	3.105
30		0.256	0.301	0.723	3.175



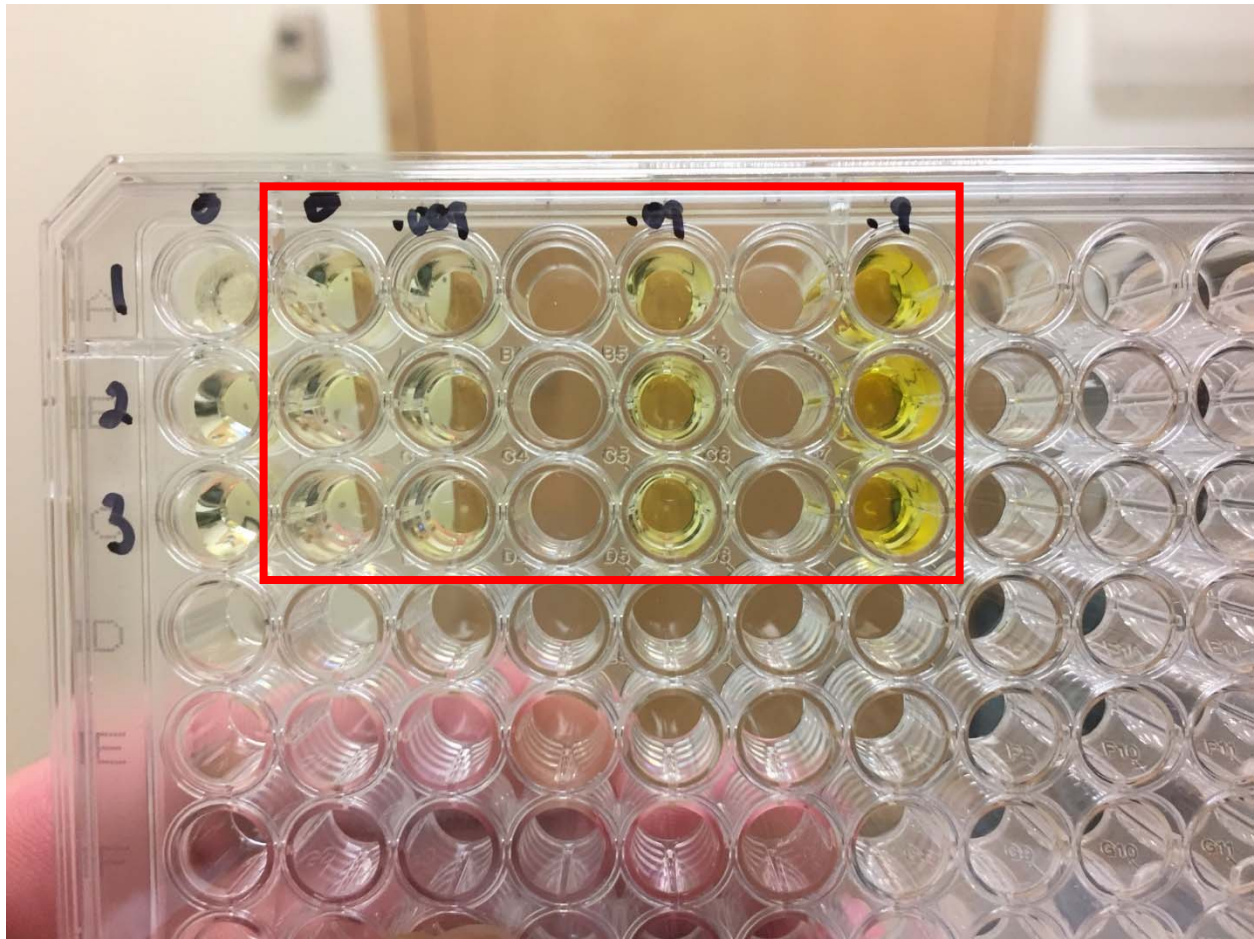
Replicate 3

	[unit/mL]	0.0	0.009	0.09	0.9
Minutes					
0		0.246	0.283	0.298	0.588
2		0.255	0.282	0.319	1.161
4		0.242	0.279	0.342	1.660
6		0.236	0.281	0.363	1.988
8		0.236	0.282	0.383	2.095
10		0.235	0.285	0.404	2.188
12		0.239	0.287	0.424	2.247
14		0.241	0.290	0.446	2.313
16		0.243	0.293	0.469	2.365
18		0.245	0.295	0.492	2.415
20		0.249	0.297	0.517	2.460
22		0.253	0.299	0.542	2.496
24		0.256	0.302	0.567	2.535
26		0.259	0.304	0.594	2.567
28		0.262	0.306	0.621	2.581
30		0.266	0.307	0.649	2.631



Supplementary Table 4. Evaluating the Assay with Different Concentrations of Acetylcholinesterase: The First Performance Test, Run 5.

The test aimed to assess the assay's ability to generate appropriate absorbance readings in response to increasing concentrations of acetylcholinesterase. It analyzed the rate of TNB²⁻ absorbance increase over a 30-min time span as acetylcholinesterase concentration increased. The lower panels of graphs depicted the changes in TNB²⁻ absorbance in response to increasing concentrations of acetylcholinesterase over the course of 30 mins. The experiment was repeated three times (n = 3).



Supplementary Figure 3. Evaluating the Assay with Different Concentrations of Acetylcholinesterase: The First Performance Test, Run 5.

A photo of the microtiter plate (ignoring the first column located on the furthest left of the plate, the 4x3 set starting from the second column within the red box) used for the run was also attached to illustrate the surprising disappearance of the crystal formation after the mixing factor had been considered for.

Replicate 1

	[unit/mL]	0.0	0.009	0.09	0.9
Minutes					
0		0.184	0.245	0.240	0.875
2		0.184	0.248	0.246	1.469
4		0.185	0.249	0.252	1.703
6		0.187	0.250	0.257	1.901
8		0.188	0.253	0.261	2.116
10		0.190	0.254	0.266	2.244
12		0.193	0.255	0.272	2.321
14		0.194	0.257	0.276	2.420
16		0.197	0.259	0.281	2.557
18		0.200	0.260	0.286	2.632
20		0.201	0.262	0.290	2.727
22		0.202	0.263	0.295	2.798
24		0.205	0.265	0.299	2.857
26		0.209	0.267	0.305	2.903
28		0.213	0.268	0.308	2.945
30		0.210	0.270	0.313	2.979



Replicate 2

	[unit/mL]	0.0	0.009	0.09	0.9
Minutes					
0		0.226	0.328	0.262	0.907
2		0.215	0.354	0.266	1.443
4		0.208	0.374	0.270	1.556
6		0.220	0.387	0.275	1.725
8		0.217	0.388	0.280	1.793
10		0.224	0.400	0.286	1.863
12		0.223	0.411	0.291	1.954
14		0.225	0.424	0.297	2.043
16		0.231	0.431	0.302	2.083
18		0.230	0.438	0.307	2.166
20		0.238	0.441	0.312	2.182
22		0.238	0.444	0.317	2.258
24		0.238	0.447	0.323	2.284
26		0.243	0.450	0.328	2.327
28		0.246	0.453	0.333	2.366
30		0.249	0.455	0.338	2.403



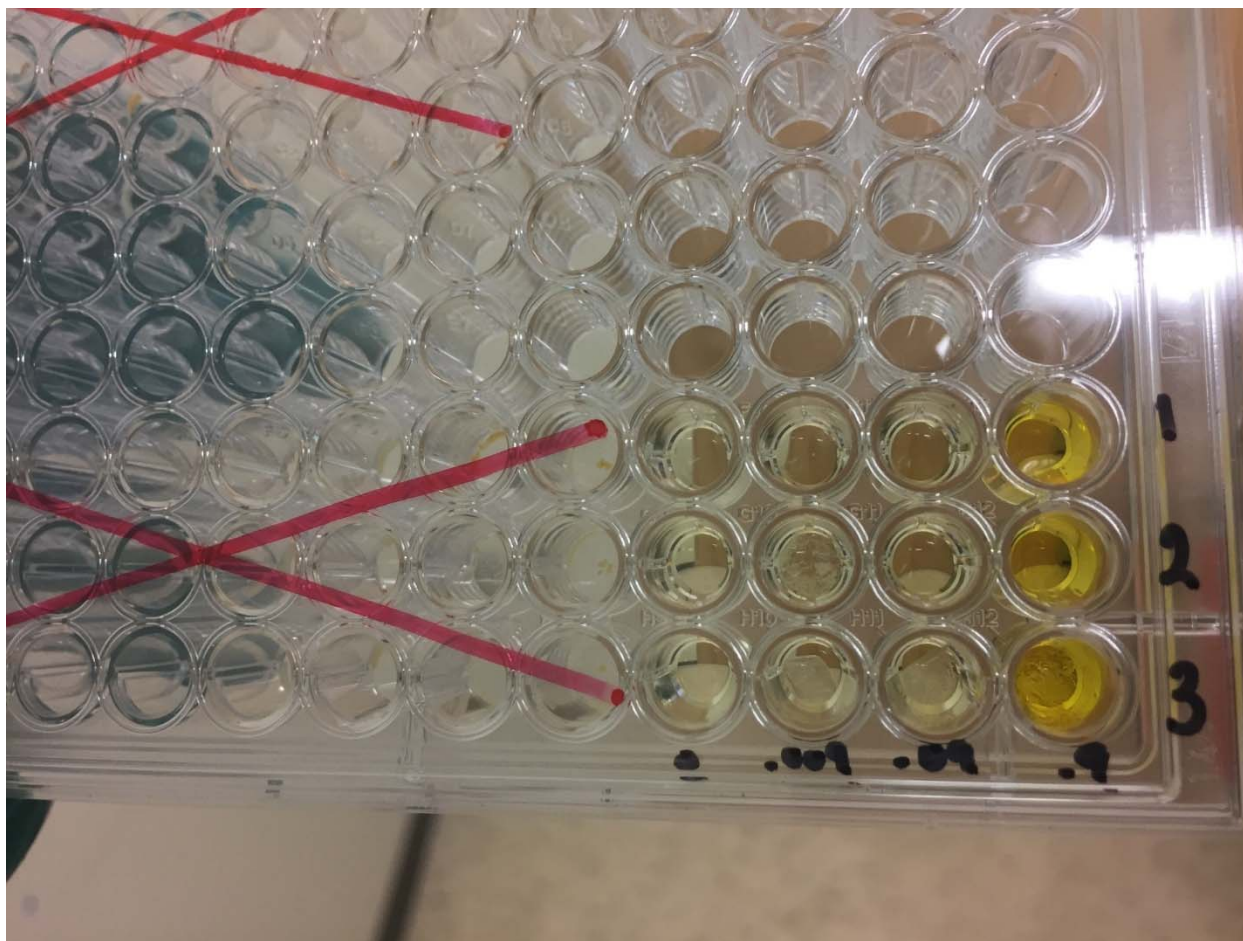
Replicate 3

	[unit/mL]	0.0	0.009	0.09	0.9
Minutes					
0		0.239	0.241	0.247	0.890
2		0.242	0.247	0.252	1.587
4		0.241	0.250	0.263	1.976
6		0.244	0.273	0.270	2.513
8		0.246	0.375	0.277	3.007
10		0.248	0.543	0.282	3.723
12		0.250	0.710	0.288	OVRFLW
14		0.252	0.781	0.301	OVRFLW
16		0.254	0.799	0.377	OVRFLW
18		0.256	0.819	0.558	OVRFLW
20		0.258	0.840	0.575	OVRFLW
22		0.261	0.857	0.593	OVRFLW
24		0.262	0.867	0.582	OVRFLW
26		0.265	0.878	0.581	OVRFLW
28		0.267	0.882	0.587	OVRFLW
30		0.269	0.888	0.598	OVRFLW



Supplementary Table 5. Evaluating the Assay with Different Concentrations of Acetylcholinesterase: The First Performance Test, Run 6.

The test aimed to assess the assay's ability to generate appropriate absorbance readings in response to increasing concentrations of acetylcholinesterase. It analyzed the rate of TNB²⁻ absorbance increase over a 30-min time span as acetylcholinesterase concentration increased. The term "OVRFLW", or "Overflow", denoted absorbance readings that exceeded the upper limit of the Synergy 2 plate reader machine's detection range and could not be measured. Black highlighted sections in the tables represented unusual data where absorbance readings resulting from treatments with lower enzyme concentrations were higher than those from treatments with higher enzyme concentrations. The lower panels of graphs depicted the changes in TNB²⁻ absorbance in response to increasing concentrations of acetylcholinesterase over the course of 30 mins. The experiment was repeated three times (n = 3).



Supplementary Figure 4. Evaluating the Assay with Different Concentrations of Acetylcholinesterase: The First Performance Test, Run 6.

A photo of the microtiter plate used for the run was also attached to illustrate the irreproducibility of the results obtained from run 5, shown by the recurrence of the crystal formation in many wells.

Replicate 1

	[unit/mL]	0.0	0.009	0.09	0.9
Minutes					
0		0.078	0.082	0.101	0.329
2		0.080	0.083	0.110	0.406
4		0.081	0.084	0.117	0.460
6		0.082	0.085	0.125	0.489
8		0.083	0.087	0.133	0.513
10		0.083	0.088	0.140	0.526
12		0.084	0.089	0.147	0.533
14		0.085	0.090	0.154	0.538
16		0.086	0.092	0.161	0.539
18		0.087	0.094	0.168	0.540
20		0.088	0.095	0.175	0.539
22		0.088	0.097	0.182	0.537
24		0.090	0.098	0.188	0.536
26		0.090	0.099	0.195	0.534
28		0.091	0.101	0.201	0.533
30		0.092	0.102	0.207	0.530



Replicate 2

	[unit/mL]	0.0	0.009	0.09	0.9
Minutes					
0		0.082	0.084	0.101	0.332
2		0.085	0.086	0.108	0.422
4		0.086	0.087	0.115	0.479
6		0.085	0.088	0.123	0.512
8		0.086	0.088	0.131	0.534
10		0.088	0.090	0.137	0.551
12		0.088	0.091	0.144	0.556
14		0.088	0.092	0.151	0.558
16		0.090	0.094	0.157	0.563
18		0.090	0.095	0.165	0.561
20		0.091	0.096	0.171	0.558
22		0.094	0.097	0.177	0.558
24		0.094	0.098	0.183	0.553
26		0.096	0.100	0.189	0.552
28		0.096	0.101	0.195	0.548
30		0.097	0.101	0.200	0.546



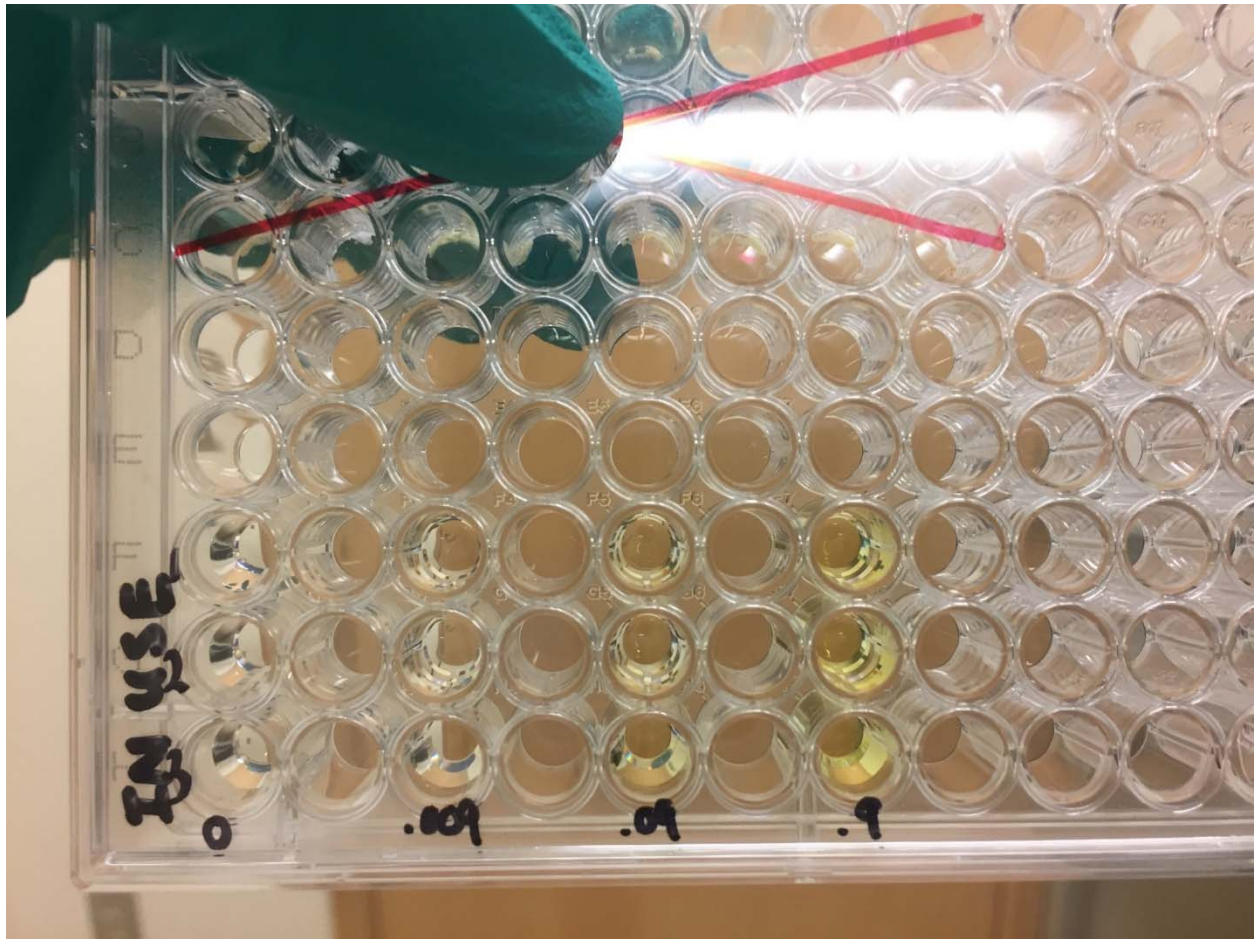
Replicate 3

	[unit/mL]	0.0	0.009	0.09	0.9
Minutes					
0		0.094	0.084	0.111	0.350
2		0.095	0.085	0.123	0.431
4		0.095	0.086	0.136	0.481
6		0.096	0.087	0.147	0.514
8		0.097	0.088	0.160	0.534
10		0.098	0.090	0.172	0.547
12		0.099	0.091	0.182	0.551
14		0.099	0.092	0.193	0.551
16		0.100	0.093	0.203	0.553
18		0.101	0.094	0.214	0.555
20		0.102	0.096	0.222	0.554
22		0.103	0.097	0.232	0.552
24		0.104	0.098	0.240	0.550
26		0.104	0.099	0.249	0.548
28		0.106	0.100	0.258	0.546
30		0.106	0.101	0.265	0.544



Supplementary Table 6. Evaluating the Assay with Different Concentrations of Acetylcholinesterase: The First Performance Test, Run 7.

The test aimed to assess the assay's ability to generate appropriate absorbance readings in response to increasing concentrations of acetylcholinesterase. It analyzed the rate of TNB²⁻ absorbance increase over a 30-min time span as acetylcholinesterase concentration increased. Black highlighted sections in the tables represented unusual data where absorbance readings resulting from treatments with lower enzyme concentrations were higher than those from treatments with higher enzyme concentrations. The lower panels of graphs depicted the changes in TNB²⁻ absorbance in response to increasing concentrations of acetylcholinesterase over the course of 30 mins. The experiment was repeated three times (n = 3).



Supplementary Figure 5. Evaluating the Assay with Different Concentrations of Acetylcholinesterase: The First Performance Test, Run 7.

A photo of the microtiter plate used for the run was also attached to illustrate the fair reproducibility of the results obtained from run 5 when treated with the same amount but at a diluted concentration of acetylthiocholine iodide by a factor of 10, as indicated by the disappearance of the crystal formation in all wells.

Replicate 1

	[unit/mL]	0.0	0.009	0.09	0.9
Minutes					
0		0.131	0.159	0.192	0.618
2		0.132	0.160	0.218	0.823
4		0.133	0.164	0.245	0.918
6		0.134	0.166	0.271	1.024
8		0.137	0.168	0.298	1.108
10		0.138	0.170	0.325	1.140
12		0.139	0.172	0.352	1.182
14		0.141	0.174	0.378	1.253
16		0.142	0.177	0.404	1.296
18		0.144	0.179	0.429	1.333
20		0.146	0.181	0.454	1.373
22		0.147	0.183	0.480	1.399
24		0.149	0.185	0.505	1.418
26		0.151	0.187	0.531	1.446
28		0.153	0.189	0.557	1.462
30		0.155	0.191	0.583	1.483



Replicate 2

	[unit/mL]	0.0	0.009	0.09	0.9
Minutes					
0		0.133	0.153	0.208	0.727
2		0.133	0.157	0.238	1.168
4		0.134	0.160	0.267	1.465
6		0.135	0.163	0.293	1.573
8		0.136	0.167	0.322	1.637
10		0.139	0.170	0.349	1.667
12		0.141	0.173	0.377	1.759
14		0.142	0.176	0.403	1.810
16		0.145	0.179	0.428	1.818
18		0.147	0.183	0.456	1.850
20		0.148	0.186	0.480	1.897
22		0.151	0.189	0.506	1.896
24		0.153	0.193	0.531	1.913
26		0.155	0.196	0.557	1.927
28		0.158	0.199	0.582	1.923
30		0.160	0.202	0.607	1.938



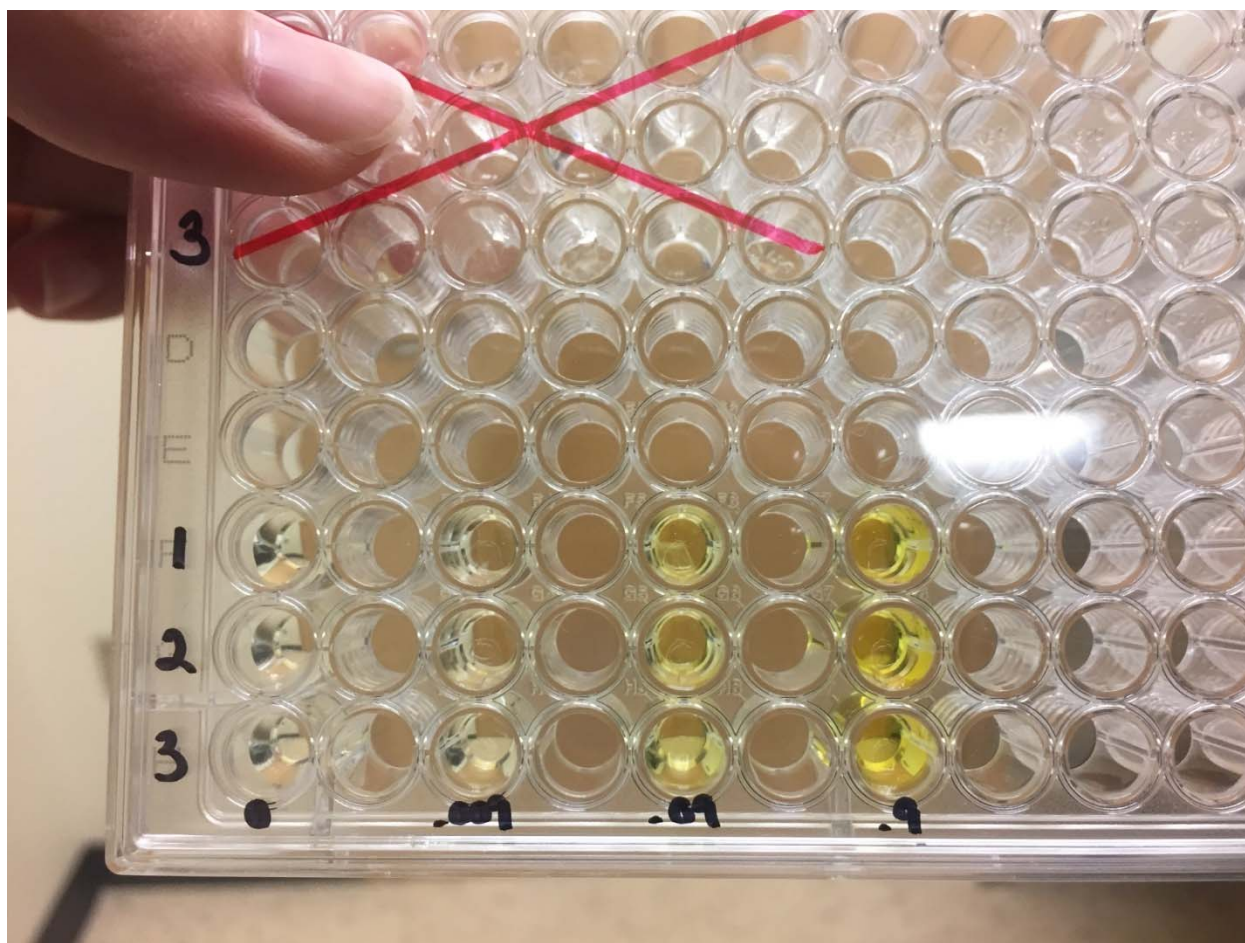
Replicate 3

	[unit/mL]	0.0	0.009	0.09	0.9
Minutes					
0		0.139	0.143	0.189	0.627
2		0.140	0.146	0.213	0.798
4		0.142	0.149	0.236	0.896
6		0.144	0.152	0.261	1.008
8		0.147	0.153	0.284	1.075
10		0.148	0.158	0.306	1.158
12		0.151	0.160	0.329	1.196
14		0.153	0.163	0.351	1.252
16		0.155	0.166	0.374	1.305
18		0.157	0.170	0.396	1.338
20		0.160	0.173	0.418	1.381
22		0.161	0.176	0.440	1.383
24		0.163	0.180	0.462	1.413
26		0.165	0.183	0.483	1.443
28		0.167	0.186	0.505	1.466
30		0.169	0.189	0.527	1.498



Supplementary Table 7. Evaluating the Assay with Different Concentrations of Acetylcholinesterase: The First Performance Test, Run 8.

The test aimed to assess the assay's ability to generate appropriate absorbance readings in response to increasing concentrations of acetylcholinesterase. It analyzed the rate of TNB²⁻ absorbance increase over a 30-min time span as acetylcholinesterase concentration increased. The lower panels of graphs depicted the changes in TNB²⁻ absorbance in response to increasing concentrations of acetylcholinesterase over the course of 30 mins. The experiment was repeated three times (n = 3).



Supplementary Figure 6. Evaluating the Assay with Different Concentrations of Acetylcholinesterase: The First Performance Test, Run 8.

A photo of the microtiter plate used for the run was also attached to illustrate the fair reproducibility of the results obtained from run 5 when treated with the same amount but at a diluted concentration of acetylthiocholine iodide by a factor of 2. Even though the crystal formation recurred in a few wells, the overall absorbance data was stable and replicable to what was observed in run 5.

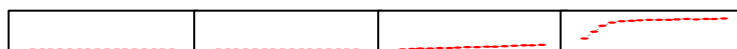
Replicate 1

	[unit/mL]	0.0	0.009	0.09	0.9
Minutes					
0		0.138	0.120	0.181	1.372
2		0.139	0.120	0.206	2.032
4		0.139	0.121	0.233	2.569
6		0.139	0.123	0.260	3.025
8		0.137	0.124	0.285	3.307
10		0.138	0.125	0.310	3.555
12		0.143	0.126	0.334	3.509
14		0.143	0.127	0.362	3.629
16		0.142	0.128	0.387	3.620
18		0.143	0.128	0.413	3.701
20		0.143	0.129	0.441	3.746
22		0.143	0.130	0.471	3.769
24		0.144	0.131	0.493	3.770
26		0.144	0.132	0.502	3.831
28		0.145	0.133	0.522	3.735
30		0.145	0.134	0.539	3.751



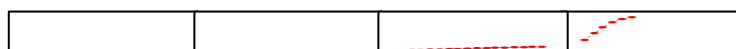
Replicate 2

	[unit/mL]	0.0	0.009	0.09	0.9
Minutes					
0		0.141	0.134	0.198	1.447
2		0.141	0.132	0.230	2.212
4		0.141	0.132	0.264	2.858
6		0.141	0.130	0.297	3.221
8		0.141	0.131	0.328	3.387
10		0.141	0.130	0.357	3.457
12		0.139	0.129	0.388	3.494
14		0.138	0.129	0.418	3.527
16		0.141	0.132	0.445	3.548
18		0.143	0.136	0.477	3.544
20		0.145	0.138	0.515	3.590
22		0.145	0.140	0.558	3.654
24		0.146	0.142	0.597	3.609
26		0.146	0.143	0.633	3.630
28		0.147	0.145	0.668	3.655
30		0.147	0.146	0.706	3.719



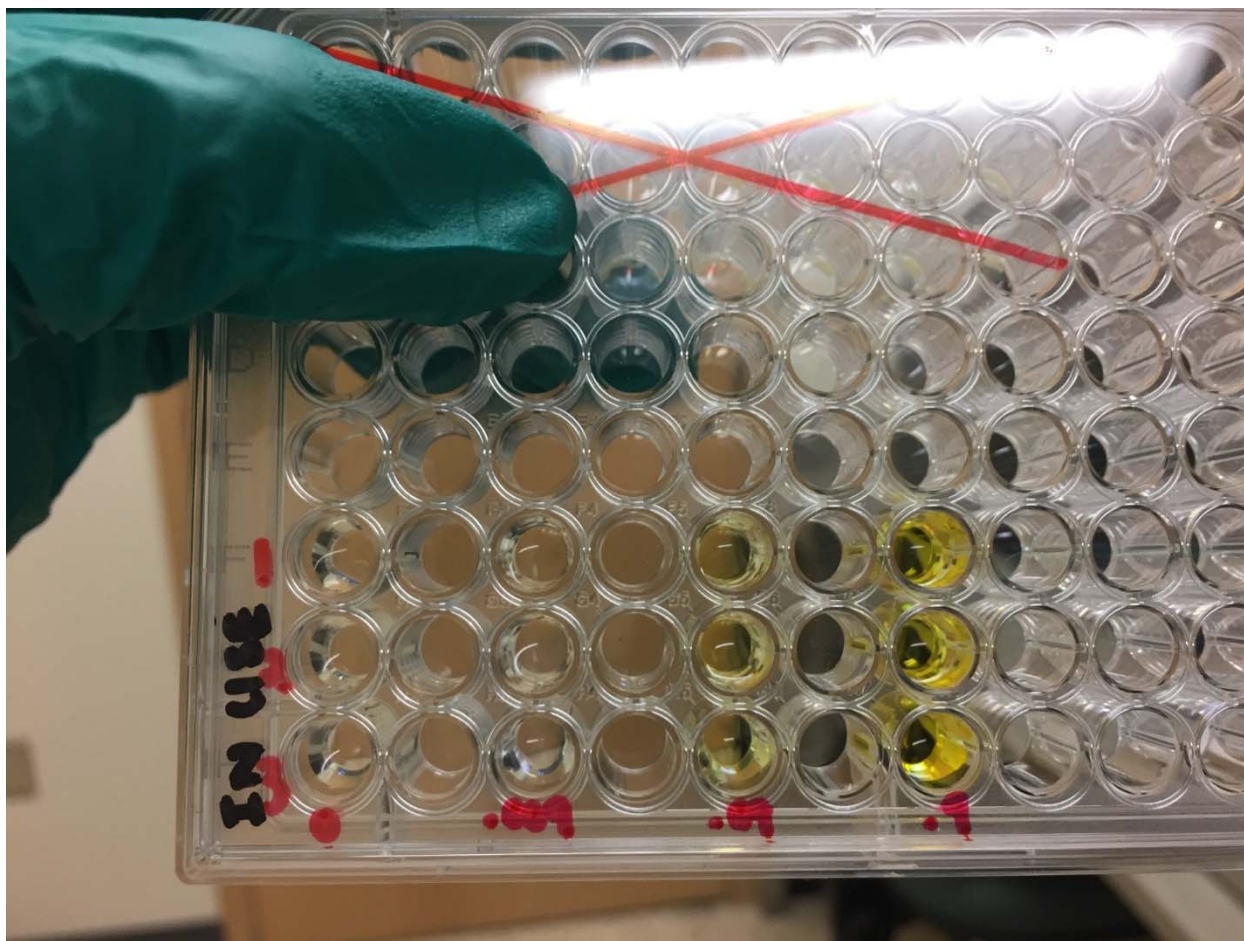
Replicate 3

	[unit/mL]	0.0	0.009	0.09	0.9
Minutes					
0		0.137	0.111	0.180	1.365
2		0.140	0.112	0.210	2.122
4		0.138	0.114	0.241	2.801
6		0.138	0.116	0.271	3.368
8		0.136	0.117	0.301	3.762
10		0.136	0.118	0.329	3.970
12		0.137	0.119	0.357	OVRFLW
14		0.138	0.120	0.385	OVRFLW
16		0.138	0.122	0.415	OVRFLW
18		0.139	0.123	0.443	OVRFLW
20		0.140	0.124	0.471	OVRFLW
22		0.140	0.125	0.499	OVRFLW
24		0.141	0.126	0.526	OVRFLW
26		0.141	0.127	0.554	OVRFLW
28		0.142	0.128	0.582	OVRFLW
30		0.143	0.129	0.610	OVRFLW



Supplementary Table 8. Evaluating the Assay with Different Concentrations of Acetylcholinesterase: The First Performance Test, Run 9.

The test aimed to assess the assay's ability to generate appropriate absorbance readings in response to increasing concentrations of acetylcholinesterase. It analyzed the rate of TNB²⁻ absorbance increase over a 30-min time span as acetylcholinesterase concentration increased. The term "OVRFLW", or "Overflow", denoted absorbance readings that exceeded the upper limit of the Synergy 2 plate reader machine's detection range and could not be measured. Black highlighted sections in the tables represented unusual data where absorbance readings resulting from treatments with lower enzyme concentrations were higher than those from treatments with higher enzyme concentrations. The lower panels of graphs depicted the changes in TNB²⁻ absorbance in response to increasing concentrations of acetylcholinesterase over the course of 30 mins. The experiment was repeated three times (n = 3).

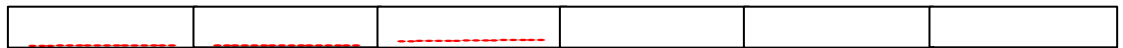


Supplementary Figure 7. Evaluating the Assay with Different Concentrations of Acetylcholinesterase: The First Performance Test, Run 9.

A photo of the microtiter plate used for the run was also attached to illustrate the almost complete reproducibility of the results obtained from run 5 when treated with the correct amount and the correct concentration of acetylthiocholine iodide, along with the correct concentration of sodium phosphate buffer in which the acetylthiocholine iodide was dissolved in. This was shown by the disappearance of the crystal formation in all wells.

Replicate 1

	[unit/mL]	0.0	0.009	0.09	0.9	4.5	9.0
Minutes							
0		0.150	0.175	0.655	OVRFLW	OVRFLW	OVRFLW
2		0.152	0.175	0.667	OVRFLW	OVRFLW	OVRFLW
4		0.153	0.175	0.677	OVRFLW	OVRFLW	OVRFLW
6		0.156	0.175	0.687	OVRFLW	OVRFLW	OVRFLW
8		0.158	0.175	0.699	OVRFLW	OVRFLW	OVRFLW
10		0.159	0.175	0.710	OVRFLW	OVRFLW	OVRFLW
12		0.160	0.175	0.721	OVRFLW	OVRFLW	OVRFLW
14		0.160	0.175	0.733	OVRFLW	OVRFLW	OVRFLW
16		0.161	0.175	0.744	OVRFLW	OVRFLW	OVRFLW
18		0.161	0.175	0.756	OVRFLW	OVRFLW	OVRFLW
20		0.161	0.175	0.766	OVRFLW	OVRFLW	OVRFLW
22		0.161	0.175	0.776	OVRFLW	OVRFLW	OVRFLW
24		0.161	0.176	0.787	OVRFLW	OVRFLW	OVRFLW
26		0.161	0.176	0.799	OVRFLW	OVRFLW	OVRFLW
28		0.162	0.176	0.809	OVRFLW	OVRFLW	OVRFLW
30		0.162	0.176	0.821	OVRFLW	OVRFLW	OVRFLW



Replicate 2

	[unit/mL]	0.0	0.009	0.09	0.9	4.5	9.0
Minutes							
0		0.173	0.165	0.236	0.958	3.107	OVRFLW
2		0.172	0.159	0.292	1.671	OVRFLW	OVRFLW
4		0.170	0.167	0.348	2.319	OVRFLW	OVRFLW
6		0.168	0.170	0.402	2.920	4.048	OVRFLW
8		0.165	0.174	0.455	3.426	3.973	OVRFLW
10		0.172	0.177	0.508	3.806	OVRFLW	OVRFLW
12		0.170	0.180	0.560	4.025	3.965	OVRFLW
14		0.169	0.183	0.611	OVRFLW	4.002	OVRFLW
16		0.169	0.186	0.662	OVRFLW	3.974	OVRFLW
18		0.169	0.188	0.712	OVRFLW	3.978	OVRFLW
20		0.169	0.192	0.761	OVRFLW	3.990	OVRFLW
22		0.169	0.194	0.811	OVRFLW	3.921	OVRFLW
24		0.169	0.197	0.857	OVRFLW	4.007	OVRFLW
26		0.170	0.200	0.906	OVRFLW	3.928	OVRFLW
28		0.170	0.202	0.952	OVRFLW	3.962	OVRFLW
30		0.170	0.205	0.999	OVRFLW	3.907	OVRFLW



Replicate 3

	[unit/mL]	0.0	0.009	0.09	0.9	4.5	9.0
Minutes							
0		0.177	0.182	0.218	0.844	3.565	OVRFLW
2		0.176	0.178	0.239	1.550	OVRFLW	OVRFLW
4		0.176	0.177	0.265	2.215	OVRFLW	OVRFLW
6		0.173	0.181	0.290	2.788	OVRFLW	OVRFLW
8		0.167	0.184	0.316	3.273	OVRFLW	OVRFLW
10		0.169	0.187	0.340	3.663	OVRFLW	OVRFLW
12		0.169	0.188	0.365	3.927	OVRFLW	OVRFLW
14		0.173	0.190	0.388	OVRFLW	OVRFLW	OVRFLW
16		0.173	0.191	0.412	OVRFLW	OVRFLW	OVRFLW
18		0.173	0.192	0.436	OVRFLW	OVRFLW	OVRFLW
20		0.173	0.194	0.459	OVRFLW	OVRFLW	OVRFLW
22		0.173	0.195	0.481	OVRFLW	OVRFLW	OVRFLW
24		0.173	0.196	0.503	OVRFLW	OVRFLW	OVRFLW
26		0.174	0.197	0.525	OVRFLW	OVRFLW	OVRFLW
28		0.173	0.198	0.546	OVRFLW	OVRFLW	OVRFLW
30		0.173	0.199	0.568	OVRFLW	OVRFLW	OVRFLW



Replicate 4

	[unit/mL]	0.0	0.009	0.09	0.9	4.5	9.0
Minutes							
0		0.190	0.194	0.226	0.757	3.647	OVRFLW
2		0.183	0.196	0.248	1.341	OVRFLW	OVRFLW
4		0.188	0.197	0.270	1.874	OVRFLW	OVRFLW
6		0.189	0.199	0.292	2.361	OVRFLW	OVRFLW
8		0.190	0.200	0.311	2.798	OVRFLW	OVRFLW
10		0.191	0.200	0.331	3.150	OVRFLW	OVRFLW
12		0.191	0.201	0.349	3.416	OVRFLW	OVRFLW
14		0.191	0.201	0.367	3.624	OVRFLW	OVRFLW
16		0.191	0.202	0.383	3.781	3.971	OVRFLW
18		0.191	0.200	0.397	3.870	3.912	OVRFLW
20		0.192	0.199	0.425	3.922	3.899	OVRFLW
22		0.192	0.202	0.452	3.953	OVRFLW	OVRFLW
24		0.192	0.206	0.474	3.858	OVRFLW	OVRFLW

26		0.192	0.208	0.495	3.858	OVRFLW	OVRFLW
28		0.192	0.211	0.515	3.683	OVRFLW	OVRFLW
30		0.193	0.212	0.533	3.801	OVRFLW	OVRFLW



Replicate 5

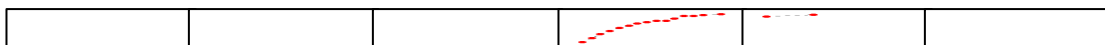
	[unit/mL]	0.0	0.009	0.09	0.9	4.5	9.0
Minutes							
0		0.182	0.188	0.206	0.854	2.923	OVRFLW
2		0.178	0.184	0.219	1.443	OVRFLW	OVRFLW
4		0.178	0.181	0.228	1.977	OVRFLW	OVRFLW
6		0.172	0.177	0.239	2.469	OVRFLW	3.974
8		0.179	0.183	0.247	2.930	OVRFLW	OVRFLW
10		0.181	0.185	0.254	3.322	OVRFLW	3.959
12		0.182	0.187	0.262	3.671	OVRFLW	OVRFLW
14		0.181	0.189	0.268	3.808	OVRFLW	OVRFLW
16		0.182	0.190	0.280	4.035	4.039	3.988
18		0.181	0.190	0.304	OVRFLW	OVRFLW	3.986
20		0.181	0.192	0.316	OVRFLW	OVRFLW	3.942
22		0.180	0.193	0.328	OVRFLW	OVRFLW	3.958
24		0.180	0.194	0.342	OVRFLW	OVRFLW	3.921
26		0.180	0.196	0.355	OVRFLW	OVRFLW	3.885
28		0.180	0.196	0.367	OVRFLW	OVRFLW	3.867
30		0.180	0.197	0.377	OVRFLW	OVRFLW	3.859



Replicate 6

	[unit/mL]	0.0	0.009	0.09	0.9	4.5	9.0
Minutes							
0		0.189	0.183	0.217	0.781	3.821	OVRFLW
2		0.188	0.172	0.223	1.264	OVRFLW	OVRFLW
4		0.188	0.170	0.231	1.715	OVRFLW	OVRFLW
6		0.188	0.153	0.235	2.109	OVRFLW	OVRFLW
8		0.186	0.167	0.241	2.466	OVRFLW	OVRFLW
10		0.187	0.173	0.246	2.711	3.989	OVRFLW
12		0.187	0.178	0.249	2.954	OVRFLW	OVRFLW
14		0.185	0.182	0.254	3.147	OVRFLW	OVRFLW
16		0.184	0.185	0.256	3.268	OVRFLW	OVRFLW
18		0.182	0.186	0.263	3.287	OVRFLW	OVRFLW

20		0.186	0.187	0.270	3.549	OVRFLW	OVRFLW
22		0.183	0.188	0.276	3.834	OVRFLW	OVRFLW
24		0.181	0.188	0.278	3.865	OVRFLW	OVRFLW
26		0.188	0.189	0.278	3.971	OVRFLW	OVRFLW
28		0.190	0.189	0.289	OVRFLW	OVRFLW	OVRFLW
30		0.186	0.190	0.304	4.040	OVRFLW	OVRFLW



Supplementary Table 9. Evaluating the Assay with Different Concentrations of Acetylcholinesterase: The First Performance Test, Run 10.

The test aimed to assess the assay’s ability to generate appropriate absorbance readings in response to increasing concentrations of acetylcholinesterase. It analyzed the rate of TNB²⁻ absorbance increase over a 30-min time span as acetylcholinesterase concentration increased. The term “OVRFLW”, or “Overflow”, denoted absorbance readings that exceeded the upper limit of the Synergy 2 plate reader machine’s detection range and could not be measured. Black highlighted sections in the tables represented unusual data where absorbance readings resulting from treatments with lower enzyme concentrations were higher than those from treatments with higher enzyme concentrations. The lower panels of graphs depicted the changes in TNB²⁻ absorbance in response to increasing concentrations of acetylcholinesterase over the course of 30 mins. The experiment was repeated three times (n = 3).